University of Alberta

Modeling the Volume-Dependent Distribution of Categorical Variables

by

Zhou Lan ©

A thesis submitted to the Faculty of Graduate Studies and Research
in partial fulfillment of the requirements for the degree of

Master of Science

in

Mining Engineering

Department of Civil and Environmental Engineering

Edmonton, Alberta
Fall 2007

Library and Archives Canada

Published Heritage Branch

395 Wellington Street
Ottawa ON K1A 0N4
Canada

Bibliothèque et Archives Canada

Direction du Patrimoine de l'édition

395, rue Wellington
Ottawa ON K1A 0N4
Canada

Your file Votre référence
ISBN: 978-0-494-33291-7
Our file Notre référence
ISBN: 978-0-494-33291-7

NOTICE:
The author has granted a non-exclusive license allowing Library and Archives Canada to reproduce, publish, archive, preserve, conserve, communicate to the public by telecommunication or on the Internet, loan, distribute and sell theses worldwide, for commercial or non-commercial purposes, in microform, paper, electronic and/or any other formats.

The author retains copyright ownership and moral rights in this thesis. Neither the thesis nor substantial extracts from it may be printed or otherwise reproduced without the author's permission.

AVIS:
L'auteur a accordé une licence non exclusive permettant à la Bibliothèque et Archives Canada de reproduire, publier, archiver, sauvegarder, conserver, transmettre au public par télécommunication ou par l'Internet, prêter, distribuer et vendre des thèses partout dans le monde, à des fins commerciales ou autres, sur support microforme, papier, électronique et/ou autres formats.

L'auteur conserve la propriété du droit d'auteur et des droits moraux qui protège cette thèse. Ni la thèse ni des extraits substantiels de celle-ci ne doivent être imprimés ou autrement reproduits sans son autorisation.

In compliance with the Canadian Privacy Act some supporting forms may have been removed from this thesis.

While these forms may be included in the document page count, their removal does not represent any loss of content from the thesis.

Conformément à la loi canadienne sur la protection de la vie privée, quelques formulaires secondaires ont été enlevés de cette thèse.

Bien que ces formulaires aient inclus dans la pagination, il n'y aura aucun contenu manquant.

Canada

University of Alberta

Library Release Form

Name of Author: Zhou Lan

Title of Thesis: Modeling the Volume-Dependent Distribution of Categorical Variables

Degree: Master of Science

Year this Degree Granted: 2007

Permission is hereby granted to the University of Alberta Library to reproduce single copies of this thesis and to lend or sell such copies for private, scholarly or scientific research purposes only.

The author reserves all other publication and other rights in association with the copyright in the thesis, and except as herein before provided, neither the thesis nor any substantial portion thereof may be printed or otherwise reproduced in any material form whatsoever without the author's prior written permission.

_____

Signature

University of Alberta

Faculty of Graduate Studies and Research

The undersigned certify that they have read, and recommend to the Faculty of Graduate Studies and Research for acceptance, a thesis entitled Modeling the Volume-Dependent Distribution of Categorical Variables submitted by Zhou Lan in partial fulfillment of the requirements for the degree of Master of Science.

Dr. Clayton Deutsch

Dr. Luciane Cunha

Dr. Carolina Diaz Goano

Dr. Oy Leuangthong

Abstract

Facies is an important categorical variable. In facies modeling, point data and scaled up block data must be considered. The scaled up facies proportions form a multivariate distribution that is dependent on the volume.

Back transformation of Logratio values satisfies the order relation constraints (non-negative proportions that sum to one), but the non-linear nature of the logratio transformation and the issue of dealing with zero proportions make it problematic to apply logratio in multiscale facies modeling.

Describing the volume dependent multivariate distribution of facies proportions and fitting the distribution at different volumetric supports is the major purpose of this thesis. Several parametric statistical distributions will be tested and practical recommendations will be made.

The volume dependent distribution of facies proportions can be predicted using a proper parametric distribution. Block kriging and sequential simulation algorithm are applied and tested in estimating the 3-dimensional distribution of facies proportions over different volumetric scales.

Acknowledgements

It is my great pleasure to thank Professor Clayton V. Deutsch for all the guidance, support and assistance during the preparation of this thesis, as well as in all the relative researches and all my studies in my Master of Science program.

I would like to thank Professor Clayton, School of Mining and Petroleum Engineering in University of Alberta and Centre for Computational Geostatistics (CCG) for the financial support on this thesis and on my studies.

Also I would like to thank Dr. Oy Leuangthong and all other professors and students for all the helps and assistance in my studies.

Table of Contents

Abstract

Acknowledgements

Chapter 1 Introduction 1
1.1 An Overview 1
1.2 Literature Review 2
1.3 A Brief Description of Facies Proportion Distribution with an Introductory Example 5
Chapter 2 Order Relations and Logratios 20
2.1 Order Relations in Facies Modeling 20
2.2 Logratio Formalism 21
2.3 Application of Logratios to Facies Modeling 24
2.4 Problem of Zero Proportions 25
2.5 Non-linearity Problems 26
2.6 Summary of the Results 29
Chapter 3 Analytical Fit to the Multivariate Distribution of Facies Proportions 32
3.1 Multinomial Distribution 32
3.2 Beta Distribution 34
3.3 Multivariate Fitting (1) – Dirichlet Distribution 35
3.4 Multivariate Fitting (2) – Ordinary Beta 38
Chapter 4 Volume Dependent Distribution of Facies Proportions Based on Ordinary Beta 51
4.1 Formalism 51
4.2 Sample Test 53
Chapter 5 An Application of Multivariate Facies Model 58
5.1 Fitting the Local Multivariate Distributions of Facies Proportions 58
5.2 Model Description 61
5.3 Sample Studies 62
5.4 Summary of Results 70
Chapter 6 Further Discussion on Multivariate Facies Distributions 85
6.1 Proportions and Probabilities 85
6.2 Facies Proportion Distribution Conditional on Local Data 88
Chapter 7 Conclusions and Future Works 98

Bibliography 100

List of Tables

1-1 Mean and standard deviation of P_0 at different scales 8

4-1 Indicator Variogram Models 54

4-2 Estimated Variances 55

5-1 Block Average Covariances 63

5-2 Kriging Variances 63

5-3a Kriging matrix for facies S_0 64

5-3b Kriging matrix for facies S_0 64

5-3c Kriging matrix for facies S_0 65

5-4 Kriging weight for facies S_0 65

5-5 Kriging variances 65

6-1 Means of P_0 conditional on the points known 89

6-2 Variances of P_0 conditional on the points known 89

List of Figures

1-1 Multiscale facies modeling 10

1-2 Slice maps of facies categories 11

1-3 Facies proportion maps 12

1-4 Scaled up facies proportions 13

1-5 Facies proportion of S_0 over different scales 14

1-6 Facies proportion of S_1 over different scales 15

1-7 Cumulative distribution of proportion of S_0 over different scales 16

1-8 Semivariograms of facies proportion for S_0 at various scales. 17

1-9 Facies proportion distribution 17

1-10 Combined facies proportions 18

1-11 Volume dependent covariances (absolute values) 18

1-12 CDF's of P_k for Cases $v = 0$ (in red) and $v = \infty$ (in black) 19

2-1 $\hat{\bar{p}}_1$ Percentile contours. 30

2-2 Map of differences between $\hat{\bar{p}}_1$ ("hatP1") and $\bar{p}_1$ ("meanP1") 31

2-3 Difference between $\hat{\bar{p}}_1$ ("hatP1") and $\bar{p}_1$ ("meanP1") 31

3-1 Binomial simulation ($\tilde{p}_k$ =0.665) 44

3-2 Semivariogram 44

3-3 Beta simulated distributions 45

3-4 Real marginal CDF's overlapped by Beta simulated CDF's 46

3-5 Beta simulated distribution for P_0 at a very small variance 47

3-6 Beta simulated fits with prior global proportion 0.0047. 47

3-7 Real marginal CDF's overlapped by Dirichlet simulated CDF's 48

3-8 Cross plots of real joint CDF's versus Dirichlet simulated joint CDF's 49

3-9 Cross plots of real joint CDF's versus Ordinay Beta simulated joint CDF's 50

4-1 Ordinary Beta simulated histograms 56

4-2 Real versus Ordinary Beta simulated joint CDF's 57

5-1 Multiscale facies models 70
5-2 Block average covariances 71
5-3 Kriging variances 72
5-4 Kriging result versus real facies proportions, from simple block Kriging with locally varying means 72
5-5 Kriging result versus real facies proportions, from ordinary block kriging 73
5-6 Kriging estimated global histograms, compared with the real histograms, from simple block kriging with locally varying means 73
5-7 Kriging estimated global histograms, compared with the real histograms, from ordinary block kriging 74
5-8 Kriging joint CDF's versus real joint CDF's 74
5-9 Residuals (kriging output – real values), from simple block kriging with locally varying means 75
5-10 Residuals (kriging output – real values), from ordinary block kriging 75
5-11 Histogram of Residuals (kriging output – real values), from Simple block kriging with locally varying means 75
5-12 Histogram of Residuals (kriging output – real values), from ordinary block kriging 76
5-13 Semivariograms reproduction from simulated realizations 77
5-14 Simulated results versus real values, based on simple block kriging with locally varying means 78
5-15 Global histograms from simulated realization, compared with the real, based on simple block kriging with locally varying means 78
5-16 Cross plots of real versus simulated Global joint CDF's, based on simple block kriging with locally varying means 79
5-17 Residual (Simulated value – real value), based on simple block kriging with locally varying means 79
5-18 Histograms of Residuals (Simulated value – real value), based on simple block kriging with locally varying means 80
5-19 Reproduction of semivariograms by simulated realizations 81

5-20 Histogram of cumulative probabilities associated with the real facies proportions based on the simulated realizations 82

5-21 Histogram of cumulative probabilities associated with the real facies proportions based on the simulated realizations, the points with facies proportion 1.0 excluded. 83

5-22 True versus simulated maps of facies proportion P_0 84

6-1 Global distributions of P_0 (based on no local information) 91

6-2 Distribution of P_k when perfect knowledge is available about a block 92

6-3 Distribution of P_0 when one point is known in the block 93

6-4 Distribution of P_0 when two points are known in the block 94

6-5 Distribution of P_0 when three points are known in the block 95

6-6 Histograms of P_0 when one point is known 96

6-7 Ordinary Beta simulated histogram (left) compared the real (right) 97

List of Nomenclature and Abbreviations

Ω : entire space of Interest

V, v : volumes of different scale

$S_1, S_2, ..., S_K$: facies categories

$\mathbf{u}$: a vector indicating the location in a two or three dimensional space

$I(\mathbf{u}, k)$: indicator of facies category S_k at location $\mathbf{u}$

$P_k, P_v(\mathbf{u}, k)$: facies proportion variable for facies category S_k at location $\mathbf{u}$

p : value of facies proportion

$\gamma_v(\mathbf{h})$: semivariogram at volumetric scale v

$D^2(v, V)$: dispersion variance

$\overline{\gamma}(v, V)$: block average semivariogram

$\overline{C}(v, V)$: block average covariance

$\Gamma^i(\mathbf{h})$: analytical function for the i^{th} nested structure of the variogram model

nst : number of nested structure

$\mathbf{a}^i$, ($a^i_{h-major}, a^i_{h-minor}, a^i_{vert}$): range of the i^{th} nested structure in horizontal major, horizontal minor and vertical direction in the variogram model

C_v^0 : nugget effect of the variogram model

C_v^i : variance contribution of the i^{th} nested structure of the variogram model

X, Y : random variables

x, y : values of random variables X and Y

$\mathbf{x}$: vector of radom variables $(X_1, ..., X_K)$

Prob[A] : probability of event A

PMF, f : probability mass function

CDF, F : cumulative distribution function

$E[X]$: expected value of variable X

$Var[X]$: variance of variable X

$COV[\mathbf{x}]$: covariance matrix of random vector $\mathbf{x}$

$C(\mathbf{u}_\alpha - \mathbf{u}_\beta)$: covariance between a variable at locations $\mathbf{u}_\alpha$ and $\mathbf{u}_\beta$

λ : kriging weight

r_i : logratio value corresponding to the facies proportion of the i^{th} facies category

$\mathcal{S}^K$: K dimensional space of compositional data

$\mathcal{S}^{K-1}$: $K-1$ dimensional positive simplex

J : Jacobian matrix

Chapter 1 Introduction

1.1 An Overview

A basic problem in reservoir modeling is to build the 3-dimentional realizations of facies, porosity and permeability at a sufficiently detailed resolution to provide a reliable basis for well planning, volumetric calculations and meaningful effective flow properties (Deutsch, 1996). Facies are important in reservoir modeling. Porosity and permeability, are highly correlated to facies types.

Consider a three-dimensional space Ω with K facies categories $S_1, S_2, ..., S_K$. Each location $\mathbf{u}_\alpha$ in the space corresponds to a facies category, that is, a set of indicator variables $I(\mathbf{u}_\alpha, k)$ $(k = 1, 2, ..., K)$, such that

$$I(\mathbf{u}_\alpha, k) = \begin{cases} 1 & \text{if facies at } \mathbf{u}_\alpha \text{ is } S_k \\ 0 & \text{otherwise} \end{cases}.$$

Such facies indicator variables are mutually exclusive and exhaustive (Deutsch, 2002), that is, for any location $\mathbf{u}_\alpha$, the following is satisfied:

$$\begin{cases} I(\mathbf{u}_\alpha, k) \cdot I(\mathbf{u}_\alpha, k') = 0 & \text{for all } k \neq k' \\ \sum_{k=1}^{K} I(\mathbf{u}_\alpha, k) = 1 \end{cases}$$

Scaling up the facies categories over a neighborhood v_α of location $\mathbf{u}_\alpha$, the proportion of category S_k is obtained by:

$$P_k = P_v(\mathbf{u}_\alpha, k) = \frac{1}{v} \int_v I(\mathbf{u}_\alpha, k) dv, \quad k = 1, 2, ..., K.$$

Here in this thesis, capital P is used to denote a facies proportion variable and lower case p denotes its value. The values and distributions of proportions $P_v(\mathbf{u}_\alpha, k)$, are volume-dependent. Figure 1-1 gives a brief illustration of the volume-dependent

distribution of the facies categories and proportions.

Two important sources of data include well data and seismic data. The well data provide accurate measurements at a small scale while the seismic data approximately reflect facies proportions at a larger volumetric support. Various other sources, such as historical production data, provide information at different scales regarding the facies. Integrating data of different scales into reservoir models is a critical issue. Furthermore, based on the available data, for some locations, perfect knowledge is available about the facies categories and proportions. But for other locations, we must treat the facies categories and facies proportions as uncertain. Estimating the multiscale distribution of facies categories and proportions and drawing realizations from these distributions is important in reservoir modeling.

This thesis focuses on three problems regarding the multiscale facies modeling: 1) A discussion on the order relation constraints and the validity of logratio transformation in multiscale facies modeling; 2) Parametric fitting of marginal and multivariate distribution of facies proportions over various volumetric scale; and 3) Application of parametric facies distributions in reservoir modeling. The topic of each subsequent chapter is as follows:

Chapter 2. Order Relations and Logratios

Chapter 3. Analytical Fits of the Multivariate Distributions of Facies Proportion

Chapter 4. Volume Dependent Distribution of Facies Proportions Based on Ordinary Beta

Chapter 5. An Application of Multiscale Facies Model

Chapter 6. Further Discussions of Multiscale Facies Modeling

Chapter 7. Conclusions and Future Works

1.2 Literature Review

Much research has been carried out regarding volume dependent distributions of facies proportions, particularly related to scaling laws governing the changes in means,

variances, covariances and variograms of facies proportions based on different volumetric supports. Some of the important previous works include:

1. Journel and Huijbregts (1978) developed a series of theoretical concepts and theorems that are widely applied as scaling laws of categorical variables in geostatistical study: For scaled up variable Z_v, volumetric support variogram $\gamma_v(\mathbf{h})$ is defined as:

$$\gamma_v(\mathbf{h}) = \frac{1}{2} E\left\{[Z_v(\mathbf{u}) - Z_v(\mathbf{u}+\mathbf{h})]^2\right\} \quad \text{where} \quad Z_v(\mathbf{u}) = \frac{1}{v}\int_{v(\mathbf{u})} Z(y)dy .$$

Given two different volumetric supports v and V and the entire space of interest Ω, three important concepts: dispersion variance $D^2(v,V)$, average variogram $\overline{\gamma}(v,V)$ and average covariance $\overline{C}(v,V)$ were defined and the following relationships were shown:

$$D^2(v,\Omega) = D^2(V,\Omega) + D^2(v,V) \qquad (\ v \subset V \subset \Omega \ )$$

and

$$D^2(v,V) = \overline{C}(v,v) - \overline{C}(V,V) = \overline{\gamma}(V,V) - \overline{\gamma}(v,v) .$$

The changes in variograms were shown predictable via a variance-variogram model.

2. C. V. Deutsch and P. Frykman (1999) gave a full discussion on semivariogram modeling at different volumetric support as well as sequential simulation based on multiscale data: the fitted variogram model at arbitrary scale v is defined as

$$\gamma_v(\mathbf{h}) = C_v^0 + \sum_{i=1}^{nst} C_v^i \Gamma^i(\mathbf{h})$$

where $\Gamma^i(\mathbf{h})$ represents i^{th} nested structure, *nst* the total number of nested structures, C_v^0 the nugget effect and C_v^i the variance contribution the i^{th} nested structure. The sum of variance contribution equals the dispersion variance; the range of the volumetric supported variogram at a larger volume V increases as the increase in volume size ($|V| - |v|$) in each particular direction; depending on the shape of large volume V, the range may increase in some directions and stay the same in other directions; the purely

random component, the nugget effect, decreases with an inverse relationship of the volume; the changes (decreases) variance contribution of each nested structure along with supporting volumes are determined by the average variogram $\bar{\Gamma}$ calculated from the nested structure Γ^i.

3. Two basic categories of algorithms are used in mapping the facies codes and proportions over a 3-dimentional space: 1) Estimation or interpolation algorithms, as named by Xu et al (1992), yield a unique response that is best in some sense. Krigings of different types form a critical family in this category. 2) Simulation, or stochastic imaging (Xu et al , 1992), provides multiple realizations of the variable of interest.

Kriging algorithms are widely used to map the facies based on well data and seismic data. Kriging with external drift, kriging with locally varying mean, block kriging and collocated cokriging are some commonly used variants. Simulation is closely related to kriging. Usually, a certain type of kriging (or cokriging) approach is used to build the conditional distribution of a variable at a certain location based on the known data, and realizations are then drawn from the conditional distribution.

Sequential simulation (Deutsch and Journel, 1998) is an effective approach in modeling the spatial distribution of facies. In the sequential simulation approach, the attributes at different locations are treated as a set of jointly distributed variables. The local distribution at each location is built based on the values of available data as well as those of related covariates. Two widely used simulation techniques for facies variables are sequential indicator simulation (sisim) (Deutsch and Journel, 1998) and truncated Gaussian simulation (Deutsch, 2002). In truncated Gaussian simulation, the local facies data are transformed to continuous Gaussian conditional data and threshold of the k^{th} facies $y_k^l(\mathbf{u})$ is set by the cumulative facies proportion $cp_k(\mathbf{u})$ as $y_k^l(\mathbf{u}) = G^{-1}(cp_k(\mathbf{u}))$. Gaussian simulation approach is applied and the threshold values are used to assign the facies categories according to the simulated value. The truncated Gaussian approach works well when facies are ordered while sisim works better in case

there is no clear ordering. Deutsch (2005) developed an advanced indicator simulation program BlockSIS that integrates data of different scales in simulating the facies categories at desired local points.

In most cases, the kriging or cokriging algorithm gives estimates of the means of facies proportions but not the estimates of facies proportions themselves. Building distributions of facies proportions conditioning on the estimated means and simulating realizations from these distributions remains a problem. Some parametric fits of the distributions of facies variables over various volumetric supports as well as an algorithm to sample from the distributions will be developed.

1.3 A Brief Description of Facies Proportion Distribution with an Introductory Example

Consider a facies category training image over a three-dimensional space 256×256×128 in terms of x×y×z coordinates. There are five facies categories, S_0, S_1, S_2, S_4 and S_5. Figure 1-2 gives the slice maps along the planes x=50, y=50 and z=50. Figure 1-3 gives the maps of the vertical facies proportions over the horizontal area. In this training image, S_0, S_1 and S_2 are the three most important categories and their proportions sum to over 90% in most of the area. Categories S_4 and S_5 take very small part.

The space is divided into blocks of equal scale using sizes of 2×2×2, 4×4×4, 8×8×8, 16×16×16, 32×32×32 and 64×64×64 and the proportion of each facies category is calculated for each block.

The following properties can be observed regarding the volume dependent facies proportion distribution:

1) Maps

Figure 1-4 gives the pixel plots of facies proportions P_0 at various volumetric

supports. At small scale, the values of the facies proportions are mostly 0 or 1. As the volumetric support increases, more and more possible values for the facies proportions P_0 occur. The true facies becomes a proportion and not a single category.

2) Continuity and Shapes:

At small scale, the facies proportions have a discrete and bimodal distribution. As the scale increases, the distributions turn to continuous, unimodal and symmetric. At scale of $v = l_1 \times l_2 \times l_3$, the facies proportions take values from the set $\left\{0, \frac{1}{v}, \frac{2}{v}, ..., 1\right\}$. Specifically, at scale of 2×2×2, the facies proportions take some values among $\left\{0, \frac{1}{8}, \frac{1}{4}, \frac{3}{8}, \frac{1}{2}, \frac{5}{8}, \frac{3}{4}, \frac{7}{8}, 1\right\}$. As the scale increases, a more continuous group of values is reached. Looking at the histograms in Figures 1-5 and 1-6, obvious bimodal distributions of facies proportions P_0 and P_2 are observed at a small scale and the distributions appear discrete. As the volumetric scale increases, more continuous distributions appear and the shapes change to unimodal but skewed. Finally, at some scale of volumetric support it becomes symmetric. Based on the central limit theorem, for a random sample, as the sample size increases, the sum, or equivalently the mean, of the sample indicator values will converge to a normal distribution. The facies categories or facies proportions are spatially correlated. Nevertheless, the central limit theorem will still partially effect the distribution of scaled up facies proportions.

The marginal cumulative distribution function (CDF) curves give us a clear picture about the continuity and shape. Figure 1-7 shows the marginal CDF curves for facies S_0 for various volumetric scales. At a small volumetric scale, the curves are discontinuous and they become more continuous as the scale increase. At the scale of $64 \times 64 \times 64$, the CDF curve is close to normal.

The change of the distribution with scales is also shown in Figure 1-12. Here, p is

the prior global proportion of the facies category. The value and distribution of P_k depend on the scale of supporting volume v. For $v=0$, $P_k = I(\mathbf{u},k)$ is an indicator variable that equals either 1 or 0, and $\text{Prob}[P_k=0]=1-p$, $\text{Prob}[P_k=1]=p$. The cumulative distribution function (CDF):

$$F_k(x)=\text{Prob}[P_k \le x]=\begin{cases}1-p & \forall 0 \le x<1 \\ 1 & \text{for } x \ge 1\end{cases},$$

see the red curve in the left of Figure 1-12. For $v=\infty$, the proportion $P_k = p$, and the CDF:

$$F_k(x)=\text{Prob}[P_k \le x]=\begin{cases}0 & \forall x<p \\ 1 & \forall x \ge p\end{cases},$$

as illustrated by black curve in the left of Figure 1-12. The right of Figure 1-12 shows how the distribution of facies proportion P_0 changes between these two extreme cases along with volumetric scales.

3). Moments: Means, variances and covariances:

Given a certain scale v, where n individual points are located in each block. The proportion $P_v(\mathbf{u}_\alpha,k)$ of facies category S_k can be defined as:

$$P_v(\mathbf{u}_\alpha,k)=\frac{1}{n}\sum_{i=1}^{n} I(\mathbf{u}_\alpha^i,k),\ k=1,2,...,K$$

Suppose the entire space of interest is divided into m blocks of the same size, then mean of the proportion P_k can be obtained by :

$$E[P_v(k)]=\frac{1}{m}\sum_{\alpha=1}^{m}\frac{1}{n}\sum_{i=1}^{n} I(\mathbf{u}_\alpha^i,k)=\frac{1}{m}\frac{1}{n}\sum_{\alpha=1}^{m}\sum_{i=1}^{n} I(\mathbf{u}_\alpha^i,k)=\frac{1}{mn}\sum_{l=1}^{mn} I(\mathbf{u}^l,k)=\mu_k .$$

The means of facies proportions over the entire area of interest are independent of the size of the scale and are equal to the global mean μ_k's.

The variance depends on the scale. As described above, according to the results of

Journel and Huijbregts (1978):

$$D^2(V,\Omega) = D^2(v,\Omega) - D^2(v,V) \quad \text{where} \quad v \subset V \subset \Omega.$$

Variance of the scaled up facies proportion decreases as the scale increases, with variance reduction factor defined as (Isaaks and Srivastava, 1989):

$$f = \frac{D^2(V,\Omega)}{D^2(v,\Omega)} = \frac{D^2(v,\Omega) - D^2(v,V)}{D^2(v,\Omega)} = 1 - \frac{D^2(v,V)}{D^2(v,\Omega)}$$

Taking as an example the facies category S_0, the mean and standard deviation (S.d.) of proportion P_0 are tabulated below:

Table 1-1 Mean and standard deviation of P_0 at different scales

Scale	2×2×2	4×4×4	8×8×8	16×16×16	32×32×32	64×64×64
Mean	0.6648	0.6648	0.6648	0.6648	0.6648	0.6648
S.d.	0.4514	0.4232	0.3898	0.3232	0.2419	0.1372

The mean remains unchanged over different scales and the standard deviation decreases as the scale increases.

The covariance value between two variables provides a measure of linear dependency between these two variables. Based on the training image, covariance values $C(P_k, P_{k'})$'s are calculated for all pairs of scaled up facies proportions $(P_k, P_{k'})$ with $k < k'$ and $k, k' \in \{0,1,2,4,5\}$. Most of the pairs have a negative covariance. The facies proportion variables are subject to a unit sum constraint, that is, the full set of facies proportions will sum to 1.0. In the case where only two facies categories exist, the increase in the proportion of one category will lead to a decrease in the other. In the multivariate cases, with more than two facies categories, things are more complicated but the increases in the proportion of one category will lead to the decrease of the total of others.

In Figure 1-11, the absolute values of covariances for each pair are plotted against

the volumetric support. Similar to the trend of variances, the absolute covariance values decrease along with the increase in volumetric scale.

4) Semivariogram:

The semivariogram is an important function giving the spatial relationship between two points with distance vector $\mathbf{h}$. For a fixed orientation, the variogram indicates the difference in the values at that distance. When the orientation changes, the variogram values also disclose directional anisotropy (Armstrong, 1998). The semivariogram of the facies categories and facies proportions are dependent on the volumetric support following the scaling laws as introduced above. Figures 1-8 give the semivariograms of facies proportion P_0 in x-direction (in red), y-direction (in green) and z-direction (in blue) at various scales. As the scale increases, the sill of indicator semivariogram in each direction decreases and the plots flatten, suggesting a trend of more continuity as the scale increases. The changes in ranges are not obvious in this case.

5) Unit Sum Constraint

Another property of facies proportions is their unit sum. Suppose only three facies S_1, S_2 and S_3 occur in the whole area, their proportions satisfy:

$$P_1 + P_2 + P_3 = 1 \quad \text{with} \quad P_1, P_2, P_3 \geq 0.$$

That is, all the points (p_1, p_2, p_3) lie in the plane determined by this equation, as illustrated in Figure 1-9. More precisely, suppose line segments AB, CD and EF in the plane represent the lines on which $P_1 = \max(P_1)$, $P_2 = \max(P_2)$ and $P_3 = \max(P_3)$, respectively. Then all the points (p_1, p_2, p_3) fall within the area of polygon $ABCDEF$. However, the density of the plane, that is, the frequency of each group of (p_1, p_2, p_3) is not even and is dependent on the volumetric support. Generally, suppose there are K facies categories $S_1, S_2, \ldots, S_K$ in the area of interest, the point $(p_1, p_2, \ldots, p_K)$ will fall on a hyperplane determined by equation:

$$P_1 + P_2 + ... + P_K = 1$$

Again, the density of the hyperplane depends on the volumetric support.

In Figure 1-10, the plots of the facies proportions of three synthetic categories from the training image are given. Here P_0 remains unchanged, P_1 and P_2 are combined and so are P_4 and P_5, denote as P_1P_2 and P_4P_5 respectively. At point scale, only 0 or 1 value occurs and the plots lie on the axis for each facies category.

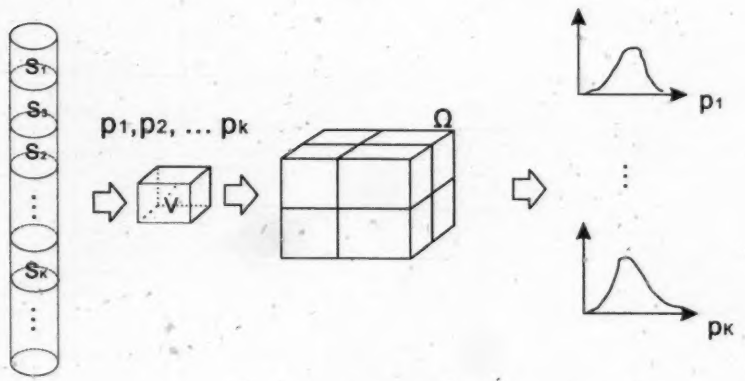

Figure 1-1 Multiscale facies modeling

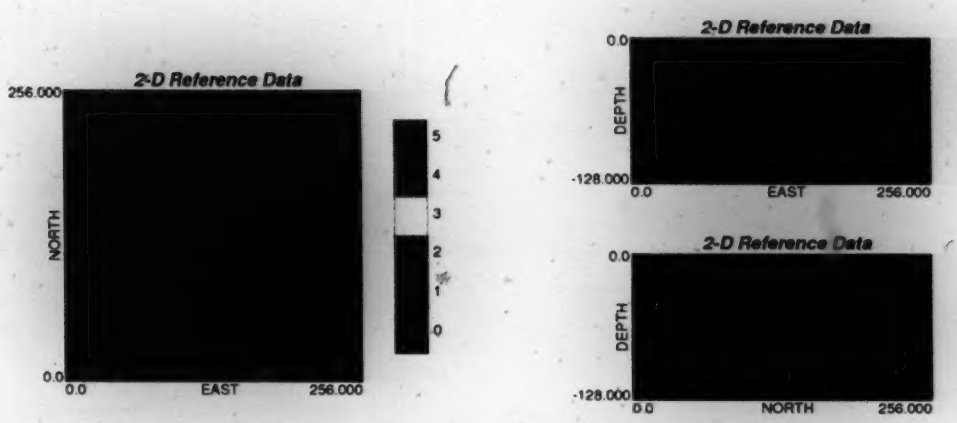

Figure 1-2 Slice maps of facies categories

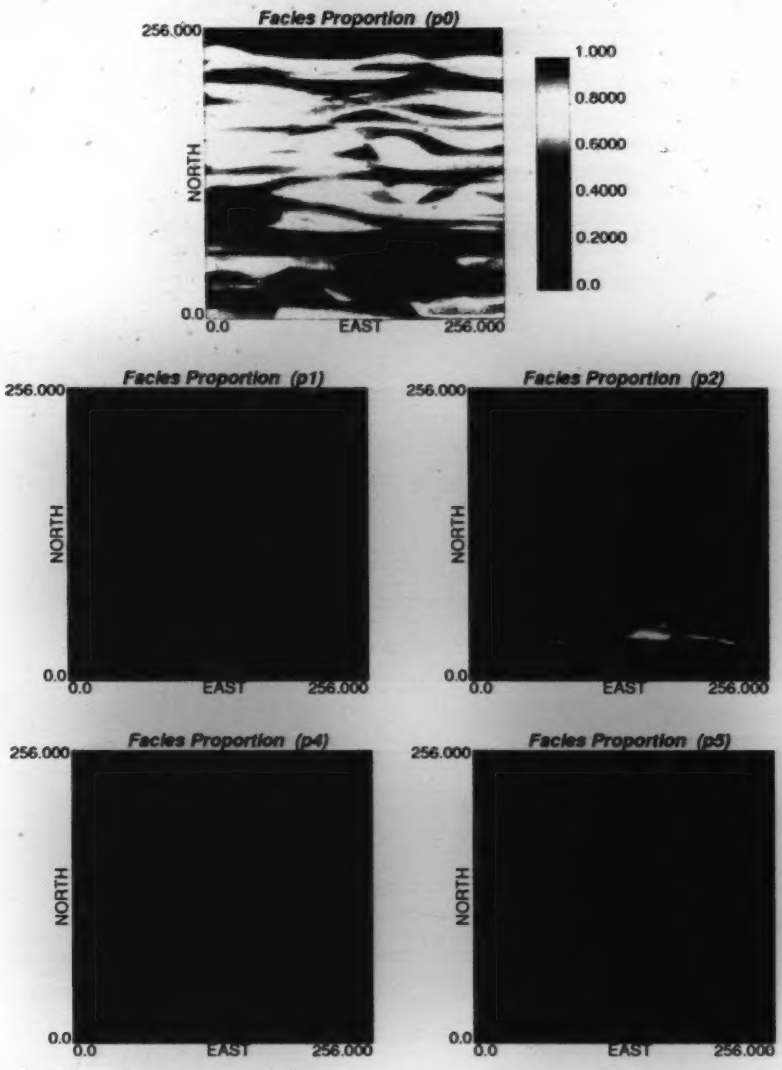

Figure 1-3 Facies proportion maps

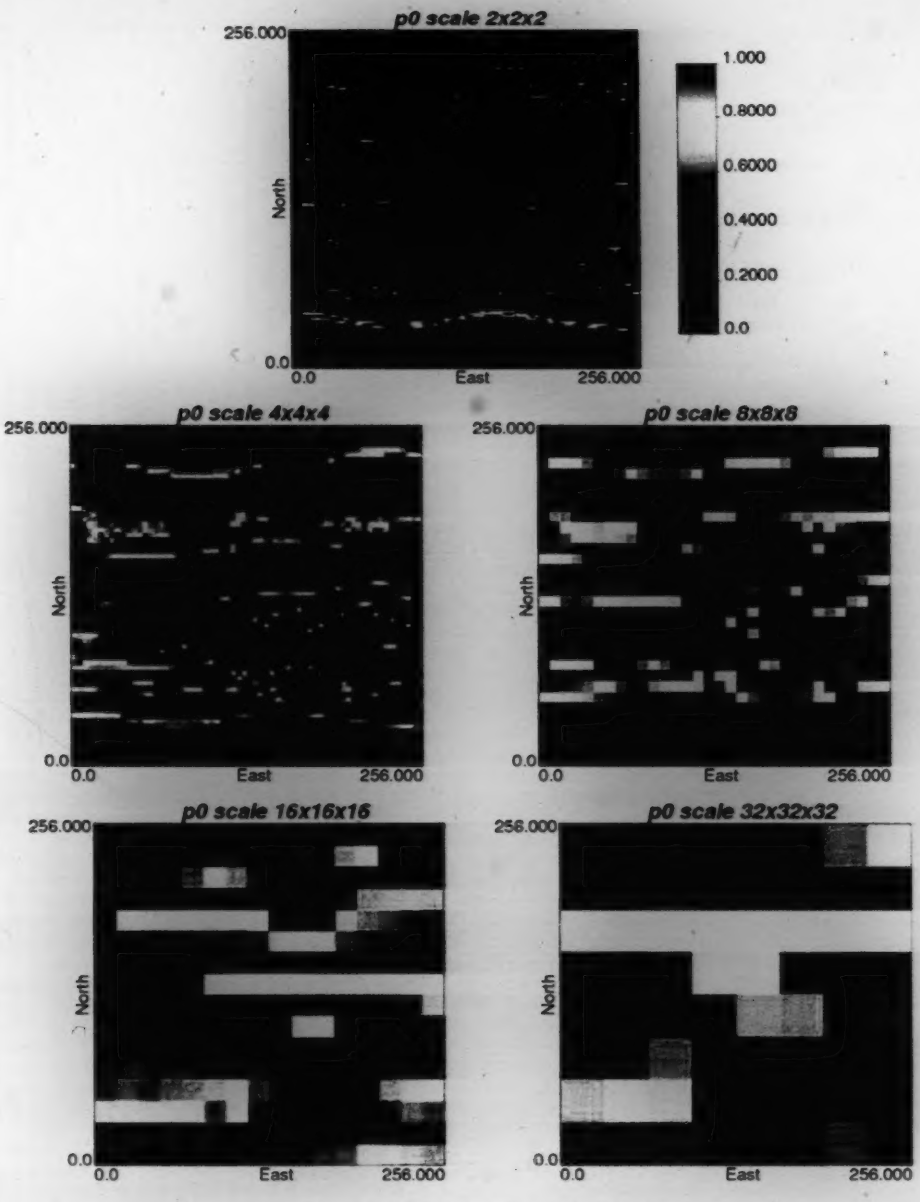

Figure 1-4 Scaled up facies proportions

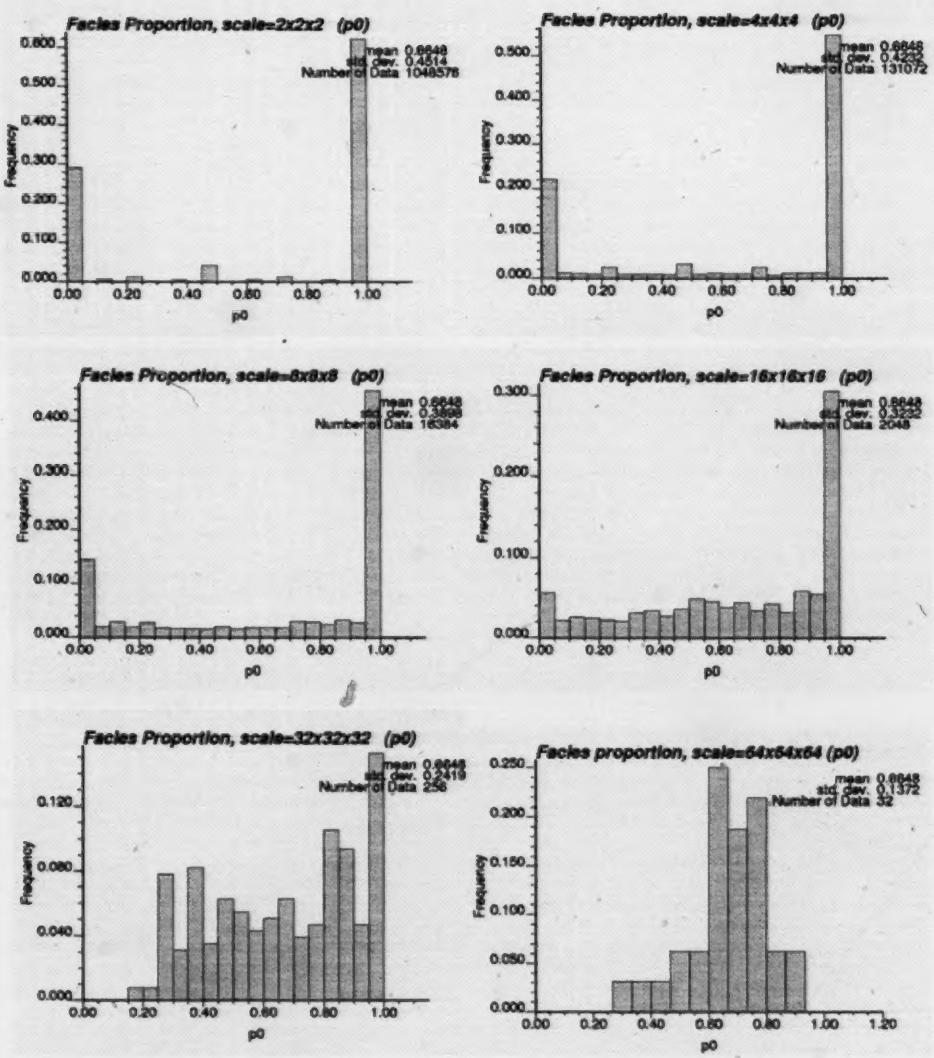

Figure 1-5 Facies proportion of S_0 over different scales

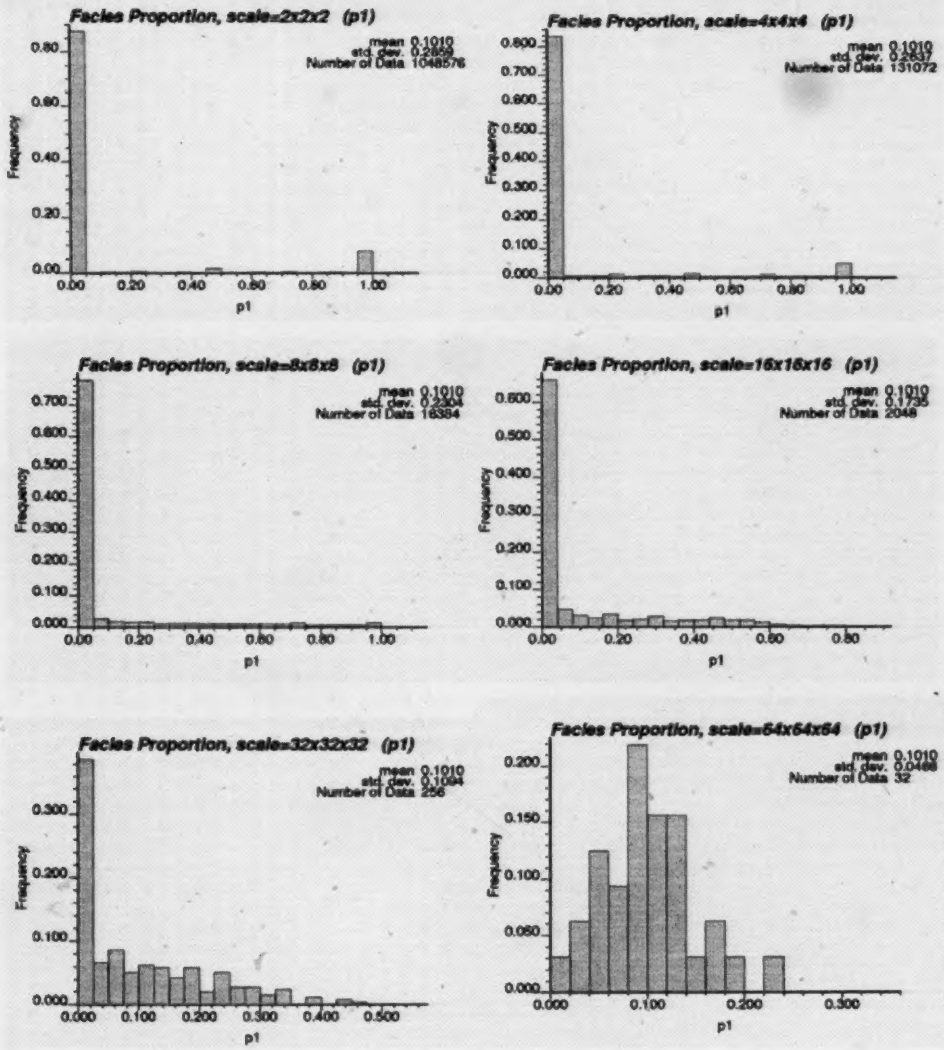

Figure 1-6 Facies proportion of S_1 over different scales

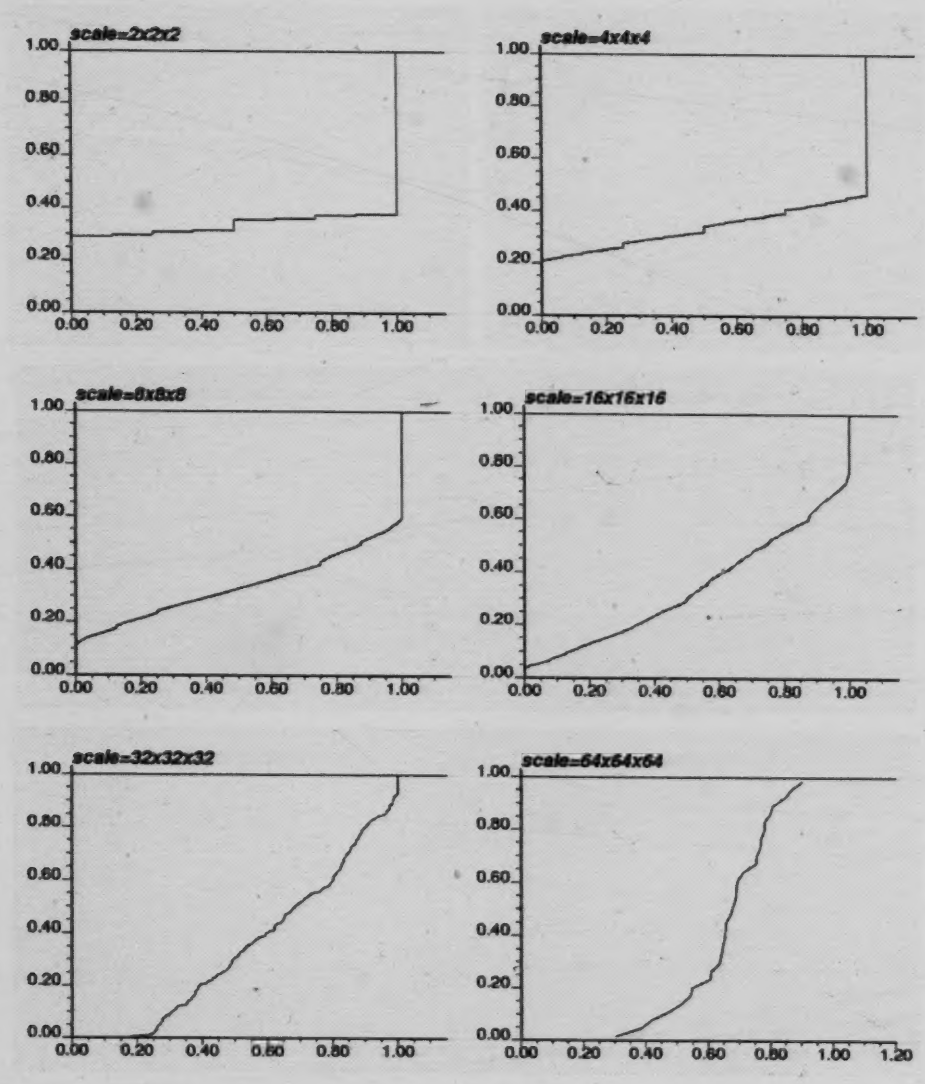

Figure 1-7 Cumulative distribution of proportion of S_0 over different scales

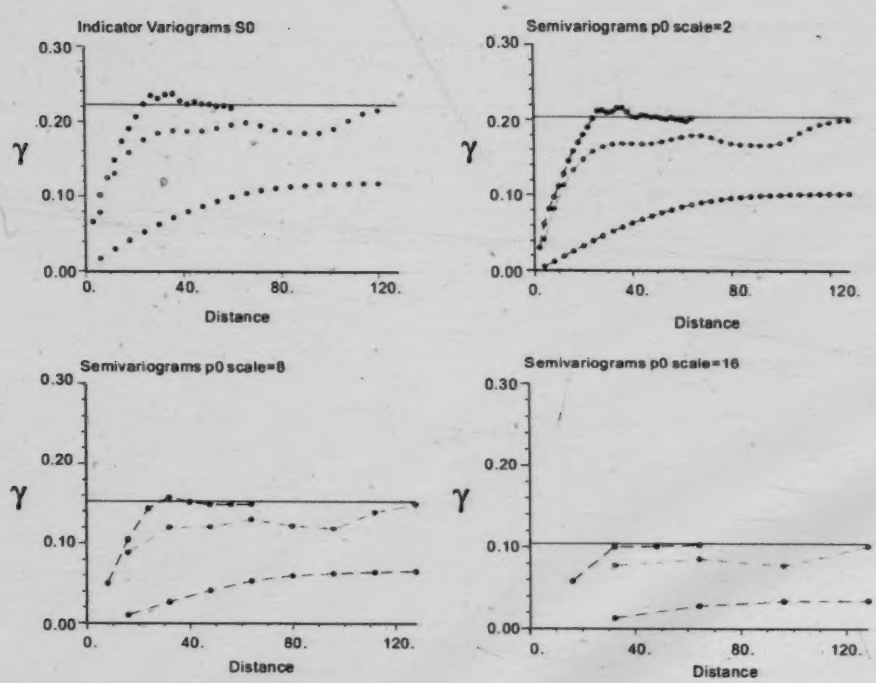

Figure 1-8 Semivariograms of facies proportion for S_0 at various scales.

(X-direction: in red. Y-direction: in green. Z-direction: in blue.)

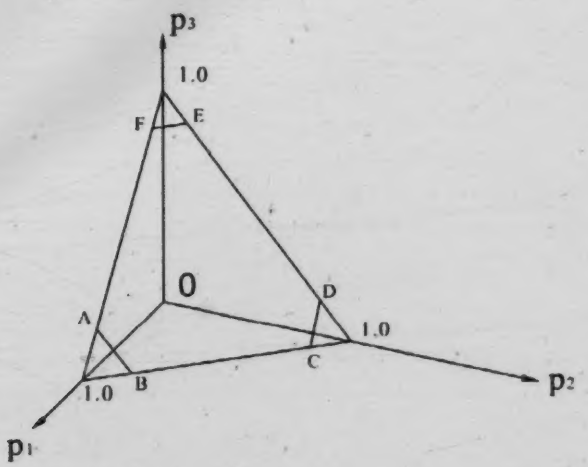

Figure 1-9 Facies proportion distribution

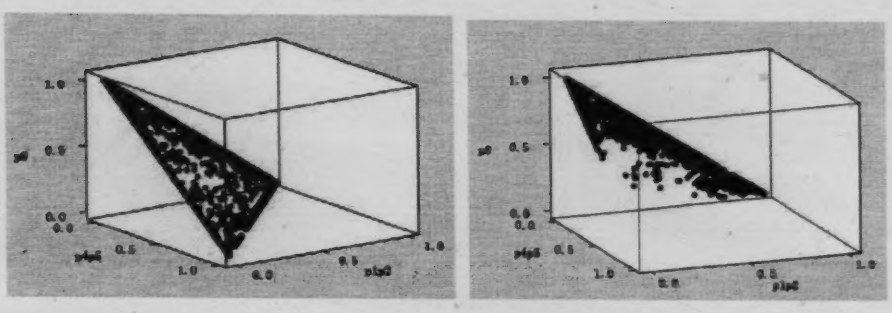

Figure 1-10 Combined facies proportions (left: scale 4x4x4, right: scale 16x16x16)

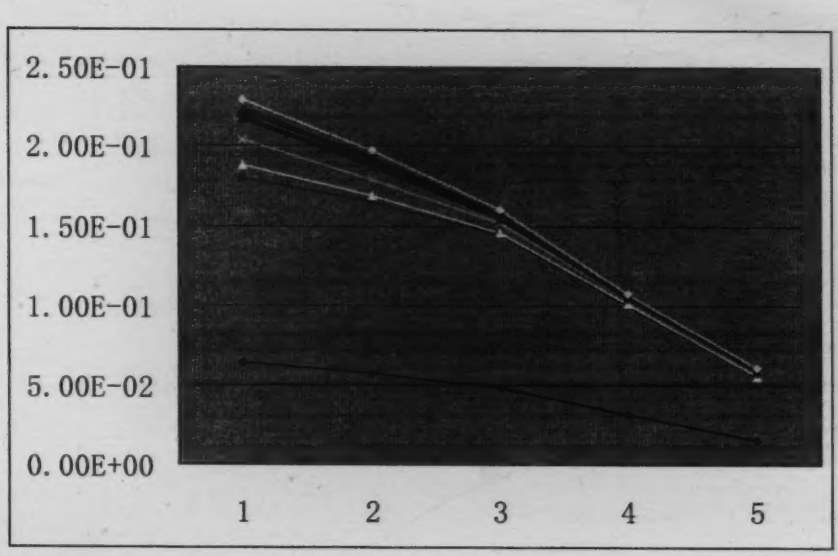

Figure 1-11 Volume dependent covariances (absolute values)

Each curve gives the covariance of one pair of facies proportions.

The horizontal axis gives the scales:

1: 2x2 x 2; 2: 4 x 4 x 4; 3: 8 x 8 x 8; 4: 16 x 16 x 16; 5: 32 x 32 x 32

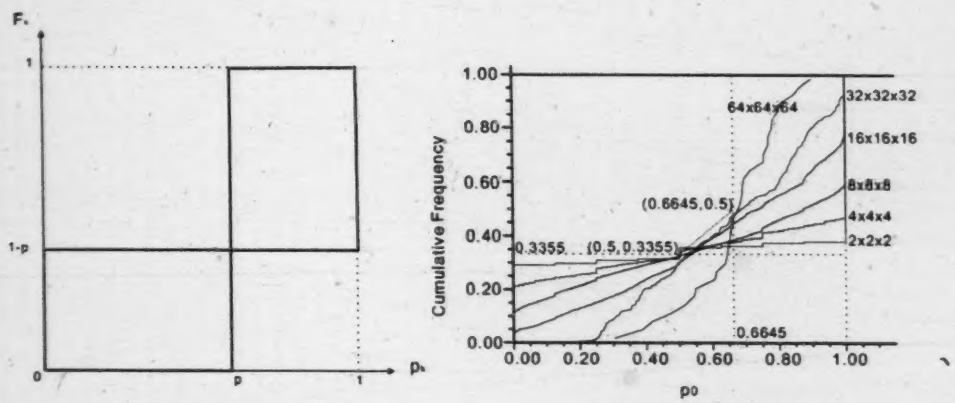

Figure 1-12 CDF's of P_k for Cases $\nu = 0$ (in red) and $\nu = \infty$ (in black)

Chapter 2 Order Relations and Logratios

2.1 Order Relations in Facies Modeling

As introduced in the previous chapter, the facies indicator variables are mutually exclusive and exhaustive, that is, for each fixed location $\mathbf{u}_\alpha$, the following constraints hold:

$$\begin{cases} I(\mathbf{u}_\alpha,k)\bullet I(\mathbf{u}_\alpha,k')=0 & \text{for all } k\neq k' \\ \sum_{k=1}^{K} I(\mathbf{u}_\alpha,k)=1 \end{cases}$$

The scaled up facies proportions are calculated by:

$$P_v(\mathbf{u}_\alpha,k)=\frac{1}{v}\int_v I(\mathbf{u}_\alpha,k)dv,\ \ k=1,2,...,K,$$

for any given location $\mathbf{u}_\alpha$, the following constraints must be satisfied:

$$\begin{cases} 0\le P_v(\mathbf{u}_\alpha,k)\le 1 \quad \text{for all } k \text{ in } 1,2,...,K \\ \sum_{k=1}^{K} P_v(\mathbf{u}_\alpha,k)=1 \end{cases}$$

This is called the order relation restriction (Deutsch, 2002).

In facies modeling, data of facies indicator or facies proportions are used to estimate the facies categories or proportions at the desired local point or block locations, using various kriging and simulation methodologies. Take as an example the simple indicator kriging algorithm:

$$p^{SK}(\mathbf{u},k)=\sum_{\alpha=1}^{n}\lambda_\alpha^{SK} I(\mathbf{u}_\alpha,k)+(1-\sum_{\alpha=1}^{n}\lambda_\alpha^{SK})p(k)\quad k=1,2,...,K.$$

This is a linear combination of the known facies indicators with the weights minimizing the kriging error with the following kriging system:

$$\sum_{\beta=1}^{n}\lambda_\beta^{SK} C_I(\mathbf{u}_\alpha-\mathbf{u}_\beta)=C_I(\mathbf{u}-\mathbf{u}_\alpha),\quad \alpha=1,2,...,n$$

Kriging minimizes the kriging error with no constraint on the range and sign of the kriging weights or estimate. It is possible to have a negative estimate or an estimate

greater than 1.0.

The violation of order relation constraints has long been a critical issue in facies modeling. Various approaches have been proposed to solve this problem, the following are two of the important methods:

Compositional kriging (CK) suggested by Dennis et al (2001). This is a straightforward extension of ordinary kriging, with two additional constraints inserted:

$$\begin{cases} \sum_{\alpha=1}^{n} \lambda_{\alpha}^{CK} I(\mathbf{u}_{\alpha}, k) \geq 0 \quad k = 1, 2, ..., K \\ \sum_{k=1}^{K} \sum_{\alpha=1}^{n} \lambda_{\alpha}^{CK} I(\mathbf{u}_{\alpha}, k) = 1 \end{cases},$$

and satisfies the order relation rules. Each constraint is connected to a corresponding Lagrange multiplier. The kriging weights are estimated by minimizing the kriging variance subject to all the constraints. And kriging estimator is expressed as:

$$p^{CK}(\mathbf{u}, k) = \sum_{\alpha=1}^{n} \lambda_{\alpha}^{CK} I(\mathbf{u}_{\alpha}, k) \quad k = 1, 2, ..., K$$

Another important alternative is Posteriori processing (Deutsch, 2002). Here the kriging estimated facies probability $\hat{p}_{iv}^{IK}$ at the unsampled location $\mathbf{u}_v$ is set to zero if it is negative and the estimated facies probability is adjusted to $\hat{p}_{iv}^{*}$ as below:

$$\hat{p}_{iv}^{*} = \frac{\hat{p}_{iv}^{IK}}{\sum_{j=1}^{k} \hat{p}_{iv}^{IK}}, \qquad i = 1, 2, ..., k$$

Now the order relation requirements are satisfied. A relative adjustment is made on the Sequential Indicator Simulation procedures by adding the correction after indicator kriging.

The use of logratio transformation of the facies is another possible choice and it is attracting the interest of geostatisticians due to its special properties.

2.2 Logratio Formalism

Logratio approach is a methodology in analysis of compositional data. According to the definition by Aitchison (1986), the compositional data give sample values of a

K dimensional space

$$\mathcal{S}^K = \left\{ \mathbf{p}^K = (P_1, P_2, ..., P_K) : P_i \geq 0 \ (i = 1, 2, ..., K), \sum_{i=1}^{K} P_i = 1 \right\}$$

that is often described by a $K-1$ dimensional positive simplex:

$$\mathcal{S}^{K-1} = \left\{ \mathbf{p}^{K-1} = (P_1, P_2, ..., P_{K-1}) : P_i \geq 0 \ (i = 1, 2, ..., K-1), \sum_{i=1}^{K-1} P_i \leq 1 \right\},$$

and the K^{th} variable is determined directly by

$$P_K = 1 - \sum_{k=1}^{K-1} P_k .$$

The positive simplex $\mathcal{S}^{K-1}$ form a principle component of compositional data base $\mathcal{S}^K$. Facies indicators and facies proportions variables make a typical compositional data.

A Logratio value, denoted by r_i, for the facies proportion p_i is defined as:

$$r_i = \log[\frac{p_i}{p_q}], \ \ i = 1, 2, ..., q-1, q+1, ..., k$$

where the denominator p_q can be any fixed one proportion among $p_1, ..., p_k$. The reverse from r_i to p_i is given by:

$$p_i = \frac{\exp(r_i)}{1 + \sum_{t=1, t \neq q}^{k} \exp(r_t)} \quad \text{for} \ \ i = 1, 2, ..., q-1, q+1, ..., k$$

and

$$p_q = \frac{1}{1 + \sum_{t=1, t \neq q}^{k} \exp(r_t)}$$

Directly from the above formulas, the constraints $0 \leq p_i \leq 1$ and $\sum_{i=1}^{k} p_i = 1$ hold for any given set of $\{r_1, ..., r_{q-1}, r_{q+1}, ..., r_k\}$ and thus the order relation requirements are satisfied.

Aitchison (1986) gave a detailed introduction on the logratio analysis for

compositional data. Some natures of the logratio transformation are worthy for its application in modeling and analysis on the compositional data:

First of all, there is a one-to-one correspondence between the original data $(p_i,\ldots,p_k)$ and the logratio vector $(r_1,\ldots,r_{q-1},r_{q+1},\ldots,r_k)$, therefore any statement in terms of logratios can be expressed as an equivalent statement in terms of raw components (Aitchison, 1986).

Secondly, logratio inference obtained from any subcompsition $(p_{(1)},\ldots,p_{(d)})$, $(d \le k)$, from the parent composition $(p_i,\ldots,p_k)$ will be exactly the same as the inference from the parent composition provided that the same component is applied as the denominator.(Aitchison, 1986). Suppose $x_i,\ldots,x_k$ denote, respectively, number of samples belong to facies $S_1,S_2,\ldots,S_k$ in an area; and $x_{(1)},\ldots,x_{(d)}$ denote, respectively, number of samples belong to facies $S_{(1)},\ldots,S_{(d)}$ and $\{S_{(1)},\ldots,S_{(d)}\} \subseteq \{S_1,\ldots,S_k\}$. Then logratio r_i for $\{S_1,\ldots,S_k\}$ is

$$r_i = \log\left([\tfrac{x_i}{\sum_{t=1}^{k} x_t}] / [\tfrac{x_q}{\sum_{t=1}^{k} x_t}] \right) = \log \tfrac{x_i}{x_q};$$

and for $\{S_{(1)},\ldots,S_{(d)}\}$, we have

$$r_{(i)} = \log\left([\tfrac{x_{(i)}}{\sum_{t=1}^{d} x_{(t)}}] / [\tfrac{x_{(q)}}{\sum_{t=1}^{d} x_{(t)}}] \right) = \log \tfrac{x_{(i)}}{x_{(q)}}.$$

$r_{(i)} = r_i$ whenever $S_{(i)} = S_i$ and $S_{(q)} = S_q$. This allows us to apply logratio analysis on any known facies collection over an area when we don't know exactly how many facies occur in the area.

Furthermore, the logarithmic operation on the ratio $\frac{P_i}{P_q}$ often leads to a set of approximately normally distributed variables that possess approximate linear relationships, making it possible to apply linear regression and linear contrast approach to

analyze and model the facies data.

Finally, the covariance structure of the original compositional data can be expressed in terms of a logratio covariance structure, determined by matrix

$$\Sigma = [\mathrm{cov}\{\log(P_i / P_q), \log(P_j / P_q)\}] \quad i, j = 1, 2, ..., k$$

Details about the logratio covariance structure were discussed by Aitchison (1986).

Due to the above characteristics, logratio transformations and modeling are frequently applied in compositional data analysis in various fields such as ecology, geology and environmental science, where original compositional data are transformed to logratio values. Then a series of statistical analysis will be applied on the logratio data:

A linear or non-linear model can be built regarding the logratio values and against a series of regressor variables acting as factors that will determine the compositional variable. In this way, the conditional logratio values can be estimated based on the given regressor variables and the significance of each regressor can be tested. The fitted logratio values can be back transformed to get the estimated compositional value given the values of regressors.

2.3 Application of Logratios to Facies Modeling

Facies indicators or proportions at un-sampled locations are estimated or simulated according to the facies data. The application of the Logratio formalism in facies modeling is straight forward. For kriging, the following steps are applied:

- Facies proportions are transformed to Logratio data and semivariogram models are built based on logratio transformed data,
- Logratio values at unsampled locations estimated by kriging,
- Estimated logratio value back transformed to get estimated facies proportions at the unsampled location.

The procedures below will be followed in sequential indicator simulation:

- The entire space is gridded and all the grid nodes are visited with a random path,

- For each of the randomly visited grid nodes, logratio values are estimated by kriging and back transformed to get the estimated facies proportions. The local conditional CDF (CCDF) of the facies is built based on the estimated facies proportions.
- Facies category is drawn and assigned to the grid node based on this local CCDF.

Two critical problems are hard to avoid and lead to fatal risks in facies modeling and analysis when logratios are used. They are 1) zero proportion problem, and 2) problem of non-linearity.

2.4 Problem of Zero Proportions

As discussed above, for any location, an indicator $I(i,\mathbf{u}_\alpha)$ is defined as:

$$I(i,\mathbf{u}_\alpha)=\begin{cases}1 & \text{if facies } \mathbf{u}_\alpha \text{ is } S_i \\ 0 & \text{otherwise}\end{cases}$$

And the facies proportion can be scaled up to a particular volume of support. A zero proportion of a particular facies category is common, especially when the scaled up facies proportion is calculated at a small scale where only one or several facies categories may occur and the rest will not. A zero value in either the denominator or numerator of $\frac{p_i}{p_q}$ will lead to an undefined logratio value. One way to solve this problem is to apply some arbitrary small values, such as 10^{-5} or 10^{-20}, in place of the zero facies proportions.

Another problem then arises: different values, such as 10^{-5} or 10^{-20}, lead to quite different logratio values. Using such values into kriging or simulation will lead to different estimation results. A number of tests show that the gaussian or uniform score transformation of logratios may partially solve the problem.

2.5 Non-linearity Problems

In multiscale facies modeling, facies categories are scaled up to facies proportions by the arithmetic average at various volumetric supports. Kriging approaches are applied to estimate facies proportions at unsampled locations based on the sampled data. Each of these involves a linear average of the data. However, the logratio transformation is not a linear transformation of the original values. That is,

$$a\log\left(\frac{p_i}{p_q}\right)+b\log\left(\frac{p_j}{p_q}\right)\neq\log\left(a\cdot\frac{p_i}{p_q}+b\cdot\frac{p_j}{p_q}\right).$$

Therefore, back transformation of either the means (arithmetic average) or kriging estimates of logratio values will not reach a valid result.

2.5.1 Problems in block means estimation

From the formula of inverse of logratio values:

$$\hat{\bar{p}}_i=\frac{\exp(\bar{r}_i)}{1+\sum_{t=1,t\neq q}^{k}\exp(\bar{r}_t)}\quad\text{for}\quad i=1,2,...,q-1,q+1,...,k$$

and

$$\hat{\bar{p}}_q=\frac{1}{1+\sum_{t=1,t\neq q}^{k}\exp(\bar{r}_t)}$$

we have

$$\bar{r}_i=\frac{1}{n}\sum_{\alpha=1}^{n}r_{i\alpha}=\frac{1}{n}\sum_{\alpha=1}^{n}\log\frac{p_{i\alpha}}{p_{q\alpha}}=\log\sqrt[n]{\prod_{\alpha=1}^{n}\frac{p_{i\alpha}}{p_{q\alpha}}}=\log\frac{\dot{p}_i}{\dot{p}_q},$$

$$(i=1,2,...,q-1,q+1,...,k)$$

reversed and finally reach

$$\hat{\bar{p}}_i=\frac{\dot{p}_i}{\sum_{t=1}^{k}\dot{p}_t}\quad\text{for}\quad i=1,2,...,k$$

with $p_{i\alpha}$ the proportion of the i^{th} facies at position $\mathbf{u}_\alpha$ ($\alpha = 1,2,...,n$), $\dot{p}_i$'s the geometric average of $p_{i\alpha}$'s in the sample. That is, back-transforming the arithmetic average of logratio values will finally reach a standardized geometric average of the proportions, rather than the arithmetic average of the facies proportions.

The nonlinearity problem can be illustrated through a small example. Assume there are only two facies and take two samples from locations $\mathbf{u}_1$ and $\mathbf{u}_2$ with proportions for facies 1 at these two sample locations as p_{11} and p_{12} respectively. The percentile contours in Figure 2-1 (solid curves) are obtained by plotting the points of all the possible combinations of proportions p_{11} and p_{12} that result at the same estimated proportion $\hat{\bar{p}}_1$ after back transformation of the mean logratios. Comparing these contours with the dot lines in Figure 2-1, which represents the percentile contours of arithmetic average, an obvious nonlinearity nature of the logratio reversed proportions $\hat{\bar{p}}_1$ is shown.

The differences (errors) between the estimated $\hat{\bar{p}}_1$ and the true $\bar{p}_1$ (that is: $\bar{p}_1 - \hat{\bar{p}}_1$) are obvious. Figure 2-2 gives the map of the errors versus p_{11} and p_{12} while Figure 2-3 gives the curves showing a series of the errors versus p_{11} for each $p_{12} \in \{0.05,0.1,0.15,...,0.95\}$. These two figures show that the difference increases symmetrically as p_{11} and p_{12} diverge from 0.5. By the way, in Figure 2-3, when p_{11} takes values less than 0.1 or greater than 0.9, the error will go up to ± 0.5.

Parametrically,

$$\hat{\bar{p}}_i = \frac{\dot{p}_i}{\dot{p}_1 + \dot{p}_2} \quad (i = 1,2).$$

Given a fixed estimated value $\hat{\bar{p}}_1 = a$, then

$$p_{12}=\frac{1-p_{11}}{1+\frac{1-2a}{a^2}\cdot p_{11}}=\frac{1-p_{11}}{1+\xi\cdot p_{11}} \text{ with } \xi=\frac{1-2a}{a^2}.$$

Note that $\xi=0$ if and only if $a=0.5$. Given a fixed estimated value a for the logratio reversed estimated proportion, the relation of the two sample proportion values p_{11} and p_{12} for facies 1 are nonlinear unless $a=0.5$. This is shown in Figure 2-1.

As will be further discussed in later chapters, scaled-up proportions at certain volumetric support are often estimated directly based on the available point and block data. Applying logratios in either up-scaling or down-scaling process is inappropriate.

2.5.2 Problems with kriging process

The same problem will also affect the validity of kriging logratios. Taking ordinary kriging as an example, p_{i0} (proportion for i^{th} facies at position $\mathbf{u}_0$) is estimated by:

$$\hat{p}_{i0}=\lambda_1 p_{i1}+\ldots+\lambda_n p_{in} \text{ with } \lambda_1+\ldots+\lambda_n=1$$

Similarly, the kriging estimator for logratios takes the form:

$$\hat{r}_{i0}=\lambda_1^* r_{i1}+\ldots+\lambda_n^* r_{in} \text{ with } \lambda_1^*+\ldots+\lambda_n^*=1$$

that is:

$$\hat{r}_{i0}=\lambda_1^* r_{i1}+\ldots+\lambda_n^* r_{in}=\log\frac{\prod_{\alpha=1}^{n}(p_{i\alpha})^{\lambda_\alpha^*}}{\prod_{\alpha=1}^{n}(p_{q\alpha})^{\lambda_\alpha^*}},$$

reversed and get

$$\hat{p}_{i0}^*=\frac{\prod_{\alpha=1}^{n}(p_{i\alpha})^{\lambda_\alpha^*}}{\sum_{t=1}^{k}\prod_{\alpha=1}^{n}(p_{t\alpha})^{\lambda_\alpha^*}}$$

Clearly, $\hat{p}_{i0}\neq\hat{p}_{i0}^*$ and expected value

$$E[\hat{p}_{i0}^*]=E\left[\frac{\prod_{\alpha=1}^{n}(p_{i\alpha})^{\lambda_\alpha^*}}{\sum_{t=1}^{k}\prod_{\alpha=1}^{n}(p_{t\alpha})^{\lambda_\alpha^*}}\right]\neq E[\hat{p}_{i\alpha}]=E[P_{i0}]$$

in general. Therefore, back transformation of a kriging estimated logratio value to the

original base will not lead to unbiased estimation. Such errors are hard to fix because the λ_α's and λ_α^*'s ($\alpha = 1,2,...,n$) in the above are estimated via two different linear regression models and it is difficult to identify the relationship between λ_α's and λ_α^*'s.

2.6 Summary of the Results

Although the logratio approach can guarantee nonnegative estimated facies proportions that also satisfy the unit sum constraint, using the logratio values directly to estimate and model the facies proportions will lead to significant bias. Furthermore, back transforming the arithmetic average of logratio values will lead to a result of standardized geometric average of facies proportions, completely different from the arithmetic average that is desired in up-scaling process. Also, the zero proportion problem is hard to avoid. These problems make it inappropriate to apply logratios in the multiscale facies modeling.

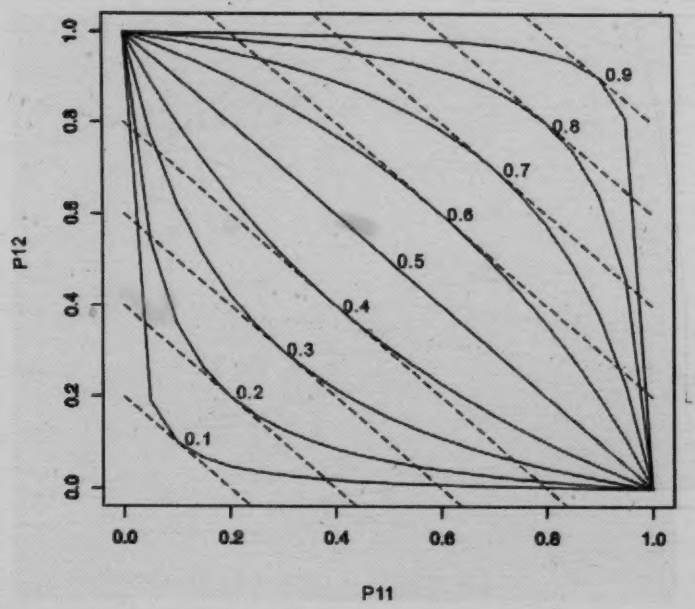

Figure 2-1 $\hat{\overline{p}}_1$ Percentile contours. Each of the solid curves is a collection of p_{11} and p_{12} that reach an identical logratio back transformed estimated facies proportion $\hat{\overline{p}}_1$. Each of the dot lines is a collection of p_{11} and p_{12} that reach an identical arithmetic average $\overline{p}_1$

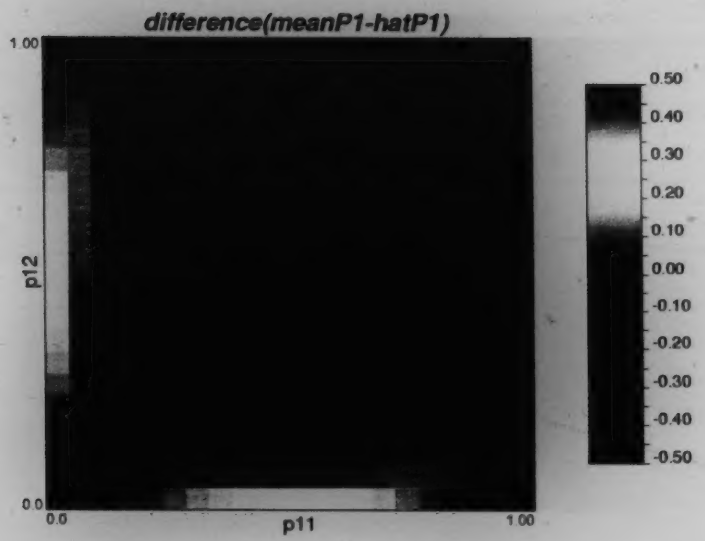

Figure 2-2 Map of differences between $\hat{\overline{p}}_1$ ("hatP1") and $\overline{p}_1$ ("meanP1")

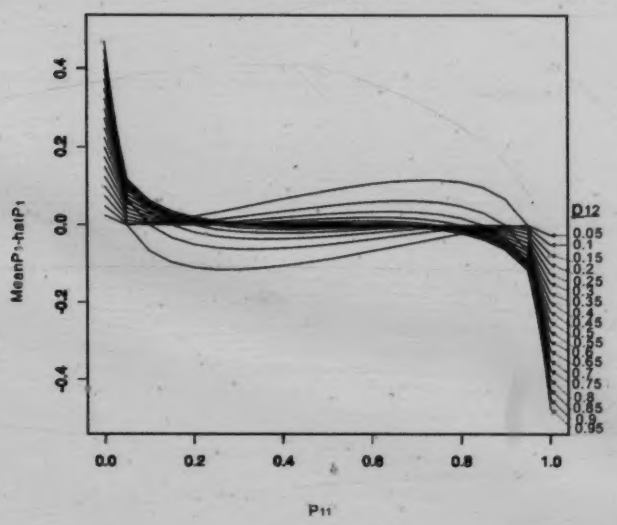

Figure 2-3 Difference between $\hat{\overline{p}}_1$ ("hatP1") and $\overline{p}_1$ ("meanP1"). Each curve represents the difference $\overline{p}_1 - \hat{\overline{p}}_1$ versus p_{11} under a distinct value of p_{12}

Chapter 3 Analytical Fit to the Multivariate Distribution of Facies Proportions

A precise understanding and estimation of the volume dependent multivariate distribution of facies proportions is the basis of multiscale facies modeling. As described in Chapter 1, when the scale increases, the facies proportions will change from a discrete bimodal distribution to a continuous unimodal distribution; the means of facies indicators and proportions will remain constant; however, the variances of facies proportions decrease along with the increase in volumetric support. The facies proportion distribution changes with volumetric support, as shown in Figure 1-12 in previous chapter.

Precisely describing and estimating the change in the multivariate distribution of facies proportions with volume is a challenge. An analytical description of the distribution of facies proportions for a fixed volumetric scale will be our first step. In this chapter, several parametric probability distributions and their fit to data are discussed and tested.

3.1 Multinomial Distribution

Consider K facies categories S_k, $k=1,2,...,K$, define variable $X_k = \sum_{i=1}^{n} I(\mathbf{u}_\alpha^i, k)$, the number of points where S_k occur within a certain block $v(\mathbf{u}_\alpha)$, and variable $P_k = \frac{X_k}{n}$ the facies proportion. Let $\tilde{p}_k$ be the prior facies proportion for category S_k. Then the following conditions are satisfied:

1) $\sum_{k=1}^{K} X_k = n$, where n is the number of grid nodes in the block

2) $\sum_{k=1}^{K} \tilde{p}_k = 1$

The above characteristics suggest a multinomial distribution of

variables $X_k, k = 1, 2, ..., K$, that is

$$\text{Prob}(X_1 = x_1, ..., X_K = x_K) = \frac{n!}{x_1! x_2! ... x_K!} \tilde{p}_1^{x_1} \tilde{p}_2^{x_2} \cdots \tilde{p}_K^{x_K}.$$

Where x_k denotes the value of variable X_k. For each individual category S_k, the marginal distribution of X_k is binomial with probability mass function (PMF) $\text{Prob}(X_k = x_k) = \binom{n}{x_k} \tilde{p}_k^{x_k} (1 - \tilde{p}_k)^{n - x_k}$. And the scaled up local facies proportion P_k follows a distribution with PMF:

$$f(y) = \text{Prob}(P_k = y) = \text{Prob}(X_k = [ny]) = \binom{n}{[ny]} \tilde{p}_k^{[ny]} (1 - \tilde{p}_k)^{n - [ny]},$$

$$y \in \left\{0, \frac{1}{n}, \frac{2}{n}, ..., 1\right\}$$

and the cumulative distribution function:

$$F(y) = \sum_{i=0}^{[ny]} \binom{n}{i} \tilde{p}_k^i (1 - \tilde{p}_k)^{n-i}, \quad y \in [0, 1]$$

where $[ny]$ is the integer part of ny.

One important assumption for the binomial distribution is that the indicator variable $I(\mathbf{u}_\alpha, k)$ and $I(\mathbf{u}_\beta, k)$ are independent from each other for any different locations $\mathbf{u}_\alpha$ and $\mathbf{u}_\beta$. However, this is not true with facies variables. See an illustration of semivariogram in Figure 3-2, those points with distance less than range a are positively correlated and those with variogram values above the sill are negatively correlated. Only those with variogram value at the sill can be considered as independent. Figure 3-1 gives the histograms from simulated multinomial realizations, which are obviously different from the true histograms. Here the parameter n denotes the volume of the scale, i.e., at scale of $2 \times 2 \times 2$, has $n = 8$.

3.2 Beta Distribution

The Beta distribution is defined for a random variable X within a closed interval [0,1] and has the probability density functions (PDF):

$$f(x)=\frac{\Gamma(\alpha+\beta)}{\Gamma(\alpha)\Gamma(\beta)}x^{\alpha-1}(1-x)^{\beta-1}$$

where the gamma function $\Gamma(z)$ is defined as $\Gamma(z)=\int_0^\infty t^{z-1}e^{-t}dt$ and has an important property:

$$\Gamma(z+1)=z\Gamma(z).$$

The shapes of the CDF curves are determined by the parameters α and β. Based on the known expected values (global mean $\tilde{p}_k$) and variances $Var_v(P_k)$, the parameters α and β are determined as:

$$\alpha=\tilde{p}_k[\frac{\tilde{p}_k(1-\tilde{p}_k)}{Var_v(P_k)}-1] \text{ and } \beta=(1-\tilde{p}_k)[\frac{\tilde{p}_k(1-\tilde{p}_k)}{Var_v(P_k)}-1].$$

Furthermore, let Ω be the entire space of interest, and $D_k^2()$ be the dispersion variances of proportion P_k based on certain supports, then

$$\frac{\tilde{p}_k(1-\tilde{p}_k)}{Var_v(P_k)}-1=\frac{D_k^2(\bullet,\Omega)}{D_k^2(v,\Omega)}-1=\frac{D_k^2(\bullet,\Omega)}{D_k^2(\bullet,\Omega)-D_k^2(\bullet,v)}-1=\frac{D_k^2(\bullet,v)}{D_k^2(\bullet,\Omega)-D_k^2(\bullet,v)}$$

$$=\frac{1}{\theta-1}$$

where $\theta=\frac{D_k^2(\bullet,\Omega)}{D_k^2(\bullet,v)}=\frac{\tilde{p}_k(1-\tilde{p}_k)}{D_k^2(\bullet,v)}$

That is: $\alpha=\frac{\tilde{p}_k}{\theta-1}$ and $\beta=\frac{1-\tilde{p}_k}{\theta-1}$, with θ defined as above.

The expected values and variances are calculated as follows:

$$E_v[P_k]=\frac{\alpha}{\alpha+\beta}, \quad Var_v[P_k]=\frac{\alpha\beta}{(\alpha+\beta)^2(\alpha+\beta+1)}.$$

Figure 3-3 gives a comparison between the true distributions (left) and simulated beta distributions (right) for P_0 at various scales while Figure 3-4 gives the overlapped curves of true CDF's and beta simulated CDF's for P_0 and P_1.

The beta simulated realizations give good reproductions of the marginal distributions at most scales and for most facies categories. The Frequencies of extreme proportion values (around 0 and 1) are slightly over or under estimated, making the simulated CDF curves over-smooth at both ends. When $Var_v(P_k)\to 0$, both α, $\beta\to\infty$, the distribution goes to a normal distribution. Figure 3-5 gives the simulated realizations for P_0 at α and β values based on some very small variance and it is a normal distribution with mean $\tilde{p}_0$=0.6648. Some other training images are tested and similar results are obtained for categories with reasonable prior global proportions. For those categories with extreme prior proportions, e.g., greater than 0.99 or less than 0.01, the beta distribution does not reproduce the true. Figure 3-6 gives some examples.

3.3 Multivariate Fitting (1) - Dirichlet distribution

A generalized form of beta distribution, the Dirichlet Distribution, is considered to fit the joint distribution of P_0, P_1,..., P_{K-1}. A Dirichlet distribution (Kotz et al, 2000), is defined for n random variables $X_1, X_2, ..., X_n$, with values $x_1, x_2, ..., x_n$, and has the joint probability density function (joint PDF) given as:

$$f(\mathbf{x};\boldsymbol{\alpha})=\frac{\Gamma(\sum_{i=1}^{n}\alpha_i)}{\prod_{i=1}^{n}\Gamma(\alpha_i)}\prod_{i=1}^{n}x_i^{\alpha_i-1}$$

where $x_1, x_2, ..., x_n \in [0,1]$ and $\sum_{i=1}^{n} x_i = 1$. And $\alpha_1, \alpha_2, ..., \alpha_n$ are the shaping

parameters. The expected value and variance of each variable are given as:

$$E[X_i]=\frac{\alpha_i}{\sum_{i=1}^{n}\alpha_i},\quad \text{and}\quad Var[X_i]=\frac{\alpha_i[\sum_{j=1}^{n}\alpha_j-\alpha_i]}{[\sum_{i=1}^{n}\alpha_i]^2[\sum_{i=1}^{n}\alpha_i+1]}$$

Let $\beta_i=\sum_{j=1,j\neq i}^{n}\alpha_j$ and we get:

$$E[X_i]=\frac{\alpha_i}{\alpha_i+\beta_i},\quad \text{and}\quad Var[X_i]=\frac{\alpha_i\beta_i}{(\alpha_i+\beta_i)^2(\alpha_i+\beta_i+1)}$$

And it can be shown that the marginal distribution of X_i follows a beta distribution with parameters (α_i,β_i). (Kotz et al, 2000)

Taking into consideration the constraint $\sum_{i=1}^{n}X_i=1$, only $n-1$ variables are free and $X_n=1-\sum_{i=1}^{n-1}X_i$. The the joint PDF for Dirichlet distribution can then be expressed as:

$$f(x_1,x_2,\ldots,x_{n-1};\boldsymbol{\alpha})=\frac{\Gamma(\sum_{i=1}^{n}\alpha_i)}{\prod_{i=1}^{n}\Gamma(\alpha_i)}[\prod_{i=1}^{n-1}x_i^{\alpha_i-1}]\cdot(1-\sum_{i=1}^{n-1}x_i)^{\alpha_n-1}$$

Now come back to facies proportion P_0, $P_1,\ldots,$ P_{K-1}, the joint PDF can then be fitted as:

$$f(p_0,p_1,\ldots,p_{K-1};\boldsymbol{\alpha})=\frac{\Gamma(\sum_{k=0}^{K-1}\alpha_k)}{\prod_{k=0}^{K-1}\Gamma(\alpha_k)}\prod_{k=0}^{K-1}p_k^{\alpha_k-1}$$

Or, taking into consideration the constraint $\sum_{k=0}^{K-1}P_k=1$, only $K-1$ variables are free and $P_{K-1}=1-\sum_{k=0}^{K-2}P_k$. The joint PDF for Dirichlet distribution can then be expressed as:

$$f(p_0,p_1,\ldots,p_{K-2};\boldsymbol{\alpha})=\frac{\Gamma(\sum_{k=0}^{K-1}\alpha_k)}{\prod_{k=0}^{K-1}\Gamma(\alpha_k)}[\prod_{k=0}^{K-2}p_k^{\alpha_k-1}]\cdot[1-\sum_{k=0}^{K-2}p_k]^{\alpha_{K-1}-1}$$

One problem occurs in fitting parameters $\alpha_0, \alpha_1, \alpha_2, ..., \alpha_{K-1}$. In case there are only two facies categories, it is simplified to a standard beta distribution and parameters α and β are uniquely determined by mean and variance of any one of the two facies proportions. In cases more than two facies categories occur, the following conditions should also be satisfied:

$$E[X_i] = \frac{\alpha_i}{\sum_{i=1}^{n} \alpha_i}, \quad \text{and} \quad Var[X_i] = \frac{\alpha_i[\sum_{j=1}^{n} \alpha_j - \alpha_i]}{[\sum_{i=1}^{n} \alpha_i]^2[\sum_{i=1}^{n} \alpha_i + 1]}, \quad i = 1, 2, ..., n$$

Here values of n variables, $\alpha_1, \alpha_2, ..., \alpha_n$, need to be determined satisfying $2n$ constraints.

One possible way might be focusing on the expected values and use only the variance of the most important category. From the mean constraints, we reach:

$$\alpha_i = E[X_i] \cdot \sum_{j=1}^{n} \alpha_j = E[X_i] \cdot \upsilon \quad \text{for all} \quad i = 1, 2, ..., n,$$

where υ denotes the sum of α's. Substitute this into the constraint regarding $Var[X_d]$ for the selected important category X_d and leads to:

$$\upsilon = \frac{E[X_d] \cdot (1 - E[X_d])}{Var[X_d]} - 1$$

and

$$\alpha_i = E[X_i] \cdot \upsilon \quad \text{for all} \quad i = 1, 2, ..., n.$$

10000 realizations are simulated, using the variance for facies category S_0 when fitting the parameters. For facies proportion P_0, the simulated CDF's are very close to those from beta distribution. Figure 3-7 gives some cross plots of joint CDF's from the real data versus the joint CDF's from the Dirichlet simulated realizations for other facies categories.

The shapes of the marginal distributions are approximately reproduced, particularly for the cases of smaller scales. The mean proportion of each facies category is

approximately reproduced. The variances for facies proportion P_0 are reproduced at different scales of volumetric support, while the variances for other facies categories are over or under estimated to some extent. For P_1 and P_2, the estimated variances are close to the real levels, but for P_4 and P_5, the variances are over-estimated and the shapes of distributions change particularly at a larger scales of supports. In Figure 3-8, the joint CDF's are approximately reproduced by Dirichlet distribution at small scales, but not at the larger scales.

3.4 Multivariate Fitting (2) – Ordinary Beta

3.4.1 Fitting of the parameters

One possible solution to the problem of not reproducing all of the variances in Dirichlet distrbution lies in a generalized beta distribution introduced by Mauldon (1959). Mauldon defined an integral transformation (ϕ_β) of n random variables $X_1, X_2, ..., X_n$ with joint CDF $F(x_1, x_2, ..., x_n)$:

$$\phi_\beta = E\left[(t - \sum_{j=1}^{n} a_j x_j)^{-\beta}\right] = \int_{-\infty}^{\infty}\int_{-\infty}^{\infty} \cdots \int_{-\infty}^{\infty} (t - \sum_{j=1}^{n} a_j x_j)^{-\beta} \, dF(x_1, ..., x_n)$$

and defined $X_1, X_2, ..., X_n$ as forming an $n-$dimensional beta distribution when there exist parameters c_{ij} and β_i $(i = 1,2,...,r)$ such that

$$\phi_\beta = \prod_{i=1}^{r} (t - \sum_{j=1}^{n} a_j c_{ij})^{-\beta_i} \quad \text{where} \quad \beta = \sum_{i=1}^{r} \beta_i$$

Those parameters c_{ij}'s form a coordinate matrix. Mauldon showed that when the coordinate matrix is a unit matrix (with all c_{ij}=1), and $X_1, X_2, ..., X_n$ fall within (0,1) and $X_1 + X_2 + ... + X_n = 1$, the joint PDF has the form:

$$f(x_1,...x_n)=\frac{\Gamma(\beta)}{\prod\Gamma(\beta_i)}\prod_{j=1}^{n}x_j^{\beta_j-1}$$

Mauldon called it the basic beta distribution. It is in fact the Dirichlet distribution discussed above. Mauldon also showed that any $n-$dimensional beta distributed variables $\mathbf{y}=(Y_1,Y_2,...,Y_K)$ can be obtained by $\mathbf{y}=M\mathbf{x}$ from basic beta distributed variables $\mathbf{x}=(X_1,X_2,...,X_n)$ through matrix M. Mauldon named this the Ordinary Beta.

The results of Mauldon are helpful in solving our problem. Let $\mathbf{p}=(P_1,P_2,...,P_K)$ be the K facies proportions, the joint distribution can be modeled by $\mathbf{p}=M\mathbf{x}$ where $\mathbf{x}=(X_1,X_2,...,X_K)$ forms a Dirichlet distribution with

$$E[X_i]=\frac{\beta_i}{\beta} \text{ and } Var[X_i]=\frac{\beta_i(\beta-\beta_i)}{\beta^2(\beta+1)}$$

and

$$E[\mathbf{p}]=M\cdot E[\mathbf{x}],\ COV[\mathbf{p}]=M\cdot COV[\mathbf{x}]\cdot M^T$$

where $COV[\mathbf{x}]$ denotes the covariance matrix of variable vector $\mathbf{x}$ and M^T the transpose of matrix M. Solving the above equation systems will results in the estimated matrix M and parameters β_i's that make $P_1,...,P_K$ honor population means, variances and covariances.

Specifically, if a diagonal matrix is used:

$$M=\begin{pmatrix} a_{11} & 0 & \cdots & 0 \\ 0 & a_{22} & \cdots & 0 \\ \vdots & \vdots & \ddots & \vdots \\ 0 & 0 & \cdots & a_{KK} \end{pmatrix},$$

and $\mathbf{x}=(X_1,X_2,...,X_K)$ form a $K-$dimensional basic Beta (Dirichlet) distribution with parameters β_i $(i=1,2,...,K)$, the following system will be reached:

$$\begin{cases} E[p_i] = \dfrac{a_{ii}\beta_i}{\beta} \\ Var[p_i] = a_{ii}^2 \cdot \dfrac{\beta_i(\beta-\beta_i)}{\beta^2(\beta+1)} & i = 1,2,...,K. \\ \beta = \beta_1 + \beta_2 + ... + \beta_K \end{cases}$$

Or, equivalently:

$$\begin{cases} a_{ii} = \dfrac{\beta \cdot Var[p_i] + Var[p_i] + (E[p_i])^2}{E[p_i]} \\ \beta_i = \dfrac{\beta \cdot E[p_i]}{a_{ii}} & i = 1,2,...,K. \\ \beta = \beta_1 + \beta_2 + ... + \beta_K \end{cases}$$

This system is solved for a_{ii} and β_i and thus we reach variables $\mathbf{p} = M\mathbf{x}$ that honor both the means and the variances. One problem is that the values $p_1, p_2, ..., p_K$ are not guaranteed to fall within [0,1] or to sum to one. This problem can be solved by resetting negative values to zero and restandardizing by:

$$p_i^* = \frac{p_i}{\sum_{j=1}^{K} p_j} \qquad i = 1,2,...,K$$

Figure 3-9 gives cross plots of the real joint CDF's versus the simulated joint CDF's. The joint CDF's are well reproduced at small scales and also reproduced at large scales. Several other training images are tested and the similar results are obtained. If a full matrix M is adopted, the covariances can also be honored and a better fit can be expected. But that will require solving a very complicated equation system.

3.4.2 Limitation and Solution

One major problem that might occur in ordinary beta distribution fitting lies in the roots of β, β_i's or a_{ii}. The system discussed above will finally lead to equations of

K^{th} order polynomials. Sometimes in each group of solutions, values for β, β_i's or a_{ii} are not all positive. It is also possible that no real root exists. Fortunately, repeated tests suggest that all the non-real roots and most of the non-positive roots occur in those extreme situations where the expected values $E[P_k]$ for some k in 1,2,..., K are greater than 0.99 or less than 0.01. Note that for all $0 \le P_k \le 1$:

$$Var[P_k] = E[P_k^2] - (E[P_k])^2 \le E[P_k] - (E[P_k])^2 \le E[P_k].$$

10^9 pairs of uniformly distributed random vectors ($\mathbf{u}$, $\mathbf{v}$), 5-dimensional or 4-dimensional, are drawn such that $0.01 < \mathbf{u}(i) < 0.99$ and $0.0005 < \mathbf{v}(i) < \mathbf{u}(i)$, treated respectively as $E[\mathbf{p}]$ and $Var[\mathbf{p}]$ and do the test. Real roots occur in all the cases and positive roots occur in more than 97.5% of the cases. In case all real roots were negative, a slight reduction on the required variances lead to positive roots. Based on this observation, when building the conditional distribution, values 0.99 and 0.01 can be assigned to $E[P_k]$ when an extreme value greater than 0.99 or less than 0.01 occurs. The result will be very close to the original one. The problem of non-positive roots can be solved by slightly reducing the maximum of the target variances.

3.4.3 Joint PDF for ordinary beta distribution

The parametric joint PDF for ordinary beta distribution can be derived applying Jacobian transformation rule. In the transformation $\mathbf{p} = M\mathbf{x}$, where $\mathbf{x}$ forms a Dirichlet distribution with joint PDF:

$$f_{\mathbf{x}}(x_1,...x_K) = \frac{\Gamma(\beta)}{\prod \Gamma(\beta_i)} \prod_{j=1}^{K} x_j^{\beta_j - 1}$$

and M an invertible matrix with inverse $M^{-1} = [b_{ij}]$, $i, j = 1, 2, ..., K$, then

$$\mathbf{x} = M^{-1}\mathbf{p}$$

or equivalently $X_i(\mathbf{p}) = \sum_{j=1}^{K} b_{ij} P_j$ $(i, j = 1, 2, ..., K)$. The Jacobian matrix for such transformation can be expressed as:

$$J = [s_{ij}], \text{ where } s_{ij} = \frac{\partial x_i(\mathbf{p})}{\partial P_j} = b_{ij} \quad (j = 1, 2, ..., K).$$

That is: $J = M^{-1}$. Denote the determinant of the Jacobian matrix J as $\det(J)$ and its absolute value as $|\det(J)|$, applying Jacobian transformation rule, the joint PDF for $\mathbf{p}$ is resulted as:

$$f_{\mathbf{p}}(p_1, ... p_K) = f_{\mathbf{x}}[x_1(\mathbf{p}), ... x_K(\mathbf{p})] \cdot |\det(J)|$$

$$= |\det(M^{-1})| \cdot \frac{\Gamma(\beta)}{\prod \Gamma(\beta_i)} \cdot \prod_{j=1}^{K} (\sum_{k=1}^{K} b_{jk} p_k)^{\beta_j - 1}$$

In case diagonal matrix is applied for M:

$$M = \begin{pmatrix} a_{11} & 0 & \cdots & 0 \\ 0 & a_{22} & \cdots & 0 \\ \vdots & \vdots & \ddots & \vdots \\ 0 & 0 & \cdots & a_{KK} \end{pmatrix}$$

where, as previously discussed, $\alpha_{ii} > 0$ for all $i = 1, 2, ..., K$, the joint PDF $f_{\mathbf{p}}$ can be simplified as:

$$f_{\mathbf{p}}(p_1, ..., p_K) = \frac{\Gamma(\beta)}{\prod_{i=1}^{K} [a_{ii} \cdot \Gamma(\beta_i)]} \cdot \prod_{j=1}^{K} \left(\frac{p_j}{a_{jj}} \right)^{\beta_j - 1}$$

$$= \frac{\Gamma(\beta)}{\prod_{i=1}^{K} [a_{ii}^{\beta_i} \cdot \Gamma(\beta_i)]} \cdot \prod_{j=1}^{K} (p_j)^{\beta_j - 1}$$

and joint CDF is derived as:

$$F_{\mathbf{p}}(p_1, ..., p_K) = \int_0^{p_1} ... \int_0^{p_K} f_{\mathbf{p}}(t_1, ..., t_K) dt_1 ... dt_K$$

$$= \frac{\Gamma(\beta)}{\prod_{i=1}^{K} [a_{ii}^{\beta_i} \cdot \beta_i \cdot \Gamma(\beta_i)]} \cdot \prod_{j=1}^{K} (p_j)^{\beta_j}$$

In order to satisfy the order relation constraints, further adjustment is done by:

$$p_i^* = \frac{p_i}{\sum_{j=1}^{K} p_j} \qquad i = 1, 2, ..., K .$$

Again, the Jacobian matrix takes the form $J_2 = \left[s_{ij}^* \right]$ with

$$s_{ij}^* = \frac{\partial p_i (\mathbf{p}^*)}{\partial p_j^*}, \quad \mathbf{p}^* = (p_1^*, ..., p_K^*)$$

Finally, using $\mathbf{p} = (p_1, ..., p_K)$ to denote the fitted facies proportions, its joint PDF has the form:

$$f_{\mathbf{p}} (p_1, ..., p_K) = \frac{\Gamma(\beta)}{\prod_{i=1}^{K} [a_{ii}^{\beta_i} \cdot \Gamma(\beta_i)]} \cdot \prod_{j=1}^{K} \left[\theta_j (p_1, ..., p_K) \right]^{\beta_j - 1} \cdot |\det(J_2)|$$

with θ_i's determined by $p_i = \theta_i \Big/ \sum_{j=1}^{K} \theta_j$, that is:

$$\sum_{k=1, k \neq i}^{K} p_i \theta_k - (1 - p_i) \theta_i = 0 \quad i = 1, 2, ..., K .$$

and Jacobian matrix

$$J_2 = \left[s_{ij}^* \right] \quad \text{where } s_{ij}^* = \frac{\partial \theta_i (\mathbf{p})}{\partial p_j} .$$

The above formalism is complicated. In practice, the joint CDF's can be approximated via large size (say 10000) of simulated sample realizations.

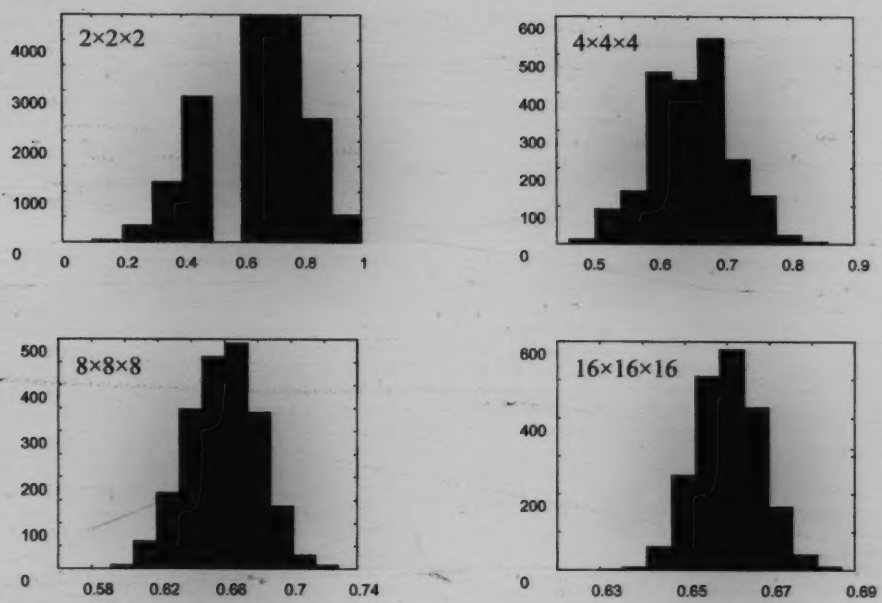

Figure 3-1 Binomial simulation ($\tilde{p}_k$ =0.665)

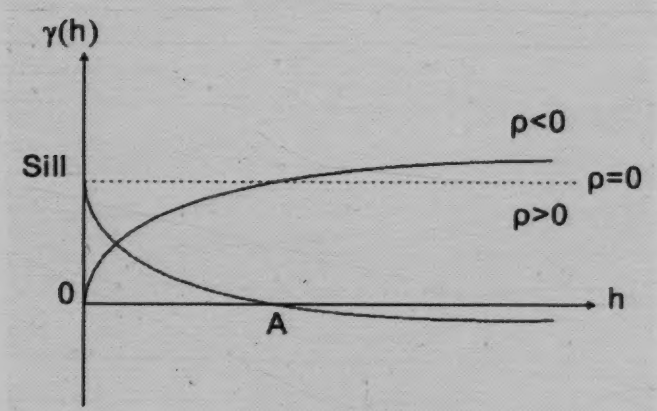

Figure 3-2 Semivariogram

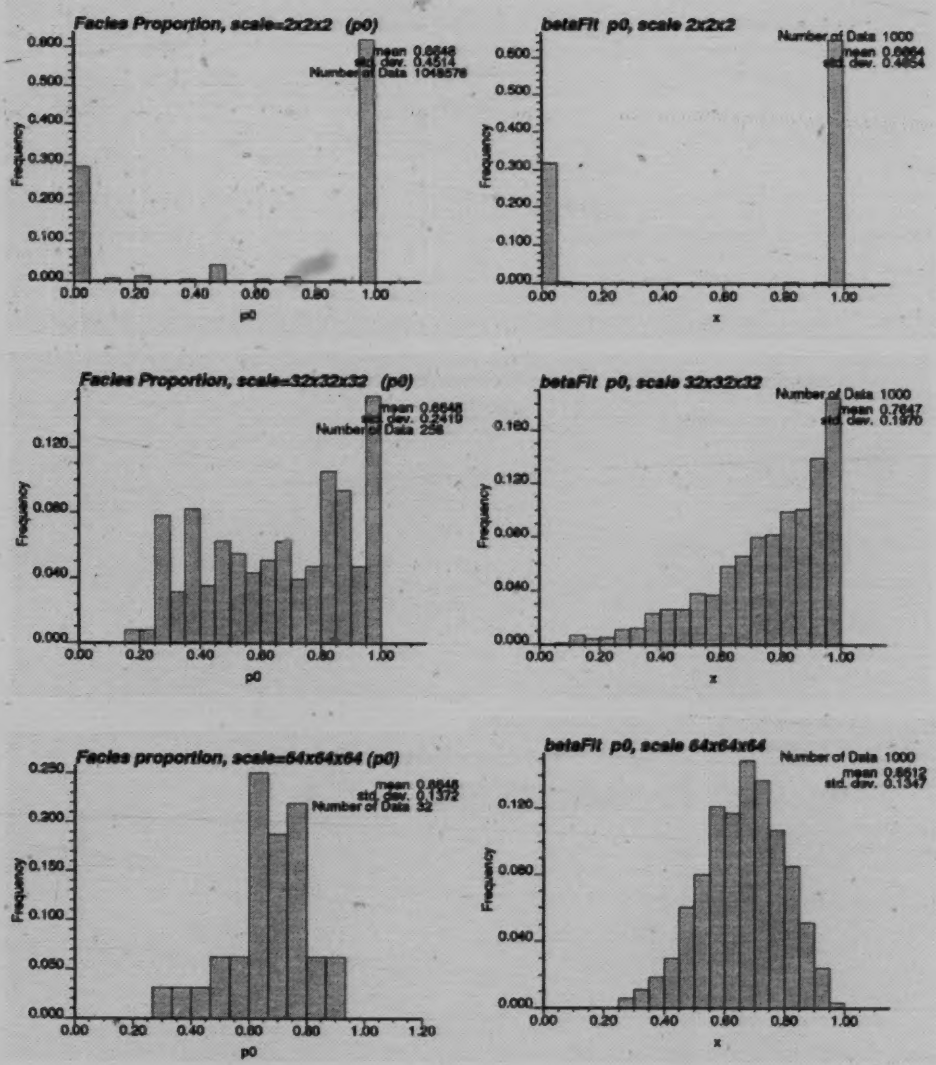

Figure 3-3 Beta simulated distributions. Histograms from data (left) compaired with the simulated Histograms (right)

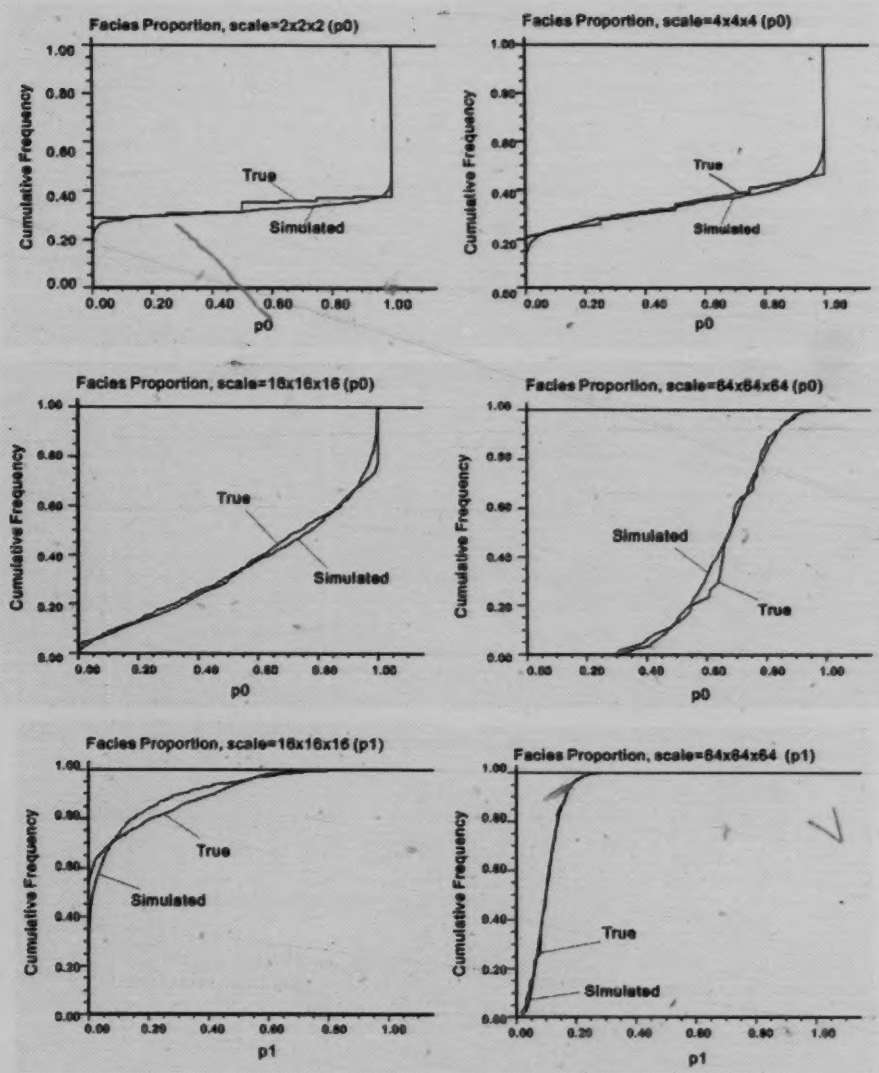

Figure 3-4 Real marginal CDF's overlapped by Beta simulated CDF's

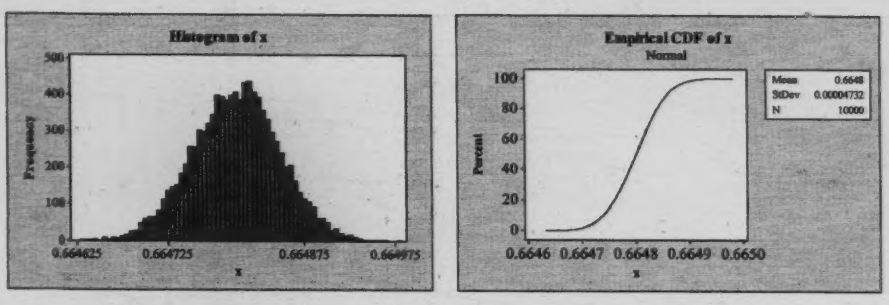

Figure 3-5 Beta simulated distribution for P_0 at a very small variance

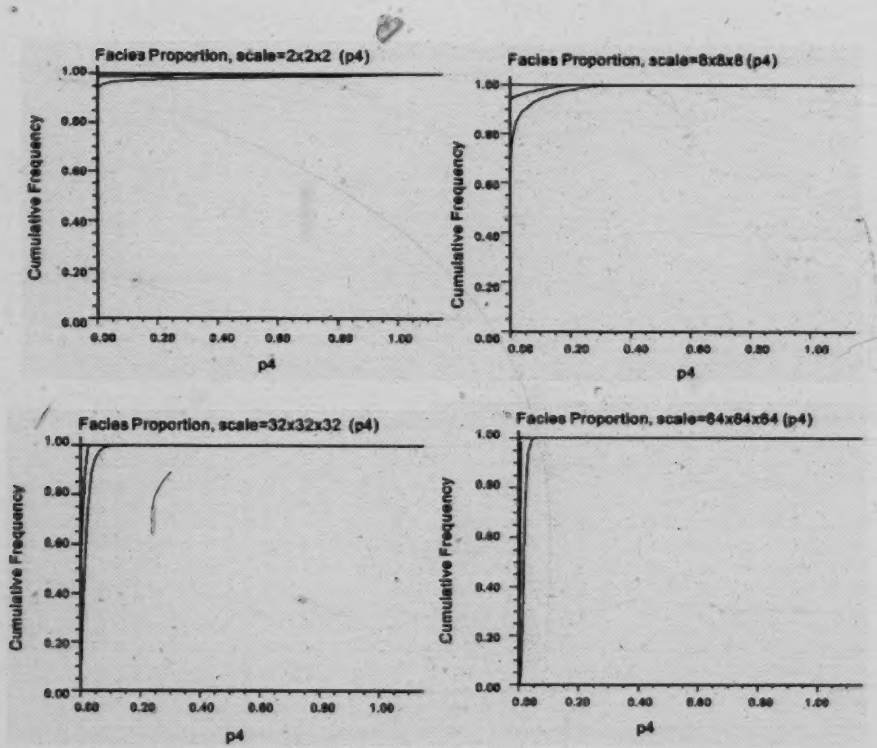

Figure 3-6 Beta simulated fits with prior global proportion 0.0047. The CDF's of simulated realizations lie below the real CDF's

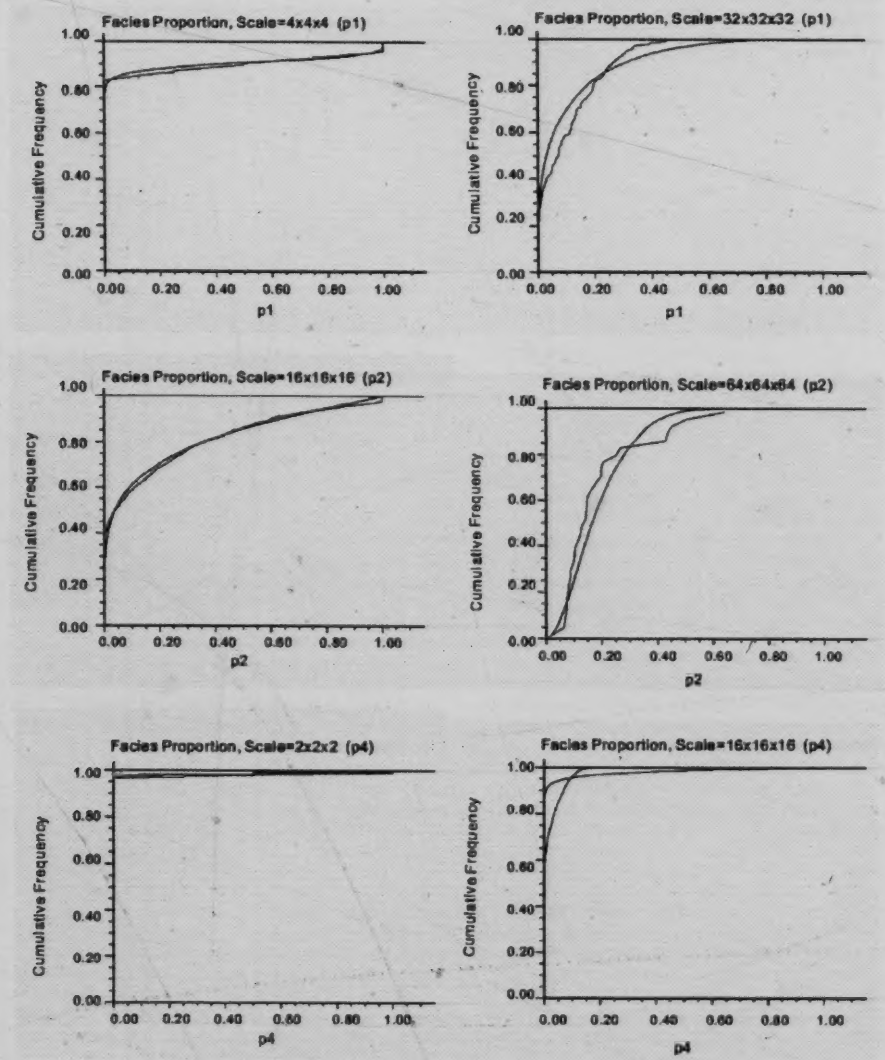

Figure 3-7 Real marginal CDF's overlapped by Dirichlet simulated CDF's

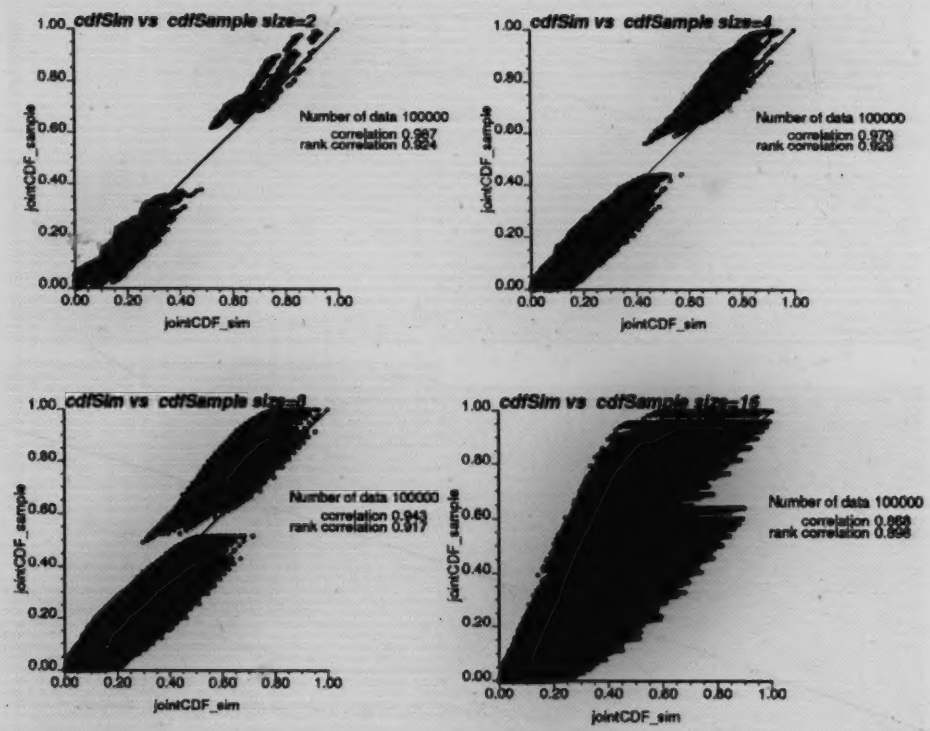

Figure 3-8 cross plots of real joint CDF's versus Dirichlet simulated joint CDF's

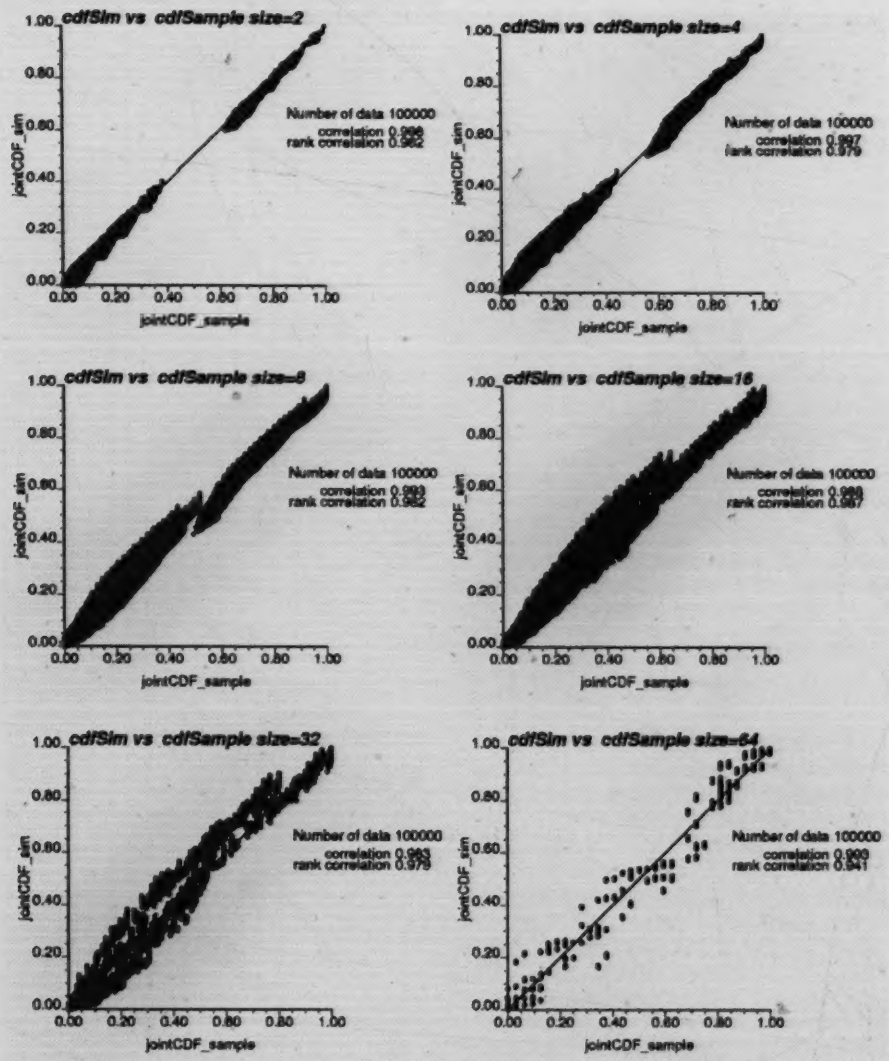

Figure 3-9 Cross plots of real joint CDF's versus Ordinay Beta simulated joint CDF's

Chapter 4 Volume Dependent Distribution of Facies Proportions Based on Ordinary Beta

4.1 Formalism

As discussed in the previous chapter, an ordinary beta distribution is determined by the means and variances of the facies proportions $P_1, P_2, \ldots, P_K$. The means remain constant and the variances are determined by the volumetric support and variance-covariance structure of facies categories over the entire 3-dimensional space of interest.

The key problem is to determine the variances of facies proportions based on the volumetric support and scaling laws. Journel and Huijbregts (1978) introduced the theoretical concepts and formalism of scaling laws. Deutsch and Frykman (1999) gave further development as well as the discussion on its applications.

Given a certain volumetric support v, the variogram model is expressed as:

$$\gamma_v(\mathbf{h}) = C_v^0 + \sum_{i=1}^{nst} C_v^i \cdot \Gamma^i(\mathbf{h})$$

where C_v^0 is the nugget effect, nst is number of nested variogram structures applied, C_v^i $(i = 1, 2, \ldots, nst)$ are the variance contributions of the i^{th} nested structure used in the variogram model, and $\Gamma^i(\mathbf{h})$ the elementary licit variogram function for the i^{th} nested structure. Both the nugget effect C_v^0 and variance contribution C_v^i are determined by variance-covariance structure and the volumetric support. Given the reference variogram model at some volumetric support v_0, the nugget effect at scale v can be obtained by:

$$C_v^0 = C_{v_0}^0 \cdot \frac{|v_0|}{|v|}$$

and the variance contribution of the i^{th} nested structure is obtained by:

$$C_v^i = C_{v_0}^i \frac{1-\bar{\Gamma}(v,v,\mathbf{a}^i)}{1-\bar{\Gamma}(v_0,v_0,\mathbf{a}^i)}$$

where $\bar{\Gamma}(v,v,\mathbf{a}^i)$ is the average variogram at volumetric support v calculated based on the i^{th} nested structure in the variogram model. The vector of ranges in the three directions

$$\mathbf{a}^i = (a^i_{h-major}, a^i_{h-minor}, a^i_{vert}),$$

corresponding to the i^{th} nested structure and is determined by the volumetric support via:

$$a^i(v) = a^i(v_0) + \Delta v$$

with Δv the change volume size ($|v| - |v_0|$) in each particular direction.

The calculation of average variograms $\bar{\Gamma}(v,v,\mathbf{a}^i)$ can be done with `gammabar` program in *Gslib* (Deutsch and Journel, 1998) using the semivariogram models for point data. Given the variogram model at some reference volumetric support v_0, the above algorithm is first applied to obtain the point variogram model and then extend to any desired scale.

The variance of the scaled up proportion at volumetric support v is the dispersion variance and is the sum of variance contributions at this volumetric support, that is:

$$D^2(v,\Omega) = C_v^0 + \sum_{i=1}^{nst} C_v^i$$

where $D_v^2(v,\Omega)$ gives the variance of scaled up values at v over the entire area of interest Ω.

Another way to calculate the variance of scaled up facies proportion is :

$$D^2(v,\Omega) = D^2(\bullet,\Omega) - D^2(\bullet,v)$$

where

$$D^2(\bullet,\Omega)=\overline{\gamma}(\Omega,\Omega) \text{ and } D^2(\bullet,v)=\overline{\gamma}(v,v)$$

Taking the entire space of interest as the target population, the above formalism suggests a function $\sigma^2(v,\Omega;v_0)$ for variance (global) of the scaled up facies proportion for each facies categories at volumetric support v conditioning on the reference variogram model at some scale v_0. Specifically, $\sigma_k^2(v,\Omega;v_0)$ is used for the k^{th} facies category.

The ordinary beta distribution has joint probability density function (joint PDF) fitted based on the parameter matrix M and vector $\boldsymbol{\beta}$ that are determined by the means (m_k) and volume dependent variances (σ_k^2). Therefore the joint distribution of scaled up facies proportion can be modeled by

$$f_{\mathbf{p}}(p_1,...,p_K;M,\boldsymbol{\beta}), \text{ with}$$

$$M=M(\mathbf{m},\boldsymbol{\sigma}^2(v,\Omega;v_0)) \text{ and } \boldsymbol{\beta}=\boldsymbol{\beta}(\mathbf{m},\boldsymbol{\sigma}^2(v,\Omega;v_0)) \ ,$$

where $\mathbf{m}$ is the vector of volume independent means and $\boldsymbol{\sigma}^2(v,\Omega;v_0)$ the volume dependent variance vector determined by the formalism as discussed above.

4.2 Sample Test

This sample is from the training image as described in Chapter 1. Here the point scale is the reference scale and the indicator variogram models are as in Table 4-1. The variances for facies proportions at volumetric supports $2\times2\times2$, $4\times4\times4$, $8\times8\times8$, $16\times16\times16$ and $32\times32\times32$ are calculated using the methods described in the previous section and tabulated in Table 4-2. The means of facies proportions are constants for all volumetric support (as given in Table 1-1). Applying the algorithm as discussed in Chapter 3, the parameter matrix M and parameter vector $\boldsymbol{\beta}$ are estimated and the

ordinary beta distribution is built. 500 realizations are then simulated and tested.

Figure 4-1 gives the simulated histograms for P_0 at various volumetric supports. Compared with the real histograms as shown in Figure 1-2 above, the marginal distributions for P_0 are approximately reproduced by the simulated distributions. The simulated histograms of other facies proportions also compare well.

The cross plots of real versus simulated joint CDF's are shown in Figure 4-2. For various volumetric supports, the cross plots are close to a 45° line, suggesting a reasonable reproduction of the global joint CDF's by the simulated realizations.

Table 4-1 Indicator Variogram Models

Facies Categories	Variogram Models
S_0	2 0.002157533 -nst, nugget effect 1 0.1510273 90.0 0.0 0.0 -it,cc,ang1,ang2,ang3 35.0 50.0 30.0 -a_hmax, a_hmin, a_vert 1 0.0625685 90.0 0.0 0.0 -it,cc,ang1,ang2,ang3 120.0 1200.0 40.0 -a_hmax, a_hmin, a_vert
S_1	2 0.000437917 -nst, nugget effect 1 0.03941259 90.0 0.0 0.0 -it,cc,ang1,ang2,ang3 15.0 30.0 25.0 -a_hmax, a_hmin, a_vert 1 0.003941259 90.0 0.0 0.0 -it,cc,ang1,ang2,ang3 40.0 60.0 30.0 -a_hmax, a_hmin, a_vert
S_2	2 0.001825218 -nst, nugget effect 1 0.12776526 90.0 0.0 0.0 -it,cc,ang1,ang2,ang3 35.0 40.0 40.0 -a_hmax, a_hmin, a_vert 1 0.05293132 90.0 0.0 0.0 -it,cc,ang1,ang2,ang3 50.0 200.0 50.0 -a_hmax, a_hmin, a_vert

Table 4-1 Indicator Variogram Models (continued)

S_4	2 0.000125341 -nst, nugget effect 1 0.008147192 90.0 0.0 0.0 -it,cc,ang1,ang2,ang3 25.0 30.0 14.0 -a_hmax, a_hmin, a_vert 1 0.004261608 90.0 0.0 0.0 -it,cc,ang1,ang2,ang3 90.0 500.0 18.0 -a_hmax, a_hmin, a_vert
S_5	2 0.000158536 -nst, nugget effect 1 0.01189023 90.0 0.0 0.0 -it,cc,ang1,ang2,ang3 20.0 25.0 16.0 -a_hmax, a_hmin, a_vert 1 0.003804874 90.0 0.0 0.0 -it,cc,ang1,ang2,ang3 200.0 500.0 18.0 -a_hmax, a_hmin, a_vert

Table 4-2 Estimated Variances

	p_0	p_1	p_2	p_4	p_5
2×2×2	0.2214	0.03740	0.1566	0.01327	0.01425
4×4×4	0.2130	0.03410	0.1496	0.01240	0.01306
8×8×8	0.1913	0.02590	0.1316	0.01020	0.0101
16×16×16	0.1531	0.01337	0.09950	0.006863	0.005626
32×32×32	0.0914	0.004157	0.04953	0.002839	0.001296

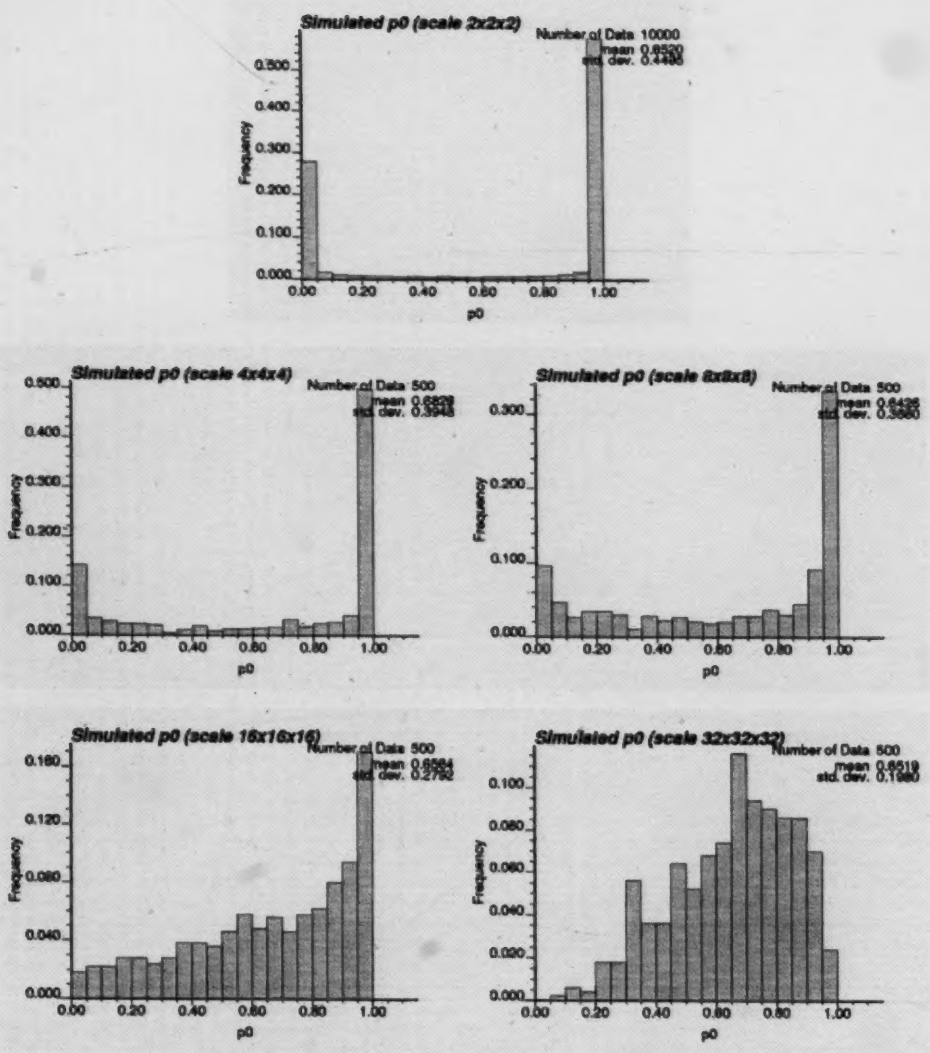

Figure 4-1 Ordinary Beta simulated histograms

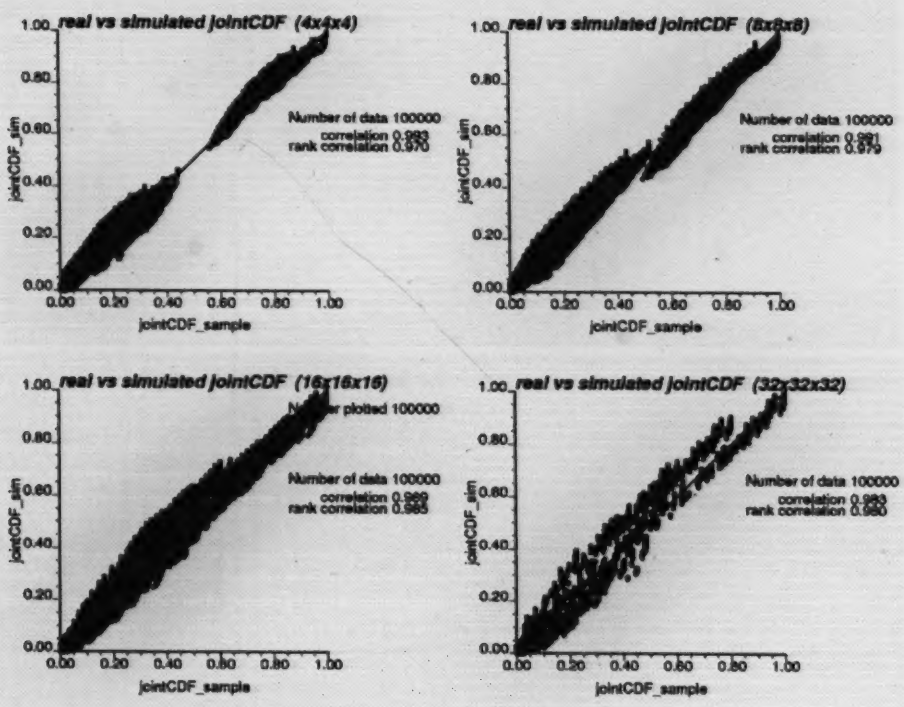

Figure 4-2 Real versus Ordinary Beta simulated joint CDF's

Chapter 5 An Application of Multiscale Facies Model

5.1 Fitting the Local Multivariate Distributions of Facies Proportions

In the previous chapter, the global multivariate and multiscale distribution of facies proportions is built as a function of means, volumetric support and a reference variogram model for each facies category at some volumetric support giving the variance-covariance structure. The volumetric scale is applied to infer the global distribution at a different volume support. The establishment of the location specific multiscale distribution, though more challenging, is often the goal. Similarly, it can be estimated by the local means and local variances. Supposed n_1 points and n_2 blocks are known, various Kriging approaches can be used to get the estimated local means of facies proportions based on the block and point data. Fitting the local variances is a challenge. One choice is the kriging variances.

1) In simple block kriging algorithm with global means, the kriging estimator is:

$$p_V^*(k,\mathbf{u}) = \sum_{\alpha=1}^{n_1} \lambda_{\alpha V\bullet}(k,\mathbf{u}) I(k,\mathbf{u}_\alpha) + \sum_{\beta=1}^{n_2} \lambda_{\beta V_v}(k,\mathbf{u}) p_v(k,\mathbf{u}_\beta) + [1 - \sum_{\alpha=1}^{n_1} \lambda_{\alpha V\bullet}(k,\mathbf{u}) - \sum_{\beta=1}^{n_2} \lambda_{\beta V_v}(k,\mathbf{u})]\bar{p}_k$$

and the kriging system:

$$\sum_{\alpha_1=1}^{n_1} \lambda_{\alpha_1 V\bullet}(k,\mathbf{u}) C(k,\mathbf{u}_{\alpha_1},\mathbf{u}_{\alpha_2}) + \sum_{\beta_1=1}^{n_2} \lambda_{\beta_1 V_v}(k,\mathbf{u}) \bar{C}(k,v_{\beta_1},\mathbf{u}_{\alpha_2}) = \bar{C}(k,V,\mathbf{u}_{\alpha_2}) \qquad \alpha_2 = 1,2,\ldots,n_1$$

$$\sum_{\alpha_1=1}^{n_1} \lambda_{\alpha_1 V\bullet}(k,\mathbf{u}) \bar{C}(k,\mathbf{u}_{\alpha_1},v_{\beta_2}) + \sum_{\beta_1=1}^{n_2} \lambda_{\beta_1 V_v}(k,\mathbf{u}) \bar{C}(k,v_{\beta_1},v_{\beta_2}) = \bar{C}(k,V,v_{\beta_2}) \qquad \beta_2 = 1,2,\ldots,n_2$$

with kriging variance:

$$\sigma_V^2(k,\mathbf{u}) = \bar{C}(k,V(\mathbf{u}),V(\mathbf{u})) - \sum_{\alpha=1}^{n_1} \lambda_{\alpha V_\bullet}(k,\mathbf{u})\bar{C}(k,\mathbf{u}_\alpha,V(\mathbf{u})) - \sum_{\beta=1}^{n_2} \lambda_{\beta V_v}(k,\mathbf{u})\bar{C}(k,v_\beta,V(\mathbf{u}))$$

2) In simple block kriging with locally varying means, we have:

$$p_V^*(k,\mathbf{u}) = \sum_{\alpha=1}^{n_1} \lambda_{\alpha V_\bullet}(k,\mathbf{u}) I(k,\mathbf{u}_\alpha) + \sum_{\beta=1}^{n_2} \lambda_{\beta V_v}(k,\mathbf{u}) p_v(k,\mathbf{u}_\beta) + [1 - \sum_{\alpha=1}^{n_1} \lambda_{\alpha V_\bullet}(k,\mathbf{u}) - \sum_{\beta=1}^{n_2} \lambda_{\beta V_v}(k,\mathbf{u})]\bar{p}(k,\mathbf{u})$$

and

$$\sum_{\alpha_1=1}^{n_1} \lambda_{\alpha_1 V_\bullet}(k,\mathbf{u}) C(k,\mathbf{u}_{\alpha_1},\mathbf{u}_{\alpha_2}) + \sum_{\beta_1=1}^{n_2} \lambda_{\beta_1 V_v}(k,\mathbf{u})\bar{C}(k,v_{\beta_1},\mathbf{u}_{\alpha_2}) = \bar{C}(k,V,\mathbf{u}_{\alpha_2}) \qquad \alpha_2 = 1,2,\ldots,n_1$$

$$\sum_{\alpha_1=1}^{n_1} \lambda_{\alpha_1 V_\bullet}(k,\mathbf{u}) C(k,\mathbf{u}_{\alpha_1},v_{\beta_2}) + \sum_{\beta_1=1}^{n_2} \lambda_{\beta_1 V_v}(k,\mathbf{u})\bar{C}(k,v_{\beta_1},v_{\beta_2}) = \bar{C}(k,V,v_{\beta_2}) \qquad \beta_2 = 1,2,\ldots,n_2$$

with kriging variance:

$$\sigma_V^2(k,\mathbf{u}) = \bar{C}(k,V(\mathbf{u}),V(\mathbf{u})) - \sum_{\alpha=1}^{n_1} \lambda_{\alpha V_\bullet}(k,\mathbf{u})\bar{C}(k,\mathbf{u}_\alpha,V(\mathbf{u})) - \sum_{\beta=1}^{n_2} \lambda_{\beta V_v}(k,\mathbf{u})\bar{C}(k,v_\beta,V(\mathbf{u}))$$

3) The ordinary block kriging estimator takes the form:

$$p_V^*(k,\mathbf{u})^* = \sum_{\alpha=1}^{n_1} \lambda_{\alpha V_\bullet}(k,\mathbf{u}) I(k,\mathbf{u}_\alpha) + \sum_{\beta=1}^{n_2} \lambda_{\beta V_v}(k,\mathbf{u}) p_v(k,\mathbf{u}_\beta) \quad \text{with } 1 - \sum_{\alpha=1}^{n_1} \lambda_{\alpha V_\bullet}(k,\mathbf{u}) - \sum_{\beta=1}^{n_2} \lambda_{\beta V_v}(k,\mathbf{u}) = 0$$

and

$$\sum_{\alpha_1=1}^{n_1}\lambda_{\alpha_1 V\bullet}(k,\mathbf{u})C(k,\mathbf{u}_{\alpha_1},\mathbf{u}_{\alpha_2})+\sum_{\beta_1=1}^{n_2}\lambda_{\beta_1 V_v}(k,\mathbf{u})\bar{C}\,(k,v_{\beta_1},\mathbf{u}_{\alpha_2})+\mu_k=\bar{C}\,(k,V,\mathbf{u}_{\alpha_2})$$
$$\alpha_2=1,2,\ldots,n_1$$

$$\sum_{\alpha_1=1}^{n_1}\lambda_{\alpha_1 V\bullet}(k,\mathbf{u})C(k,\mathbf{u}_{\alpha_1},v_{\beta_2})+\sum_{\beta_1=1}^{n_2}\lambda_{\beta_1 V_v}(k,\mathbf{u})\bar{C}\,(k,v_{\beta_1},v_{\beta_2})+\mu_k=\bar{C}\,(k,V,v_{\beta_2})$$
$$\beta_2=1,2,\ldots,n_2$$

$$\sum_{\alpha_1=1}^{n_1}\lambda_{\alpha_1 V\bullet}(k,\mathbf{u})+\sum_{\beta_1=1}^{n_2}\lambda_{\beta_1 V_v}(k,\mathbf{u})=1$$

with kriging variance:

$$\sigma_V^2(k,\mathbf{u})=\bar{C}(k,V(\mathbf{u}),V(\mathbf{u}))-\sum_{\alpha=1}^{n_1}\lambda_{\alpha V\bullet}(k,\mathbf{u})\bar{C}(k,\mathbf{u}_\alpha,V(\mathbf{u}))$$
$$-\sum_{\beta=1}^{n_2}\lambda_{\beta V_v}(k,\mathbf{u})\bar{C}\,(k,v_\beta,V(\mathbf{u}))-\mu_k$$

Each equation for kriging variances is in fact a difference between two parts. For example, in simple block kriging, the kriging variance is the difference between

$$\bar{C}(k,V(\mathbf{u}),V(\mathbf{u}))$$

and

$$\sum_{\alpha=1}^{n_1}\lambda_{\alpha V\bullet}(k,\mathbf{u})\bar{C}(k,\mathbf{u}_\alpha,V(\mathbf{u}))+\sum_{\beta=1}^{n_2}\lambda_{\beta V_v}(k,\mathbf{u})\bar{C}(k,v_\beta,V(\mathbf{u}))\,.$$

The first part is the block average covariance over the estimated block, and depends only on the target volumetric support. The second part is the sum of variances and block average covariances of the data points and data blocks with kriging weights. In ordinary block kriging formalism, Lagrange constant μ_k is also subtracted from the block average of covariances. Both the simple and ordinary block kriging variances can be considered a function of desired volumetric support, the univariate proportions, local data and variograms. As the volumetric support increases, the block average covariance will decrease and thus tend to decrease the kriging variances. The second part of kriging variances contains uncertainties based on the available data set. It is possible that the kriging variances either overestimate or underestimate the true variances. Further

discussion will be done in our sample studies in sections below.

5.2 Model Description

Two typical cases in multiscale facies modeling are shown in Figure 5-1. The left of Figure 5-1 illustrates a regular grid, where the point data and facies proportions of regular blocks at a certain volumetric support (say, the bigger blocks) are given and facies proportions of regular blocks at some other volumetric support (say, the smaller) are estimated. The right of Figure 5-1 shows the case of irregular grids where the point data and the facies proportions over blocks A and B are known, while facies proportions over blocks C, D and F are desired. A general description of the multiscale facies model is suggested as follows:

The following data are supposed known:

- Exact facies category at each data point.
- Facies proportions:
  - Facies proportions for each regular grid data block over entire area of interest. Or
  - Facies proportions for each irregular block, as well as the (x,y,z) coordinates at all the finest grid nodes within the block.

Blocks to estimate:

- Regular blocks, block grid structures are given
- Irregular blocks, (x,y,z) coordinates at all the finest grid node within the block are supposed to be known.

Based on the kriging proportion $p_V^*(k,\mathbf{u})$ (considered as mean proportion for a local block) and kriging variance, multivariate distributions for facies proportions $(P_1,...,P_K)$ are built applying ordinary beta distribution.

In order to better honor the spatial relationship of facies proportions, the sequential simulation approach is applied, where the local multivariate distribution of each desired

location is built conditioning on previously simulated blocks that are the most related covariate with current estimated/simulated block. Here all the blocks adjacent to current estimated block are considered. In a 3-dimensional space that is regularly gridded, each block has 26 adjacent blocks (either with common edge or common corner point), except those at the corner or on the boundary of the space. Either all or some of the previously simulated adjacent blocks can be used in the sequential simulation and the following steps are applied:

1) A random path is built to reach all the blocks over the entire space of interest
2) For the first block selected, local multivariate distribution is built based on the kriging estimated means and kriging variances from the original data and a realization is simulated.
3) For any subsequent blocks, all or some of the adjacent blocks may be used for block kriging. A realization is drawn.
4) step 3) is repeated until all blocks are randomly visited.
5) A number, say 100, of realizations are simulated following steps 1) to 4).

5.3 Sample Studies

Here the facies category training image described in Chapter 1 will be considered. The examples are limited to cases where block data are collocated with the block to be estimated. The indicator variogram models are fitted based on the point data from the training image and are as shown in Table 4-1 in Chapter 4.

5.3.1 Small Sample Cases

A small sample is drawn from the training image. Suppose point data are available at locations (4,4,4), (4,8,4), (8,4,4), (8,8,4), (4,4,8), (4,8,8), (8,4,8), (8,8,8) and the facies proportions are to be estimated over blocks of scales $2\times2\times2$, $4\times4\times4$, $8\times8\times8$, $16\times16\times16$ and $32\times32\times32$, but with the same upper corner at (4,4,4). Simple block

kriging algorithm is used and Tables 5-1 and 5-2 give the block average covariances and kriging variances. Figures 5-2 and 5-3 show the block average covariances and kriging variances along with volumetric scales. The block average covariances decrease as the volumetric scale increases. The kriging variances also decrease but fluctuate based on the kriging weights determined by the variance-covariance structure as well as the spatial relation of the data.

Table 5-1 Block Average Covariances

Scale	p0	p1	p2	p4	p5
2x2x2	0.2052	0.04002	0.1736	0.01153	0.01450
4x4x4	0.1968	0.03672	0.1666	0.01066	0.01332
8x8x8	0.1801	0.03032	0.1526	0.008977	0.01104
16x16x16	0.1387	0.01646	0.1180	0.005261	0.006066
32x32x32	0.07792	0.005058	0.06511	0.002134	0.002242

Table 5-2 Kriging Variances

Scale	p0	p1	p2	p4	p5
2x2x2	0.08216	0.02049	0.06472	0.006149	0.007311
4x4x4	0.04100	0.008482	0.03140	0.002763	0.002973
8x8x8	0.08042	0.01106	0.06729	0.003596	0.004111
16x16x16	0.06119	0.004966	0.05089	0.001962	0.001814
32x32x32	0.02688	-0.0000823	0.02153	0.0003268	0.0001374

A further look at the fit is taken from the following small samples regarding the estimation of one block at scale $16\times16\times16$ with the upper corner at (0,0,0) using 5 sample points at different locations. Group 1) of data points are collocated or closed to the estimating block, say at: (4,8,4), (4,8,8), (20,12,12), (24,16,8), (16,16,24). Group 2) of points are farther, located at (32,64,32), (48,48,64), (36,64,48), (64,48,24), (16, 48, 24). Group 3) of data points are even farther, located at (96,64,32), (72,96,32), (64,84,28), (72,64,28) and (72,48,28) Also, collocated $32\times32\times32$ block data are used in the block

kriging.

Tables 5-3 to 5-4 give the kriging matrices (right-hand-side "r" and columns "a" of upper triangle of the left-hand-side), kriging weights, kriging variances for these small samples. As the data points located farther to the estimated block, the values of corresponding terms in the kriging matrix are getting smaller and smaller except for the diagonal terms, the variances, which remain constant at a fixed volumetric support under a stationary semivariogram model. The Kriging weights reduce as the distances of data points from the estimated block increase. The Kriging variances are complicated, for some facies categories, they are increasing among these three groups; for other facies categories, they are decreasing.

Table 5-3a Kriging matrix for facies S_0

Group 1	r(1) = 0.1436 a= 0.2136 r(2) = 0.1292 a= 0.1742 0.2136 r(3) = 0.1257 a= 0.0972 0.0818 0.2136 r(4) = 0.1029 a= 0.0794 0.0748 0.1606 0.2136 r(5) = 0.0743 a= 0.0501 0.0302 0.0959 0.0609 0.2136 R(6) = 0.0779 a= 0.0650 0.0539 0.0956 0.0833 0.0977 0.0779

Table 5-3b Kriging matrix for facies S_0:

Group 2	r(1) = 0.0341 a= 0.2136 r(2) = 0.0327 a= 0.1847 0.2136 r(3) = 0.0197 a= 0.0667 0.0823 0.2136 r(4) = 0.0146 a= 0.0692 0.0826 0.1644 0.2136 r(5) = 0.0113 a= 0.0329 0.0399 0.0987 0.0878 0.2136 r(6) = 0.0779 a= 0.0586 0.0586 0.0338 0.0302 0.0252 0.0779

Table 5-3c Kriging matrix for facies S_0:

Group 3	r(1) = 0.0084 a= 0.2136 r(2) = 0.0084 a= 0.1262 0.2136 r(3) = 0.0108 a= 0.0682 0.1227 0.2136 r(4) = 0.0054 a= 0.0527 0.0880 0.1248 0.2136 r(5) = 0.0012 a= 0.0531 0.0599 0.0365 0.0447 0.2136 r(6) = 0.0779 a= 0.0166 0.0165 0.0201 0.0139 0.0058 0.0779

Table 5-4 Kriging weight for facies S_0

	Point 1	Point 2	Point 3	Point 4	Point 5	Collocated block
Group 1	0.33939	0.15489	0.22266	-0.00188	-0.01806	0.36111
Group 2	-0.06037	-0.09068	0.00545	-0.02216	-0.04806	1.13538
Group 3	-0.02466	-0.00126	-0.02410	-0.01861	-0.00740	1.01562

Table 5-5 Kriging variances

	p0	p1	p2	p4	p5
Group 1	0.07340	0.009464	0.06275	0.002758	0.003153
Group 2	0.06451	0.01137	0.05507	0.002963	0.003685
Group 3	0.06118	0.01140	0.05289	0.003102	0.003727

5.3.2 Big Sample Case

The example below represents a $256\times256\times32$ space drawn from the training image. The following data are known:

1) facies category at each $4\times4\times4$ grid node
2) facies proportions over each $32\times32\times32$ block in the entire space, only the block data collocated with the estimated block are used for each of the desired estimated block.

Based on the above, the facies proportions over each $16\times16\times16$ block are estimated using both block kriging and sequential simulation approaches.

5.3.2.1 Block Kriging Estimations

Both simple block kriging and ordinary block kriging methods are used to estimate the means and variances of facies proportions $p_V^*(k,\mathbf{u})$ for each local block. Figures 5-4 to 5-12 give the results.

Cross plots of kriging facies proportions versus real values (Figures 5-4 and 5-5) lie around a 45° straight line, suggesting a good estimated result by both simple and ordinary block kriging methods. The histograms of kriging estimated facies proportions compared with the real histograms (Figures 5-6, 5-7) show that global marginal distributions are reproduced by the kriging results. The real global joint CDF's are reproduced by both the simple kriging and ordinary kriging results (see Figure 5-8, the cross plots kriging estimated joint CDF's versus real joint CDF's). The scatter plots of residuals (kriging value minus the real values) versus kriging results in Figures 5-9 and 5-10 are evenly spread and are surrounding a horizontal line at zero, Figures 5-11 and 5-12 give distributions of residuals, showing that both ordinary block kriging and simple block kriging output reproduce real values well.

5.3.2.2 Sequential Simulation

One hundred realizations are simulated. As discussed above, the kriging variances may either overestimate or underestimate the variabilities of local facies proportions. The real local block variances are also unknown. One important reference is the variograms of the scaled up proportions. Let's look at the reproduction of the semivariograms by the simulated realizations (Figure 5-13).

The shapes of semivariograms are approximately reproduced by the simulated realizations but the values are higher than the true reference results at all lag distances

and for all facies categories. This may suggest a systematic overestimation of the variances. In order to solve this problem, the target local variances are reduced to some fraction of the kriging variances. Based on the shapes of the simulated semivariograms, we assume the real local variances of facies proportions are overestimated by the kriging variances to a similar extent over the entire area of interest. Two approaches are tried to adjust the local variances:

In the first approach, the derived global variances $D_k^2(v,\Omega)$ are used. It is calculated from the variogram models at the reference scale using scaling laws, as described in Chapter 4. The global variances from a simulated realization $\hat{\sigma}_k^2(v)$ are compared with $D_k^2(v,\Omega)$. When $\hat{\sigma}_k^2(v) > D_k^2(v,\Omega)$ or when $\frac{|\hat{\sigma}_k^2(v) - D_k^2(v,\Omega)|}{D_k^2(v,\Omega)}$ is greater than some given level, say 0.05, use factor $f_k(v) = \frac{D_k^2(v,\Omega)}{\hat{\sigma}_k^2(v)}$ to adjust the target variances and redo the sequential simulation. This procedure is repeated until the simulated global variances are closed to the derived values $D_k^2(v,\Omega)$. But this method does not lead to a good fit in this sample.

In the second approach, a series of fraction values $\frac{n}{m}$ ($m = 2,3,...,10$; $n = 1,2,...,m$.) are applied as a variance reduction factor to each facies category, where the factor for one facies category may be different from others. The simulated variograms are compared with the reference variograms. Finally in this example, the factor with value of $\frac{1}{6}$ applied to all facies categories leads to a pretty good result. Figures 5-14 to 5-19 give the final results based on simple block kriging with locally varying means (similar results are obtained from simulation based on ordinary kriging after adjusting the kriging variances).

The cross plots (Figure 5-14) of simulated results versus real values are around the 45° line; the global marginal histograms are reproduced (Figure 5-15); also cross plots of

simulated versus true joint CDF's (Figure 5-16) show a good reproduction of the multivariate distribution by the simulated realizations; residuals (simulated value minus true) plots and residual histograms show they are centered at zero and has a reasonable distribution, suggesting a good fit by the simulated realizations (Figures 5-17 and 5-18).

The above simulated histograms show that that the global variances of the proportions of all facies categories are reproduced by simulated realizations. Figure 5-19 gives the reproduction of semivariograms. Here, after the adjustment of kriging variances, the variograms are well reproduced by simulated realizations.

Test of Accuracy is performed on the simulated distributions. For a probability distribution (treated as continuous random variables), accuracy and precision are based on the actual fraction the true values falling within symmetric probability intervals of varying width p^*. A probability distribution is accurate if the fraction of true values falling in the p^* interval exceed the p^* for all p^* within [0,1]; the precision of an accurate probability distribution is measured by the closeness of the fraction of true values to p^* for all p^* within [0,1] (Deutsch, 2002). One way to test the accuracy and precision is to check the distribution of the true quantile, the cumulative probability associated to each true value based on simulated realizations. That is, $F_{P_k}(x) = \text{Prob}[P_k \leq x]$ for real facies proportion P_k at each local block conditioning to the simulated realizations. A probability distribution is accurate and precise if the cumulative probabilities associated to true values follow a uniform distribution (Deutsch, 1996).

Figure 5-20 gives the histograms of the cumulative probabilities (shown on horizontal axis) of true values based on the simulated realizations using sequential simulation from simple block kriging. The frequency at cumulative probability 1.0 is much higher than at those other values. We observed that most cumulative probability values 1.0 occur at the point where the true facies proportion is 1.0. Excluding those

points with true facies proportion equal to 1.0 and plotting histograms of the cumulative probabilities of the remaining points, approximate uniform distributions are obtained as shown in Figure 5-21. Such results suggest that the probability distributions from simulated realizations are accurate for facies proportions except those extreme values.

Figure 5-22 shows the true and simulated maps of facies proportion P_0 in an arbitrary slice; the spatial distribution is reproduced.

5.3.3 Discussion

Both simple and ordinary block kriging algorithms work well in estimating the facies proportion in desired locations at certain volumetric support. In the simulation algorithm, the building of local multivariate distribution of facies proportions needs a further adjustment on the kriging variances. In the above sample study, we observe that the shapes of the simulated semivariogram based on the kriging variances are above and approximately parallel to the real reference semivariograms. Thus we assume the real local variances of facies proportions are overestimated by the kriging variances to a similar extent over the entire area of interest. The true semivariograms are used as a reference and this leads to a factor (about 1/6) applied to decrease the kriging variances.

In practice, the real semivariograms of the facies proportion at the desired volumetric scale are usually unknown. The variogram models can be built based on the semivariograms at the reference scale following the scaling laws, as described in Chapter 4, and can be taken as a reference to adjust the kriging variances, following the similar method as using the reference variograms. In case a common factor is not suitable for all locations, further information is required to estimate or correct the local variances in order to fit the ordinary beta distribution for each local block. Correctly estimating the local variances remains a tricky question. No general solution is available by now and further research is desired.

5.4 Summary of Results

Block kriging approaches using simple kriging and ordinary kriging algorithms are efficient in estimating the facies proportions at unknown block locations of desired volumetric support based on the data of different scales, including point data and collocated block data of difference volumetric supports.

Ordinary beta distribution is efficient in fitting the multivariate distribution of facies proportions for any unknown local blocks and thus can be applied in sequential simulation to build the multi-realization maps of facies proportions provided the means and variances of facies proportions can be obtained.

One big challenge in applying the ordinary beta distribution in multivariate facies modeling is how to determine the appropriate local variances to build the distribution. Kriging variances are one important and reasonable reference and are determined by the volumetric supports, variance-covariance structure and spatial distribution of data. But kriging variances alone do not lead to a good fit. Further adjustments are still required based on variogram models or other information.

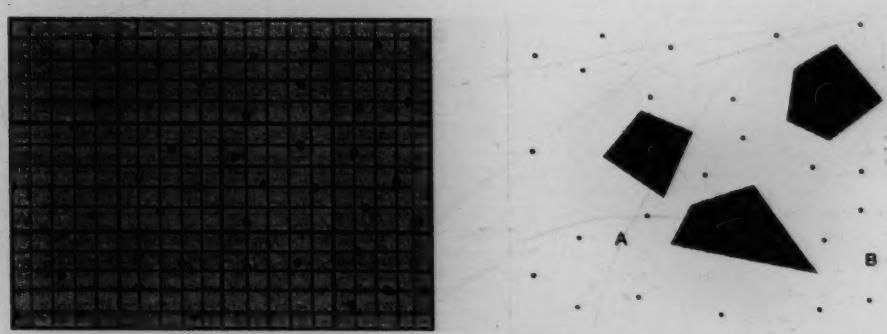

Figure 5-1 Multiscale facies models

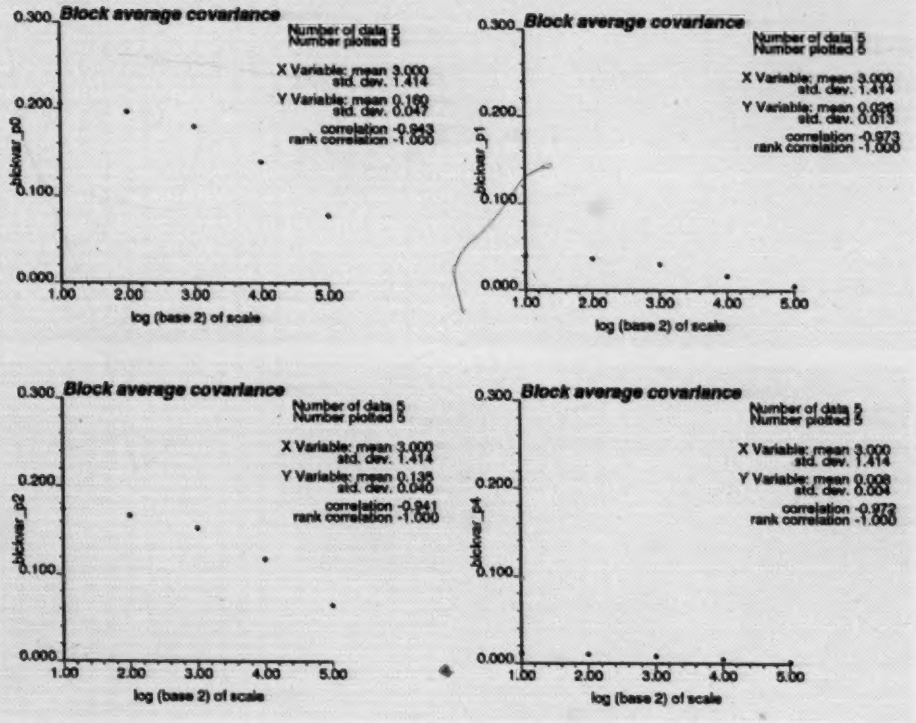

Figure 5-2 Block average covariances

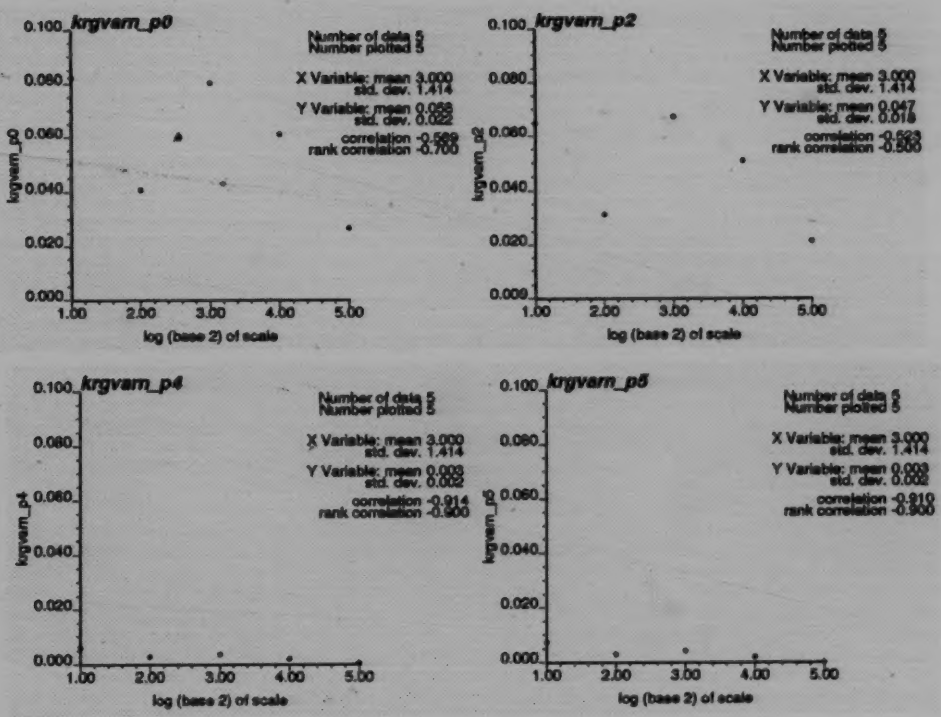

Figure 5-3 Kriging variances

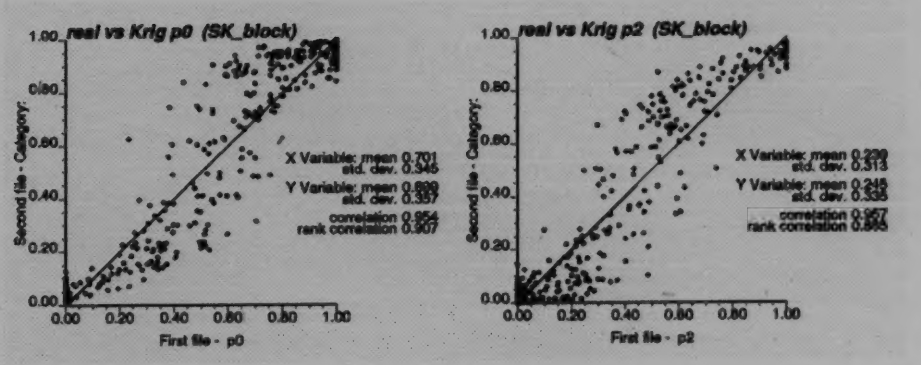

Figure 5-4 Kriging result versus real facies proportions, from simple block kriging with locally varying means

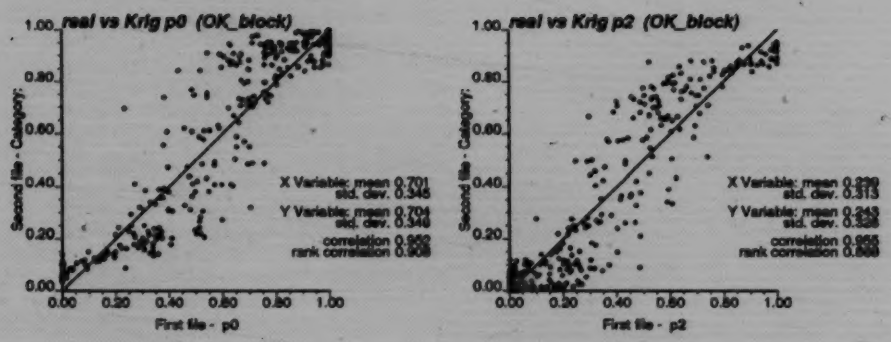

Figure 5-5 Kriging result versus real facies proportions, from ordinary block kriging

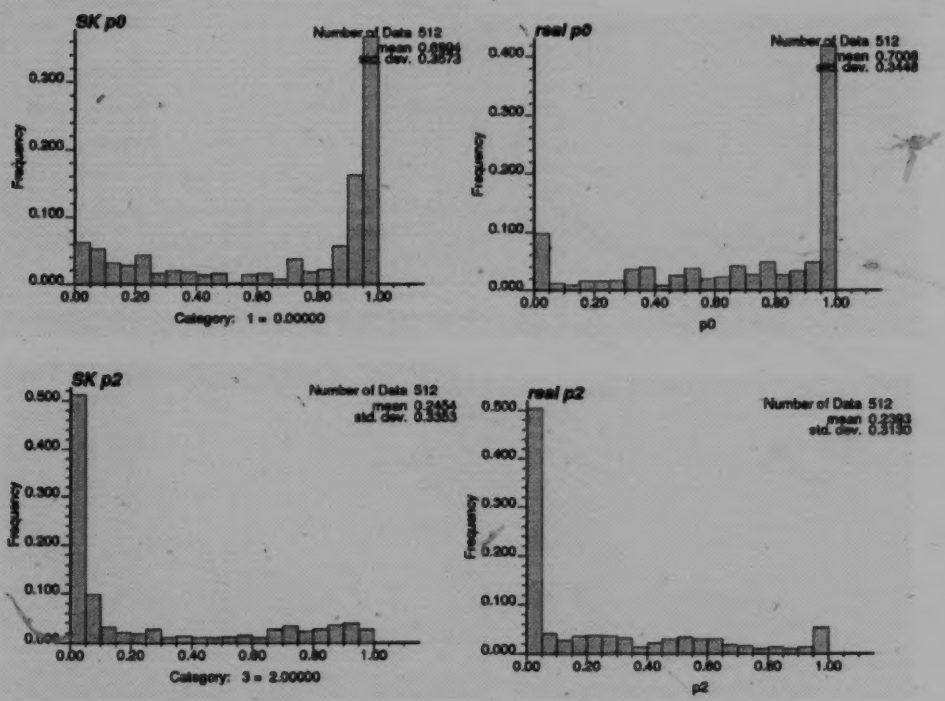

Figure 5-6 Kriging estimated global histograms, compared with the real histograms, from simple block kriging with locally varying means

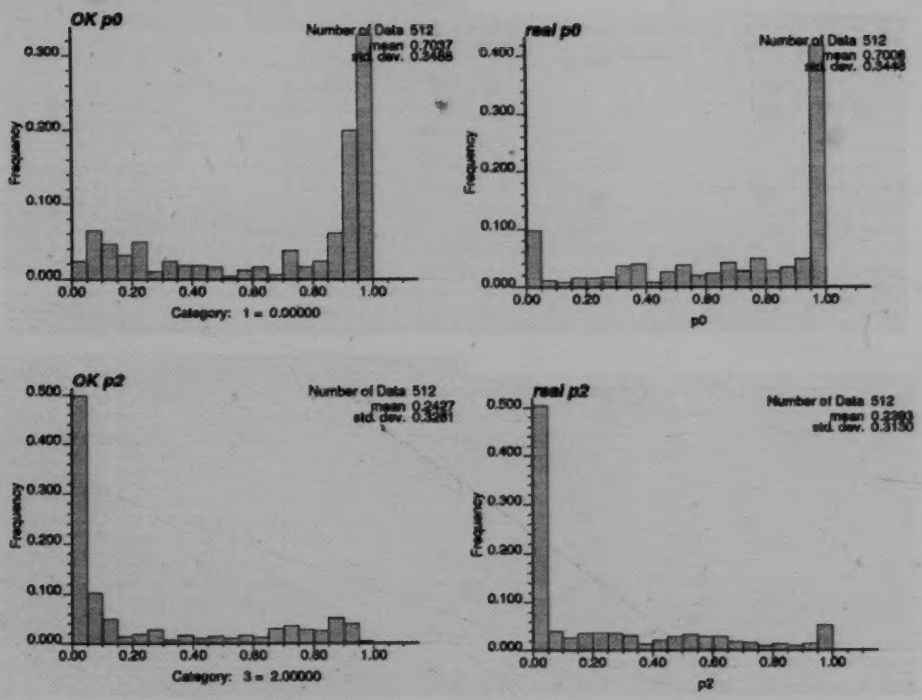

Figure 5-7 Kriging estimated global histograms, compared with the real histograms, from ordinary block kriging

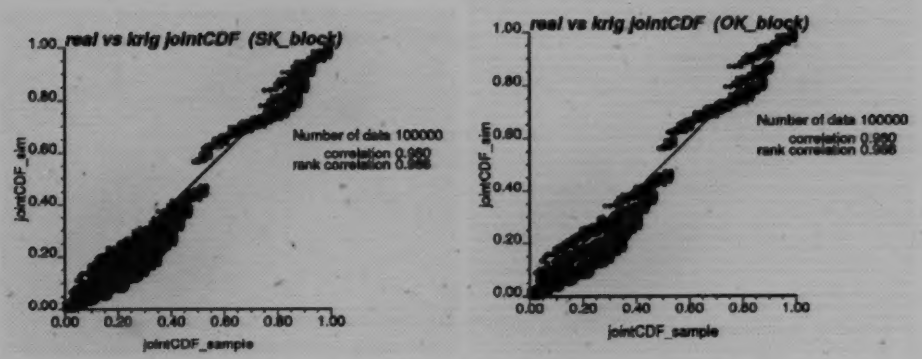

Figure 5-8 Kriging joint CDF's versus real joint CDF's

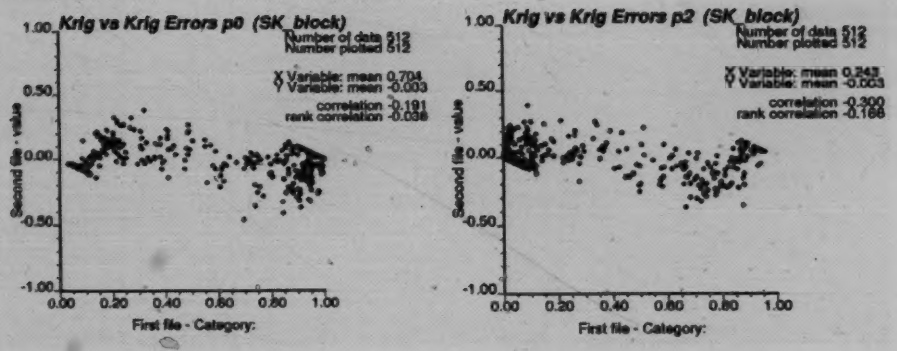

Figure 5-9 Residuals (kriging output – real values), from simple block kriging with locally varying means

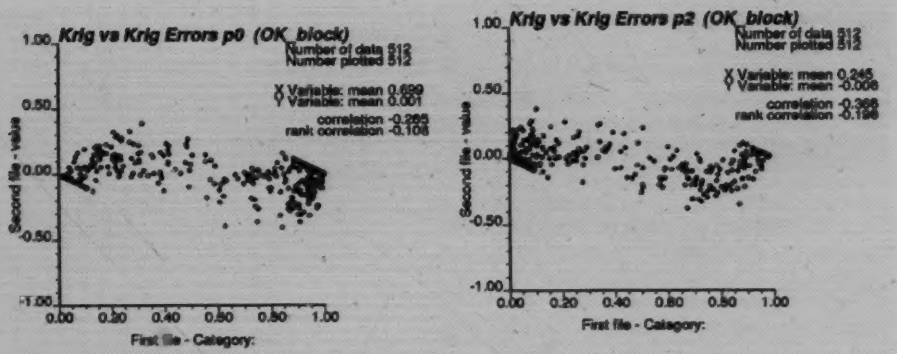

Figure 5-10 Residuals (kriging output – real values), from ordinary block kriging

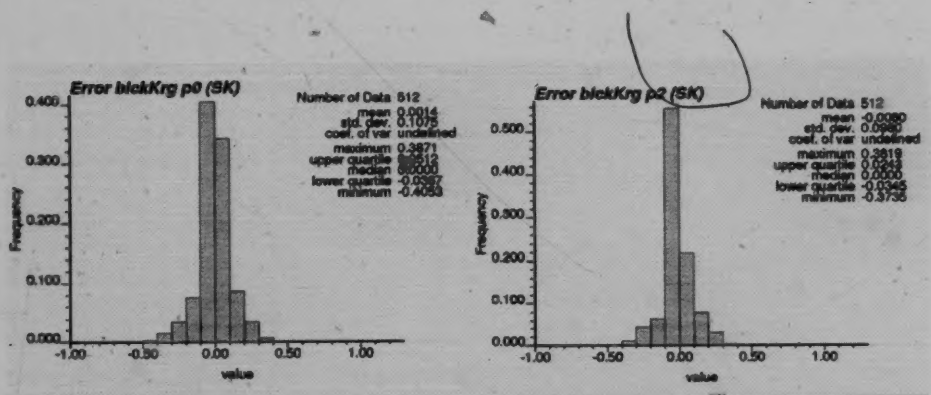

Figure 5-11 Histogram of Residuals (kriging output – real values), from simple block kriging with locally varying means

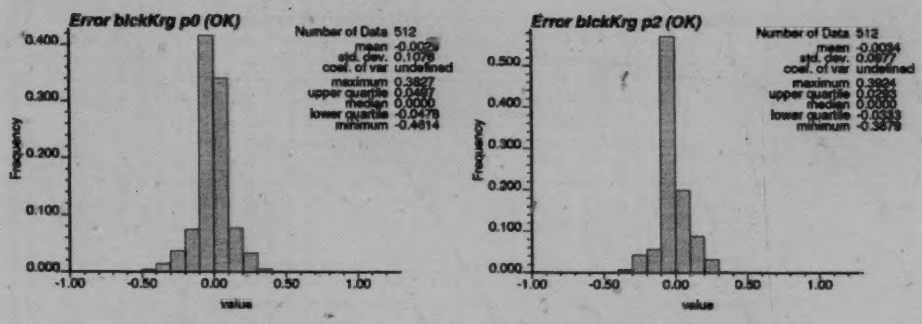

Figure 5-12 Histogram of Residuals (kriging output – real values), from ordinary block kriging

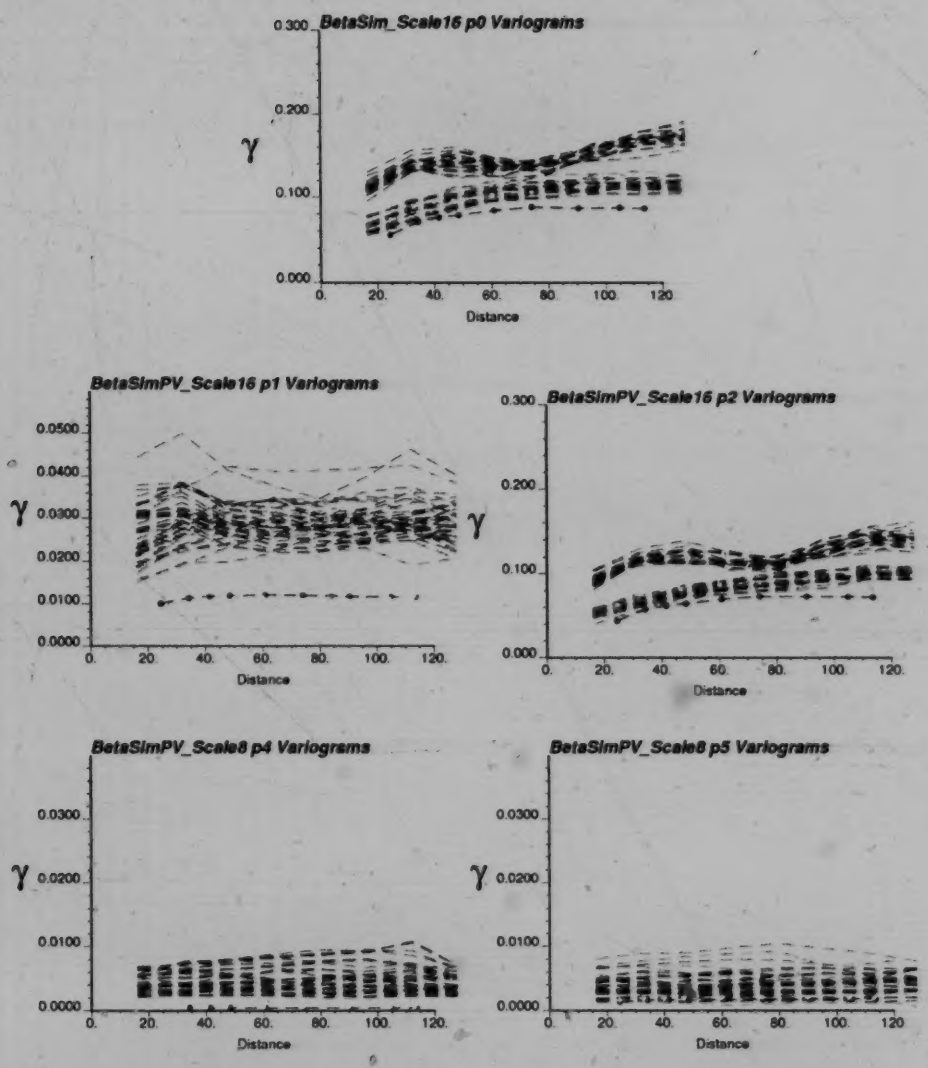

Figure 5-13 Semivariograms reproduction from simulated realizations, based on simple block kriging with locally varying means. Blue and yellow dash-point curves give, respectively, the real variograms in X and Y directions. According to the variogram maps, X direction is the major direction of continuity in the training image. The light blue and red dash curves give, respectively, the simulated variograms in X and Y directions.

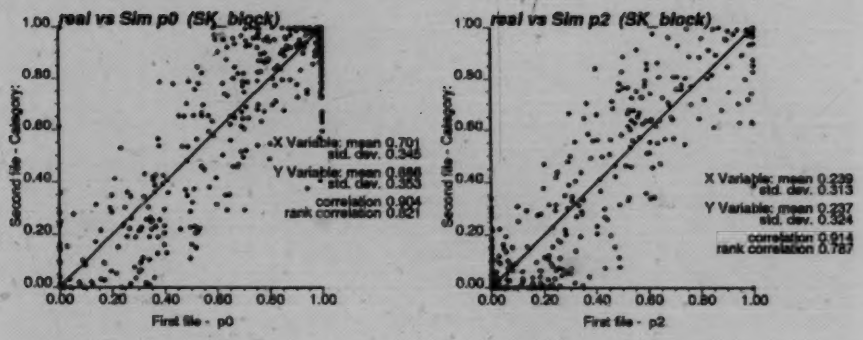

Figure 5-14 Simulated results versus real values, based on simple block kriging with locally varying means

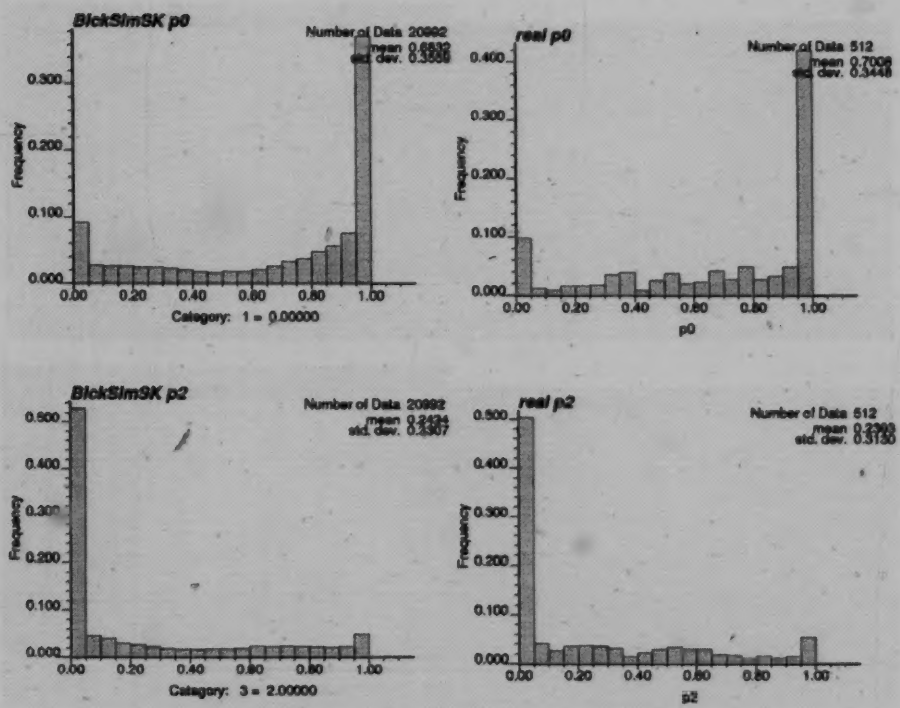

Figure 5-15 Global histograms from simulated realization, compared with the real, based on simple block kriging with locally varying means

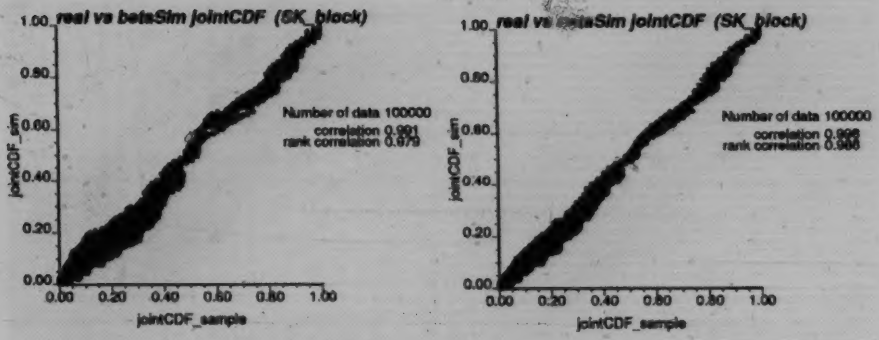

Figure 5-16 Cross plots of real versus simulated Global joint CDF's, based on simple block kriging with locally varying means

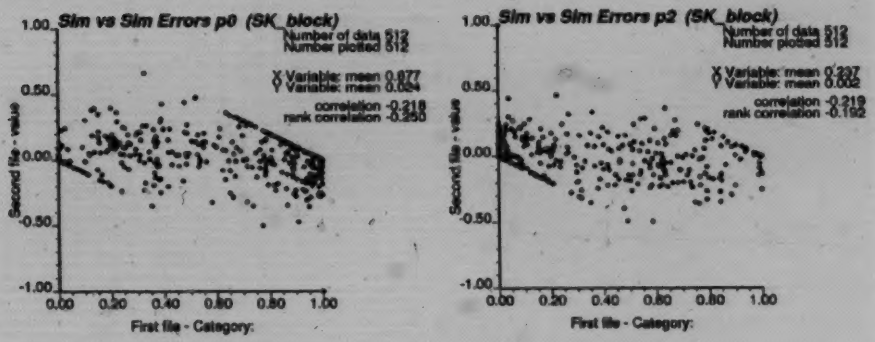

Figure 5-17 Residual (Simulated value – real value), based on simple block kriging with locally varying means

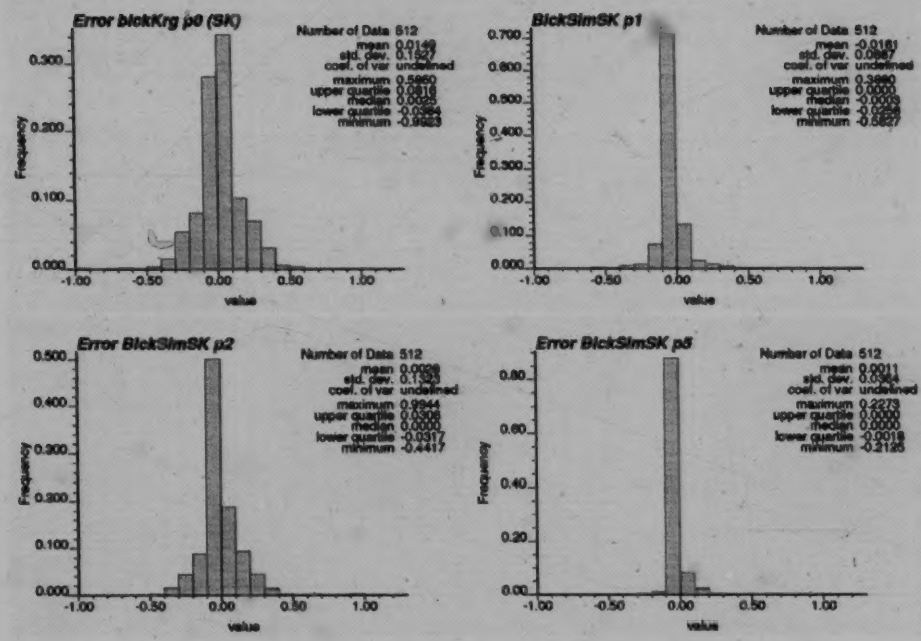

Figure 5-18 Histograms of Residuals (Simulated value – real value), based on simple block kriging with locally varying means

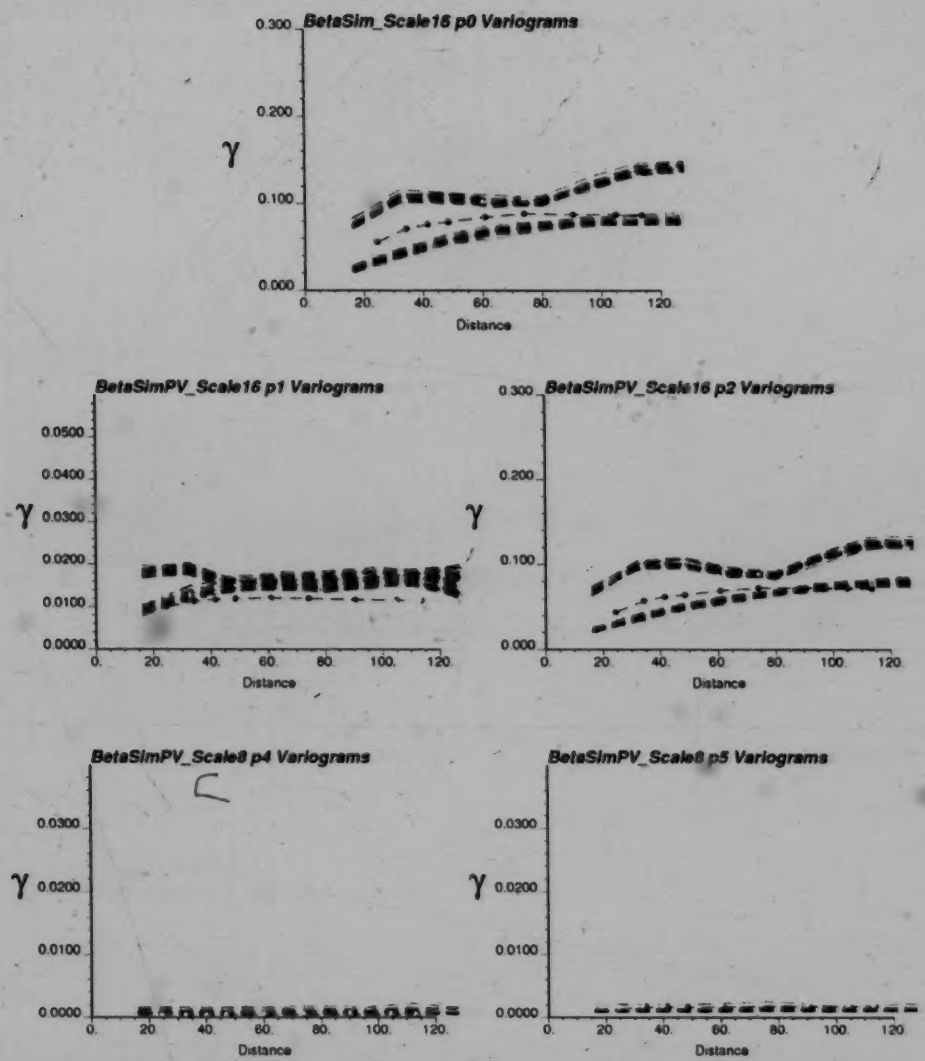

Figure 5-19 Reproduction of semivariograms by simulated realizations, based on simple block kriging with locally varying means. Blue and yellow dash-point curves give, respectively, the real variograms in X and Y directions. According to the variogram maps, X direction is the major direction of continuity in the training image. The light blue and red dash curves give, respectively, the simulated variograms in X and Y directions.

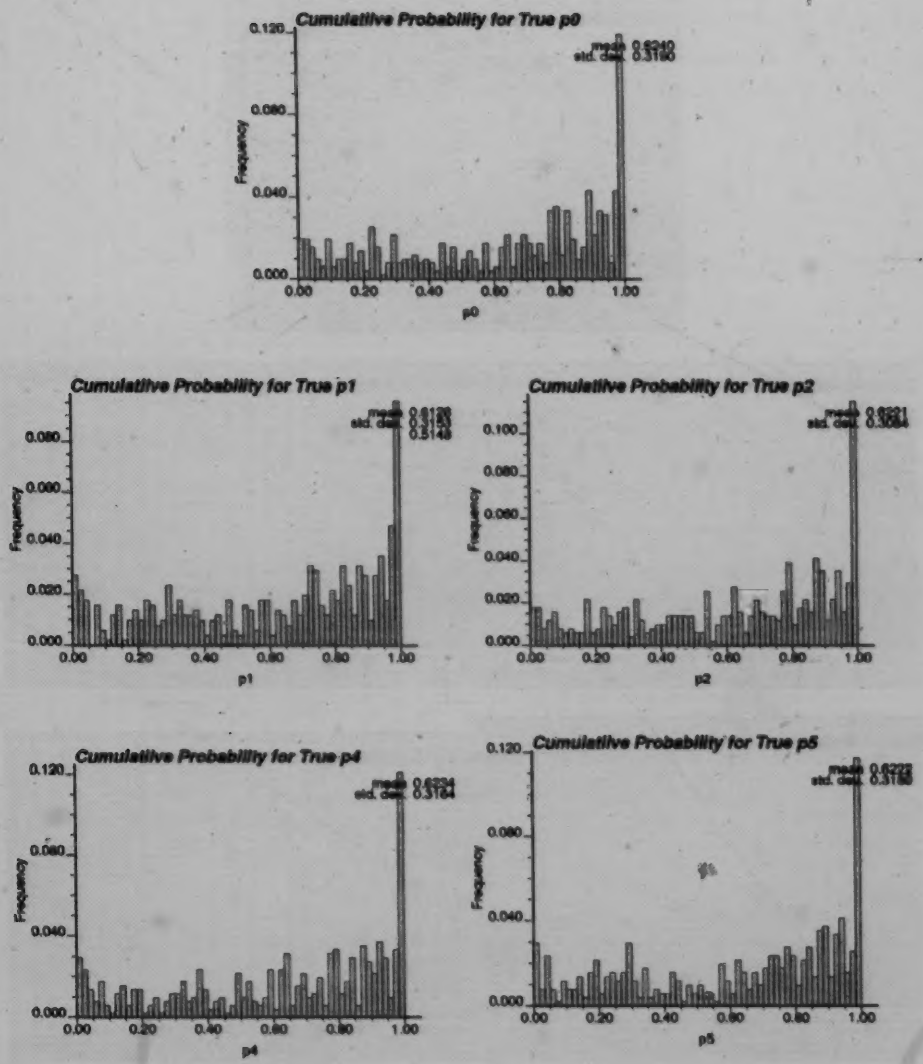

Figure 5-20 Histogram of cumulative probabilities associated with the real facies proportions based on the simulated realizations (based on simple block kriging with locally varying means)

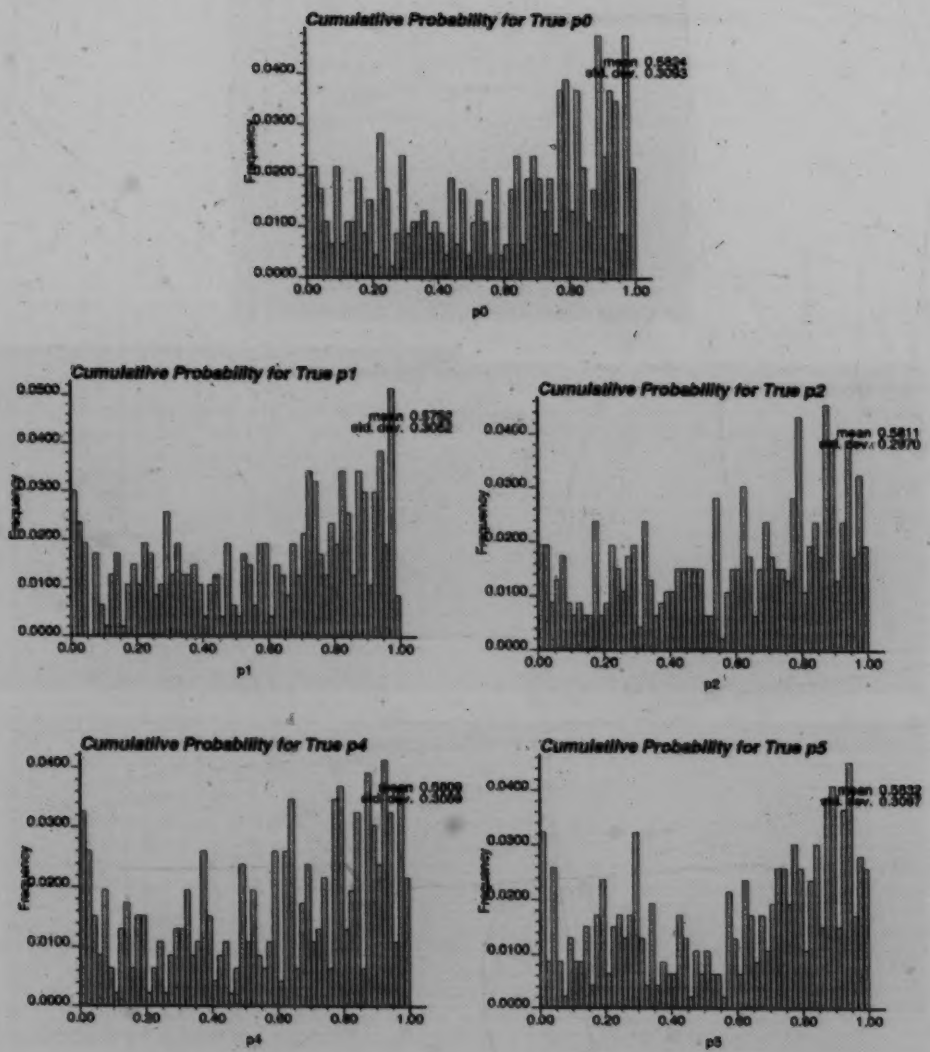

Figure 5-21 Histogram of cumulative probabilities associated with the real facies proportions based on the simulated realizations, the points with facies proportion 1.0 excluded. (Based on simple block kriging with locally varying means)

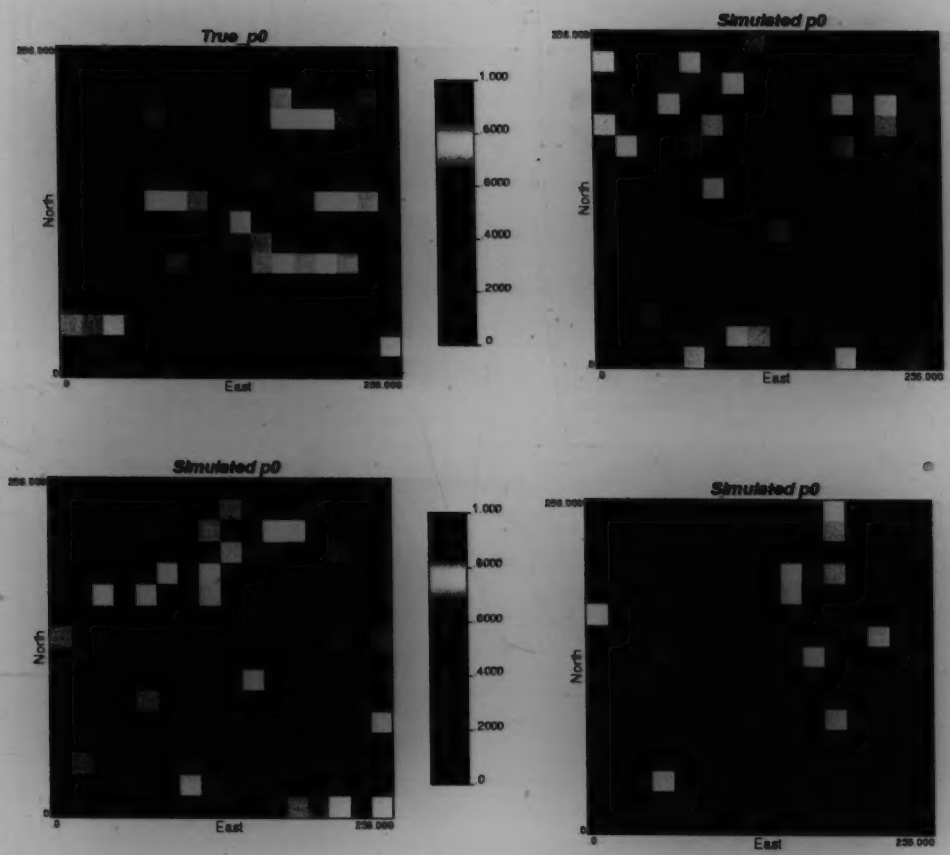

Figure 5-22 True versus simulated maps of facies proportion P_0

Chapter 6 Further Discussions on Multiscale Facies Distributions

6.1 Proportions and Probabilities

The key question in multiscale facies modeling is to estimate and simulate the values and the three dimensional distribution of the facies proportions

$$p_k = p_V(\mathbf{u},k) = \frac{1}{V}\int_V I(\mathbf{u}_\alpha,k)dV .$$

For any given local block at some volumetric support, the values of proportions p_k's, $(k=1,2,...,K)$ are unknown and are estimated or simulated. Various kriging approaches have been applied and the kriging estimates, say $p^*_{k(V)}$'s are treated as the estimated means of facies proportions for facies categories S_k's. This is reasonable because they are unbiased. For example, the simple kriging estimator has the form:

$$\begin{aligned} p^*_{k(V)} = p^*_V(k,\mathbf{u}) = &\sum_{\alpha=1}^{n_1}\lambda_{\alpha V\bullet}(k,\mathbf{u})I(k,\mathbf{u}_\alpha)+\sum_{\beta=1}^{n_2}\lambda_{\beta V v}(k,\mathbf{u})p_v(k,\mathbf{u}_\beta) \\ &+[1-\sum_{\alpha=1}^{n_1}\lambda_{\alpha V\bullet}(k,\mathbf{u})-\sum_{\beta=1}^{n_2}\lambda_{\beta V v}(k,\mathbf{u})]m(k,\mathbf{u}) \end{aligned}$$

where $m(k,\mathbf{u})$ denotes locally varying mean for variable P_k and v the scale support of block data. The expected value of $p^*_{k(V)}$ can be derived:

$$\begin{aligned} E[p^*_{k(V)}] &= \sum_{\alpha=1}^{n_1}\lambda_{\alpha V\bullet}(k,\mathbf{u})E[I(k,\mathbf{u}_\alpha)]+\sum_{\beta=1}^{n_2}\lambda_{\beta V v}(k,\mathbf{u})E[P_v(k,\mathbf{u}_\beta)] \\ &\quad +[1-\sum_{\alpha=1}^{n_1}\lambda_{\alpha V\bullet}(k,\mathbf{u})-\sum_{\beta=1}^{n_2}\lambda_{\beta V v}(k,\mathbf{u})]m(k,\mathbf{u}) \\ &= \sum_{\alpha=1}^{n_1}\lambda_{\alpha V\bullet}(k,\mathbf{u})m(k,\mathbf{u})+\sum_{\beta=1}^{n_2}\lambda_{\beta V v}(k,\mathbf{u})m(k,\mathbf{u}) \\ &\quad +[1-\sum_{\alpha=1}^{n_1}\lambda_{\alpha V\bullet}(k,\mathbf{u})-\sum_{\beta=1}^{n_2}\lambda_{\beta V v}(k,\mathbf{u})]m(k,\mathbf{u}) \\ &= m(k,\mathbf{u}) = E[P_k] \end{aligned}$$

That is, $p^{\bullet}_{k(V)}$ is an unbiased estimator of the local means of facies proportion P_k.

On the other hand, we should realize that in most cases, it is not an estimator of the facies proportion itself. For example, at point scale the means of facies proportions take some value within interval [0,1] while the exact facies proportions are either 0 or 1. But usually, $E[p^{\bullet}_{k(\bullet)}]$ does not equal 0 or 1. In fact, such an estimator contains information in two distinct and equally important aspects: 1) the facies proportion $p_v(\mathbf{u},k)$ itself and 2) the probability that the facies proportion variable P_k take some value. The information of these two parts is often combined.

Given some volumetric scale V, there is a set of possible values $\{0,\frac{1}{V},\frac{2}{V},...,1.0\}$ for the facies proportion. Using $x_q=\frac{q}{V}$, $q=0,1,...,V$ to denote the possible values of facies proportions at volumetric support V, the expected value of facies proportions have the form

$$E[P_k]=\sum_{q=0}^{V}\text{Prob}[P_{k(V)}=x_q]\bullet x_q .$$

This is a linear combination of all possible values with the weights to be their probabilities and $p^{\bullet}_{k(V)}$ is an unbiased estimator of this combination.

Now, focus on just one facies category S_k. Consider the facies proportions at two extreme volumetric supports V =0 and $V=\infty$. The first case represents the point scale and the second case can be regarded as the entire area of interest, $V=\Omega$. At a very large scale, there is exactly one unit in the population, that is, the entire space. All other values of x_q have the probability 0 except one, say $x_{q'}$, with probability 100% . In this case, $E\left[p^{\bullet}_{k(V)}\right]=E[P_k]=100\%\bullet x_{q'}$ and $p^{\bullet}_{k(\infty)}$ or $p^{\bullet}_{k(\Omega)}$ is the estimate of this facies proportion value. At the point scale, the facies proportion $P_{\bullet}(\mathbf{u},k)$ is the same as the facies indicator $I(\mathbf{u},k)$ and takes exactly 0 or 1. There is a large population of points

and different points might have different indicator values. Here $E\left[p^{\bullet}_{k(V)}\right] = E[P_k] = \text{Prob}[P_{k(V)} = 1.0] \bullet 1.0$. $p^{\bullet}_{k(\bullet)}$ is therefore the estimate of probability $\text{Prob}[P_{k(V)} = 1.0]$. This is in fact the probability that facies S_k occurs at the point. These two extreme cases are relatively simple and clear. At other volumetric scales $0 < V < \Omega$, the probabilities and the proportions are mixed. Figure 1-5 in Chapter 1 gives the histograms of proportions for facies S_0 at various volumetric supports. Note that at scales $2\times2\times2$ and $4\times4\times4$, about 80% or 90% of the real facies proportion values are either 0 or 1. In these cases, $p^{\bullet}_{0(V)}$ can give a very good estimation about probability that facies category S_0 occupies the whole block and the probability that no facies category S_0 occurs in the block. At scale $8\times8\times8$, 60% percent of facies proportions take values of either 0 or 1. At scale $64\times64\times64$, about 60% of the real facies proportion values go between 50% to 70%, surrounding the means of the facies proportion 66.48%. Similar observations are true for other facies categories and other training images.

The uncertainty also depends on the volume. At point scale, there is a large population of points taking values of either 0 or 1, each has some probability. The uncertainties, that is, variances of estimated facies proportions, are the largest. As scale increases, a series of facies proportion values occur but their variance decreases. At a very large scale $V = \Omega$, there is exactly one unit in the population and no uncertainty of this type. This can be illustrated by dispersion variance defined as:

$$D^2(V,\Omega) = E\left\{\frac{1}{N}\sum\left[P_{k(V)} - p_{k(\Omega)}\right]^2\right\}.$$

Here $p_{k(\Omega)}$ is the means of facies proportion $P_{k(V)}$ over the entire area of interest. At point scale, $P_{k(V)} = P_{k(\bullet)}$ takes either 0 or 1, while at various other scales $V \neq 0$, more values of $P_{k(V)}$ are larger than 0 or smaller than 1 and getting closer to the means. For

any fixed global mean $p_{k(\Omega)}$, $\sum [P_{k(V)} - p_{k(\Omega)}]^2$ is the largest when $V = 0$ and will decrease as V increases.

Another source of uncertainty comes from the modeling and estimating approach itself. Taking as an example the simple kriging algorithm, just as discussed in previous chapter, the kriging variance is the difference between two parts. The first part is the block average covariance over the estimated block and is dependent on the volumetric support. The second part is the sum of variances and block average covariances of the data points and data blocks with kriging weights and is determined by spatial relationship of the data with estimated block, as well as the variance covariance structure used. As the desired volumetric support increases, the block average covariance decreases and thus tends to decrease the kriging variance and thus decrease the uncertainty.

6.2 Facies Proportion Distribution Conditional on Local Data

The facies proportion distribution of a block is conditional on the information (data) available regarding this block. In the training image in this thesis, for block of each desired volumetric scale, there is a global distribution as described in Chapter 1 and the marginal CDF's are as listed in Figure 6-1. When there is no local information, the block is treated as one unit among the population following the global distribution. Based on some data regarding that local block, the conditional distribution changes. In case of perfect knowledge, we are 100% sure that the facies proportion for category S_k is $x_{q^*} = \frac{q^*}{V}$, for a unique value q^* within $0,1,...,V$ and distribution of P_k becomes

$$F_k(x) = \text{Prob}[P_k \le x] = \begin{cases} 0 & \forall x < x_{q^*} \\ 1 & \forall x \ge x_{q^*} \end{cases}.$$

The shape is shown in Figure 6-2. Different blocks might correspond to different values of x_{q^*}, but for a given block, this value is unique.

The above paragraph discusses two extreme cases: 1) there is no local information about a block; 2) full information is available. Usually, some information is available but not full. In this case, the possible value of facies proportion for category S_k is not unique but is part of the population with the unconditional global distribution. Here are three examples: 1) one point known: suppose among the regular grid in the training image, it is known that category S_0 occurs at the north-west top corner of a block; 2) two points known: suppose the facies category at the middle of the block is also S_0; 3) three points known: besides on 1) and 2), suppose it is known that the facies category at the south-east bottom corner is S_1. Figures 6-3 to 6-5 give the marginal CDF curves for P_0 at different volumetric scales and Tables 6-1 and 6-2 give the means and variances. Also Figure 6-6 gives the marginal histograms.

Table 6-1 Means of P_0 conditional on the points known

	2x2x2	4x4x4	8x8x8	16x16x16	32x32x32	64x64x64
3 points	0.9789	0.866	0.7966	0.7487	0.7958	0.6802
2 points	0.9956	0.9814	0.9565	0.8951	0.828	0.7295
1 points	0.9403	0.9262	0.8616	0.7731	0.6989	0.6600

Table 6-2 Variances of P_0 conditional on the points known

	2x2x2	4x4x4	8x8x8	16x16x16	32x32x32	64x64x 64
3 points	0.004476	0.027656	0.023378	0.03052	0.028527	0.010588
2 points	0.00117	0.004436	0.00996	0.023348	0.028968	0.009722
1 points	0.0147	0.038064	0.063303	0.073984	0.056787	0.020909

The following properties are observed:

a) At small scale, the histograms often show a unimodal shape rather than bimodal as in global distribution, but with a stronger skew.

b) The means are no longer constant. At small scale, means get close to either 0 or 1

while at large scale, they converge to the global means

c) The variances decrease as more points are known, but they are not strictly decreasing. As the local data increase, the mean of conditional distribution of facies proportion will get closer to the truth and the uncertainty will decrease.

Ordinary beta approach can also be applied to fit the multivariate distribution conditional on the data if the means and variances can be obtained. Figure 6-7 compares the simulated histograms with the true in some cases for facies proportion P_0 and shows a well reproduction of the distributions.

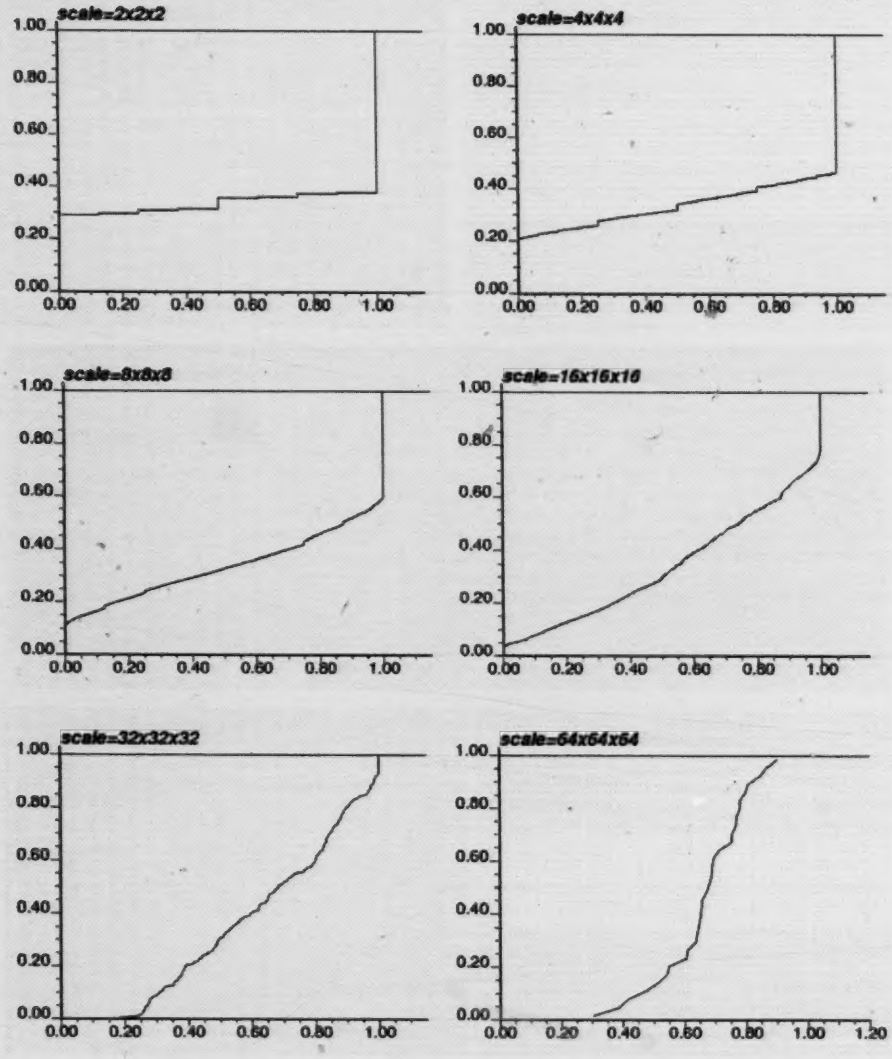

Figure 6-1 Global distributions of P_0 (based on no local information)

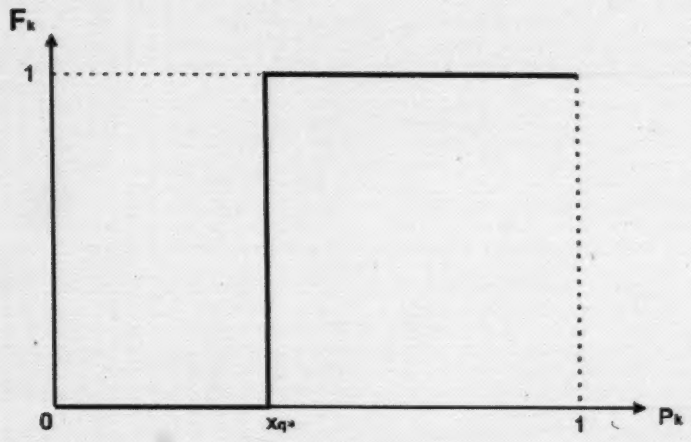

Figure 6-2 Distribution of P_k when perfect knowledge is available about a block

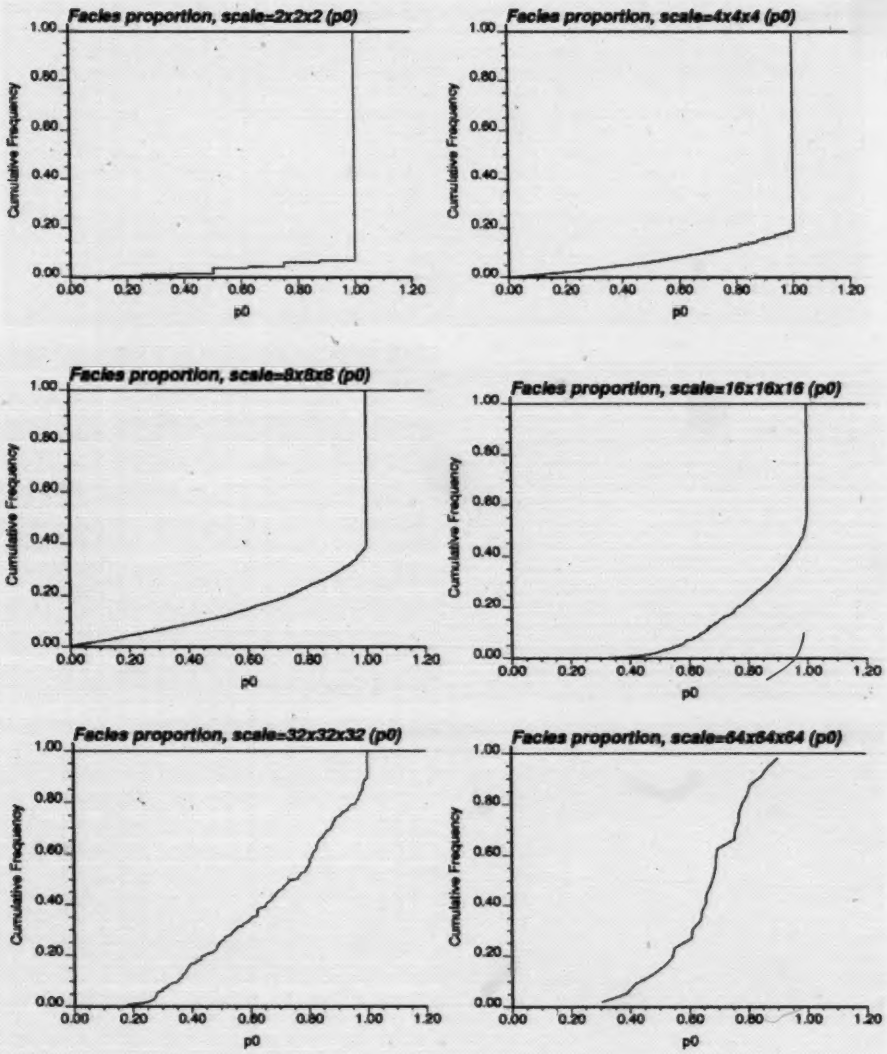

Figure 6-3 Distribution of P_0 when one point is known in the block

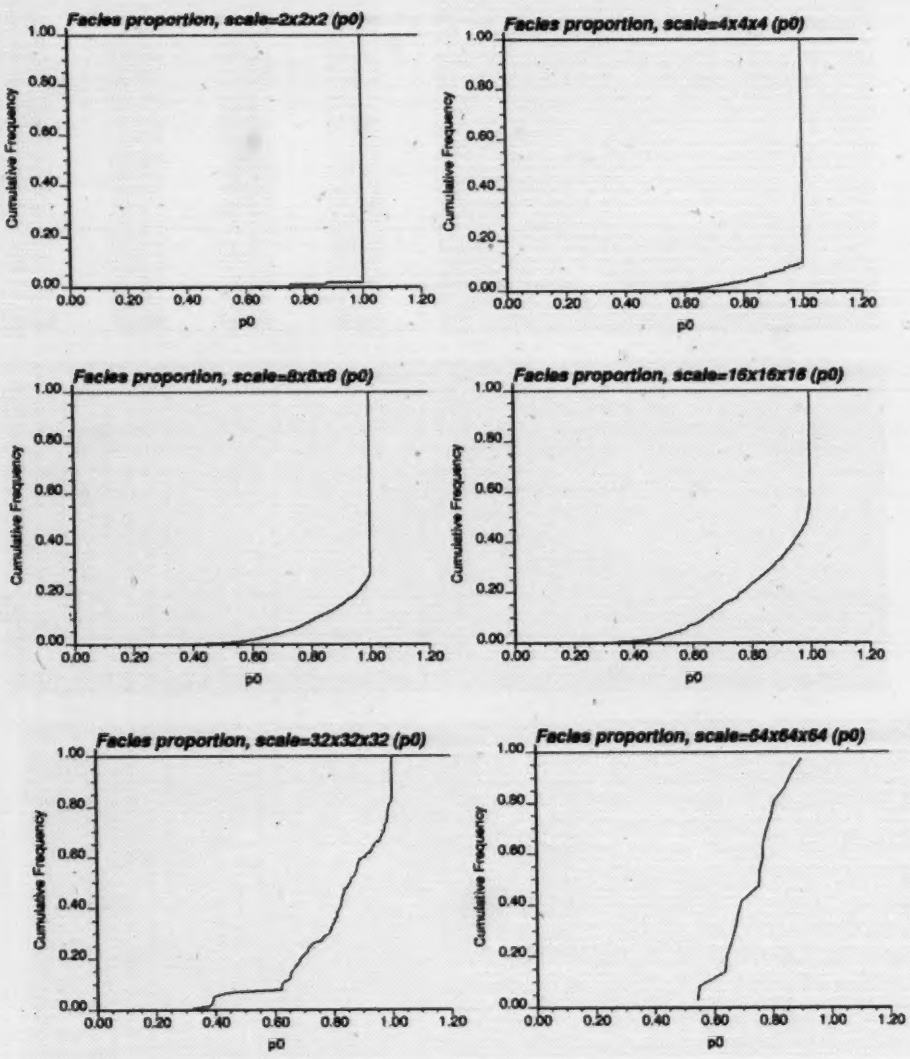

Figure 6-4 Distribution of P_0 when two points are known in the block

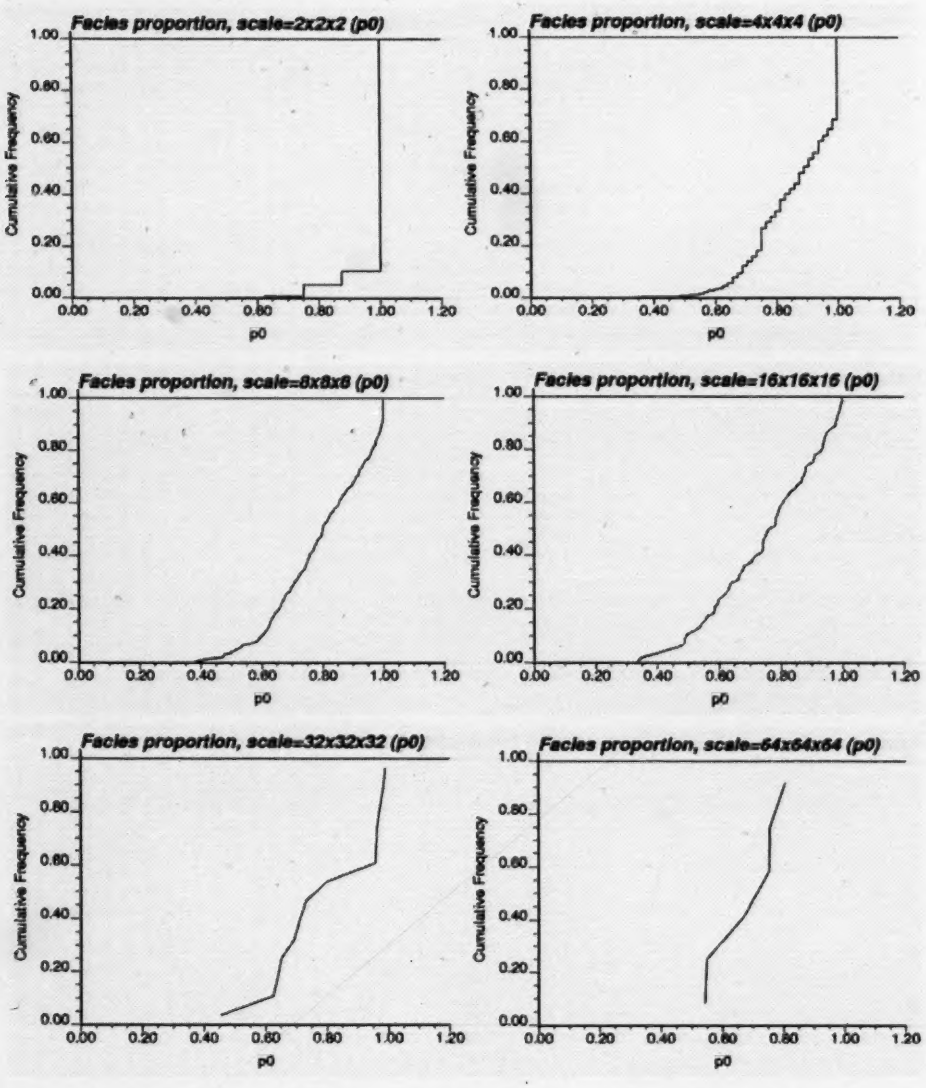

Figure 6-5 Distribution of P_0 when three points are known in the block

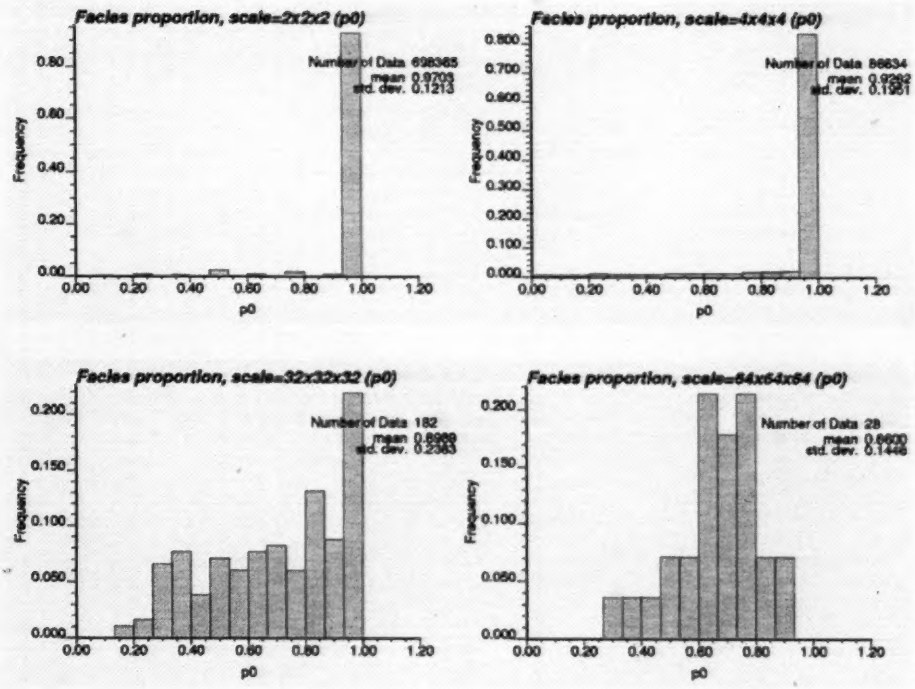

Figure 6-6 Histograms of P_0 when one point is known

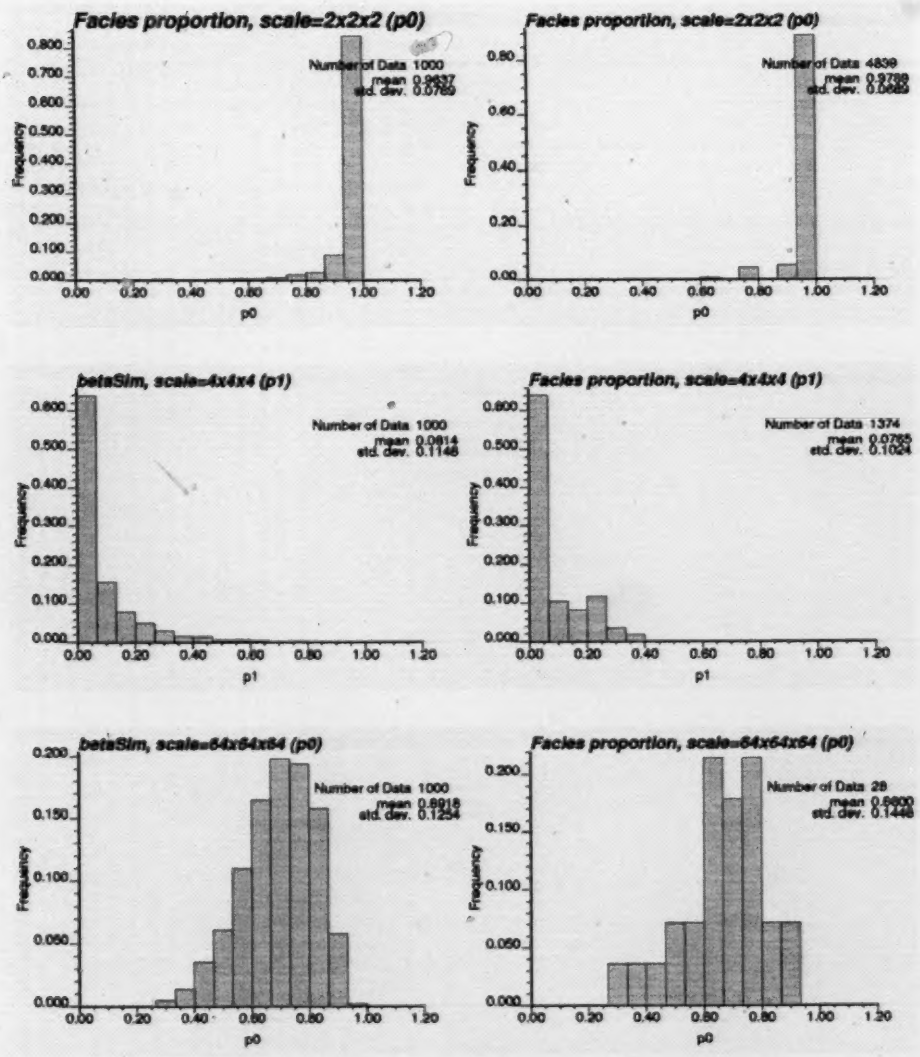

Figure 6-7 Ordinary Beta simulated histogram (left) compared the real (right).
Top and middle row: three points known; Bottom row: one point known

Chapter 7 Conclusions and Future Works

The multivariate distributions of facies indicators and facies proportions are volume dependent and determined by mean, the volumetric support and the variance-covariance structure of facies categories within the domain of interest. The global means of facies proportions are independent of the volumetric support while the variances of the facies proportions decrease with an increase in the volumetric support. Due to constant sum constraints, a negative covariance often occurs between the proportions of two facies categories within the space of interest.

Logratio transformation of facies proportions will guarantee the satisfaction of order relation constraints when applied in kriging or other estimation approaches. However, zero-proportions will lead to problems. Furthermore, the nonlinear nature of logratio transformation always leads to geometric average results when back transforming an arithmetic average of logratio values thus leading to significant bias when it is used to estimate the mean that is an arithmetic average.

The beta distribution and the ordinary beta distribution are shown to efficiently fit the marginal and joint distribution of facies proportions at different volumetric supports. Block kriging approaches using simple kriging and ordinary kriging algorithms estimate the facies proportions at unsampled block locations based on the data of different scales, including point data and collocated block data of difference volumetric supports.

One big challenge in applying the ordinary beta distribution in multivariate facies modeling is how to determine the appropriate local variances to build the distribution. Kriging variances are one important and reasonable reference and are determined by the volumetric support, variance-covariance structure and spatial distribution of data. But kriging variances tends to overestimate or underestimate the local variances. Further adjustments are required based on variogram models or other information.

Several factors determining the uncertainty of facies proportions include: 1)

volumetric support, 2) spatial distribution of available data and variances-covariance structure within the entire area, 3) modeling and estimating approach itself and 4) amount of local data and local information available. In general, at a larger volumetric support, or having more local data or local information available, uncertainty tends to decrease.

The following future works are desired:

First, as discussed in Chapter 5, further research is needed on estimating and adjusting the local variances which are required to fit the local facies distribution. Kriging variances are a reference in estimating the local variances but further adjustments are needed. Supposed there is a factor $f_k(\mathbf{u},v)$ such that $\sigma_k^2(\mathbf{u},v) = f_k(\mathbf{u},v)\cdot\hat{\sigma}_k^2(\mathbf{u},v)$, where $\sigma_k^2(\mathbf{u},v)$ is the true local variance for facies category S_k and $\sigma_k^2(\mathbf{u},v)$ is the kriging variance, the factor $f_k(\mathbf{u},v)$ may depend on i) the location of the estimated block, ii) the magnitude of kriging estimate, iii) the conditioning data, iv) the multivariate distribution of the facies proportion and v) other factors.

Second, the research in this thesis is based on analysis and process on the training images. Application in industrial and production practices is still subject to further development and test.

Bibliography

J. Aitchison (1986). *The Statistical Analysis of Compositional Data.* Chapman and Hall, New York

M. Armstrong (1998). *Basic Linear Geostatistics.* Springer-Verlag Berlin Heidelberg.

R. A. Behrens, M. K. Macleod, T. T. Tran, A. O. Alimi (1998). *Incorporating Seismic Attribute Maps in 3D Reservoir Models.* SPE 36499

D. Dennis, J. J. Walvoort, de Gruijter (2001) "Compositional Kriging: A Spatial Interpolation Method for Compositional". Mathematical Geology, Vol. 33, No. 8, p.951-966

C. V. Deutsch (1996). *Direct Assessment of Local Accuracy and Precision.* Geostatistics Wollongong'96. Volume 1, p.115-125.

C. V. Deutsch and A. G. Journel (1998). *GSLIB: Geostatistical Software Library and User's Guide.* Oxford University Press, New York, second Edition.

C. V. Deutsch and P. Frykman(1999). *Geostatistical Scaling Laws Applied to Core and Log Data.* SPE 56822.

C. V. Deutsch (2002). *Geostatistical Reservoir Modeling.* Oxford University Press, New York.

C. V. Deutsch (2005). *A Sequential Indicator Simulation Program for Categorical Variables with Point and Block data: BlockSIS.* Centre for Computational Geostatistics (CCG) Annual Report. p.402-1 – 402-22.

L. Devroye (1986). *Non-Uniform Random Variate Generation.* Springer-Verlag, New York.

E. D. Isaaks and R. M. Srivastava (1989) *An Introduction to Applied Geostatistics.* Oxford University Press, New York.

A. G. Journel and Ch. J. Huijbregts (1978) *Mining Geostatistics*. Academic Press, London, New York, San Francisco

W. J. Kennedy and J. E. Gentle (1980). *Statstical Computing*. Mercel Dekker, Inc. New York and Basel

S. Kotz, N. Balakrishnan, N. L. Johnson (2000). *Continuous Multivariate Distributions*. John Willey & Sons, Inc.

J. G. Mauldon (1959). *A Generalization of the Beta-Distribution*. The Annals of Mathematical Staitstics, Vol. 30, No. 2. p.509-520.

W. H. Press, S. A. Teukolsky, W. T. Vetterling, B. P. Flannery (1986). *Numerical Recipes in Fortran 77 (Second Edition)*. Press Syndicate of the University of Cambridge.

W. Xu, T. T. Tran, R. M. Srivastava, A. G. Journel (1992). *Integrating Seismic Data in Reservoir Modeling: The Collocated Cokriging Alternative*. SPE 24742